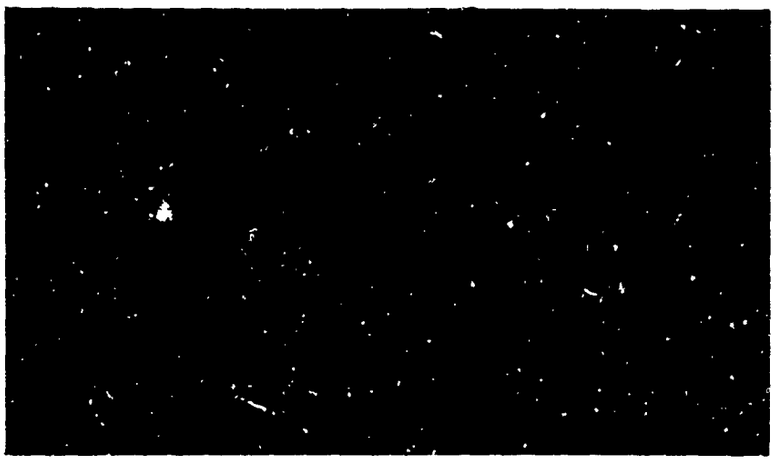

UNIVERSITY OF PENNSYLVANIA

ELECTROCHEMISTRY LABORATORY

PHILADELPHIA 4, PENNSYLVANIA

AD 60001

SCIENTIFIC AND TECHNICAL INFORMATION FACILITY

operated for National Aeronautics and Space Administration by Documentation Incorporated

Post Office Box 5700
Bethesda, Md. 20014

Telephone 656-2850
656-2851

FACILITY CONTROL NO. 10541

DATE 11-5-64

ATTACHED IS A DOCUMENT ON LOAN

FROM: Scientific and Technical Information Facility

TO: Defense Documentation Center
Attn: DDC-IRC (Control Branch)
Cameron Station
Alexandria, Va. 22314

In accordance with the NASA-DOD Cooperative AD Number Assignment Agreement it is requested that an AD number be assigned to the attached report.

☑ As this is our only available copy the return of the document (with AD number and any applicable distribution limitations) to the address below is essential.

☐ This document may be retained by DDC. If retained, please indicate AD number and any applicable distribution limitations on the reproduced copy of the title page and return to the address below.

Return Address: Scientific and Technical
Information Facility
Attn: INPUT BRANCH
P. O. Box 5700
Bethesda, Md. 20014

FL 244

HYDROGEN EVOLUTION:

THE EFFECT OF SURFACE CONCENTRATION

Final Report

to

Office of Naval Research
Contract Nonr 551(22) NR 036-028
Contract Ending March 31, 1962

Principal Investigator - J. O'M. Bockris

Research Associate - M. A. V. Devanathan

Electrochemistry Laboratory

The University of Pennsylvania

Philadelphia 4, Pennsylvania

1. INTRODUCTION:

The objective of this project is the acquisition of fundamental knowledge concerning the behavior of atomic hydrogen at corrodible metal surfaces, in particular the formation and transfer of atomic hydrogen into the bulk metal. Such knowledge is a prerequisite to the control and the final elimination of hydrogen embrittlement which causes weakening and eventual breakdown of structures in corrosive environments.

The problem can be resolved into two stages. First, a knowledge of the concentration of atomic hydrogen on the surface of the corroding metal must be determined. Secondly, the rate of transfer of the hydrogen into the metal bulk under various conditions must be measured. The solution, therefore, requires first the development of new techniques whereby the necessary information may be acquired. The establishment from this data of a general theory of the kinetics of formation and transfer of atomic hydrogen into metals will then enable the development of practical methods of control of hydrogen embrittlement.

2. FACTORS WHICH CONTROL THE SURFACE CONCENTRATION OF HYDROGEN

Atomic hydrogen is produced during the natural corrosion of ferrous materials, during cathodic protection by externally impressed cathodic currents, and during plating of protective metal films. In all these instances the hydrogen is produced by a cathodic hydrogen evolution reaction. The problem of surface concentration with adsorbed atomic hydrogen is therefore intimately connected with the kinetics and mechanism of the hydrogen evolution reaction. The variation of the surface concentration or coverage factor θ can therefore be formulated in general

terms as follows.

(A) Hydrogen embrittlement and surface concentration of H

Consider a metal surface in solution upon which H_2 is evolved (fig. 1).

Then, if the surface coverage with H is in the steady state,

$$k_1 \cdot (1 - \theta) c_{H^+} - k_{-1}\theta - k_2\theta - (k_D)_1\theta = 0 \qquad (1)$$

where the k values are rate constants appropriate to the reactions indicated in fig. 1; c_{H^+} is the proton source concentration in the double layer.

Hence (1)

$$\theta = \frac{k_1 c_{H^+}}{k_1 c_{H^+} + k_{-1} + k_2 + (k_D)_1} \qquad (2)$$

Thus, suppose $k_1 c_{H^+} \ll k_2$, and $k_2 \gg k_{-1}$ (condition of slow discharge control of the hydrogen evolution reactions), then:

$$\theta = \frac{k_1 c_{H^+}}{k_2 + (k_D)_1} \qquad (3)$$

Or, suppose that $k_2 \ll k_1$ and $k_{-1} \ll c_{H^+}$ then:

$$\theta = \frac{1}{1 + (k_D)/k_1 c_{H^+}} \qquad (4)$$

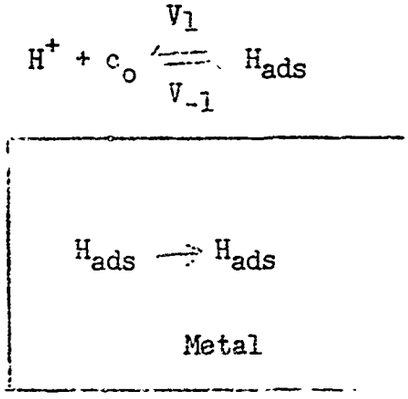

Fig. 1

(3) and (4) represent limiting expression for the coverage of an electrode with H, assuming a path of electrochemical desorption.

Thus, the rate of diffusion of H into the metal is:

$$v_D = (k_D)_1 \theta. \qquad (5)$$

Equation (1), and the resulting equation (5) apply for conditions of steady H_2 evolution and it is assumed that little or no H exists in the metal. If v_D is appreciable, the concentration of adsorbed H grows with time and may result in embrittlement. When the steady state for H diffusion into the metal has been reached:

$$(k_D)_1 \theta = (k_D)_{-1} c_H, \qquad (6)$$

where c_H is the concentration of adsorbed H and $(k_D)_{-1}$ is the rate constant for diffusion of H out of the metal and c_H is the concentration of absorbed H atoms. For a given metal the embrittlement is probably proportional to the concentration of adsorbed H and (6) shows:

$$c_H = \frac{(k_D)_1}{(k_D)_{-1}} \theta \qquad (7)$$

i.e., the absorbed H and hence for a given metal the embrittlement, is proportional to the surface concentration, θ.

Hence, the amount of surface adsorbed H, may be regarded as the most basic quantity for the study of the H embrittlement of a metal.

The variation of degree of H embrittlement in a series of metals depends upon: (a) The embrittlement caused per atom in the metal lattice; (b) The surface coverage during H_2 evolution, upon which the concentration of adsorbed H directly depends. Among the various metals (Conway and Bockris, 1957), it is known qualitatively that the concentration of surface adsorbed H is greatly variable. It is therefore possible that an important determinative factor in the degree of H embrittlement among the various metals is the surface concentration of adsorbed H.

3. THE DOUBLE CHARGING METHOD

The methods available for the determination of the fraction of electrode surface covered, θ, have been reviewed in detail elsewhere (Bockris and Devanathan, 1957).

The most direct method is that of:

(A) Rapid galvanostatic charging

The method was originated by Bowden (1929) and used by Pavson and Butler (1939) and others (Breiter, Knorr and Völkl, 1955). Difficulties associated with the readsorption of hydrogen from dissolved hydrogen molecules in solution, or from bubbles on the electrode, are minimized by the use of high anodic current densities, whereby the anodic dissolution of the adsorbed atomic hydrogen is completed before readsorption becomes appreciable. Breiter, Knorr and Völkl (1955) used this method for the noble metals Pt, Pd, Ir, Rh and Au under cathodic polarization. The method can only be successfully applied if there is a considerable potential difference between the potential corresponding to the completion of hydrogen dissolution and that corresponding to the commencement of the next anodic process (e.g., oxide formation, evolution of oxygen, etc.), a condition found only with the noble metals. When the succeeding anodic processes overlap the hydrogen dissolution, the definition of the potential region of hydrogen dissolution becomes diffuse, and the rapid galvanostatic charging method becomes inapplicable.

(β) Double charging method

Figure 2, which represents a typical potential time curve obtained on platinum by the rapid charging method, shows the potential gap B-C separating the hydrogen dissolution stage A-B and the oxide formation stage C-D. Figure 3 (curve 1) shows a similar curve for silver under analogous conditions. No clear region attributable to hydrogen dissolution is discernible. In the present method, a compensating curve enables subtraction of the current due to the irrelevant anodic processes to be made from the total current due to hydrogen dissolution and these other anodic processes.

4. THEORY OF THE DOUBLE CHARGING METHOD

Suppose an electrode is polarized to an overpotential, η, with a steady cathodic current, i_c. Let this current be switched off and a constant anodic current of magnitude i_a switched on "immediately".

Then, after switching in a (total) galvanostatic current density, i_a,

$$C_v\left(\frac{\partial V}{\partial t}\right)_t = i_a - i_{F,t} \qquad (8)$$

where C_v is the capacity of the double layer at a potential V, t is the time, and i_F the total c.d. for the Faradaic processes occurring at the potential V (i.e. for the dissolution of adsorbed H, together with the formation of oxides).

If the degree of surface coverage with H is θ,

$$i_F = i_{H,\theta} + i_{an}(1 - \theta) \qquad (9)$$

where $i_{H,\theta}$ is the current due to the dissolution of H from a total of 1 cm^2 of electrode area (whatever the fraction of this area occupied by H);

and i_{an} is the current due to some anodic process when this process occurs on 1 cm^2 of an electrode surface which is free from H. Thus $i_{H,\theta}$ and $i_{an}(1 - \theta)$ are both partial currents on 1 cm^2 of electrode.

From (8) and (9),

$$C_v\left(\frac{\partial V}{\partial t}\right)_{t,1} = i_a - \left(i_{H,\theta} + i_{an}(1 - \theta)\right) \tag{10}$$

Suppose galvanostatic charging is now begun on an electrode free from H (e.g., suppose it is begun at a potential sufficiently anodic to the reversible H_2 potential, so that all the adsorbed H has been dissolved off the electrode before charging is commenced). Then:

$$C_v\left(\frac{\partial V}{\partial t}\right)_{t,2} = i_a - i_{an} \tag{11}$$

For a given potential in the first charging process, from (10) and (11),

$$C_v\left[\left(\frac{\partial V}{\partial t}\right)_{t,2} - \left(\frac{\partial V}{\partial t}\right)_{t,1}\right] = i_{H,\theta} - i_{an}\,\theta \tag{12}$$

If, therefore, the potential-time gradients at a series of identical potentials, i.e. $(dV/dt)_{1,v}$ and $(dV/dt)_{2,v}$ are measured, the value of $(i_{H,\theta} - i_{an}\,\theta)_v$ at a series of potentials can be obtained, knowing the value of C_v at the various potentials chosen for the series of $(dV/dt)_v$ values.

Consider now a plot of $\left[i_{H,\theta} + (1 - \theta)i_{an}\right]_v$ as a function of a potential. Such a plot is shown in fig. 4, where the corresponding values of i_{an} are also shown. For sufficiently cathodic values of V, both $\left[i_{H,\theta} + (1 - \theta)i_{an}\right]$ continues to increase because of the increasing contribution of i_{an}. Correspondingly, i_{an} is initially small because the

potential is not sufficiently anodic, but at sufficiently high anodic potentials it increases rapidly and finally coincides with $i_{H,\theta} + (1 - \theta)i_{an}$. This occurs when the adsorbed atomic hydrogen has dissolved completely from the surface of the metal and the entire faradaic current is carried by anodic processes such as oxide formation.

The corresponding plot of the difference of the functions $\left[i_{H,\theta} + i_{an}(1 - \theta) \right]_V$ and $(i_{an})_V$ is shown in an example in fig. 5. In the vicinity of the reversible electrode potential, the difference of the two functions rises sharply, passes through a maximum and falls asymptotically towards zero at the potential corresponding to the completion of H dissolution.

The difference of the two functions $\left[i_{H,\theta} + i_{an}(1 - \theta) \right]$ and i_{an} plotted as a function of potential in fig. 4 can now be plotted as a function of the time needed to reach given potentials during the first type of charging process (namely, that described by equation (10), when H is being dissolved from the surface). Examples of a plot of this difference (i.e., of $i_{H,\theta} - i_{an}\,\theta$) against V are given in figs. 6 and 7. The area under this curve is equal to:

$$A = \int_0^{t_\infty} i_{H,\theta}\left(1 - \frac{i_{an}\,\theta}{i_{H,\theta}}\right)dt \qquad (13)$$

where t_∞ is the time at which the plot falls to zero value.

When this function has a maximum value, namely, at small times, and potentials near to the reversible potential, it is seen from the plot in Fig. 7 that i_{an} is very small. This suggests that $i_{an}\,\theta / i_{H,\theta} \ll i_{H,\theta}$.

Further,

$$\frac{i_{an}\,\theta}{i_{H,\theta}} = \frac{1}{1 + \Delta/i_{an}\,\theta} \cdot \qquad (14)$$

where $\Delta = i_{F_1} - i_{an}$ and $i_{F_1} = i_{H,\theta} + (1 - \theta)i_{an}$, the faradaic current in the first charging process. At short times, inspection of fig. 4 shows that $\Delta/i_{an} \gg I$ and therefore the "error term" in equation (13) tends to be negligible. At long times, $\theta \rightarrow 0$, and the error term is hence correspondingly small.

Neglecting, therefore, the effect of the term $i_{an}\theta/i_{H,\theta}$ the integral of equation (13) gives the amount of adsorbed H on the electrode under the conditions of cathodic polarization corresponding to the beginning of the first anodic charging process.

5. STUDIES ON SILVER

Silver was selected for these studies. With alkaline solutions on anodic charging, oxide formation should overlap with and succeed the dissolution of H, and then be followed by oxygen evolution. Thus, the solution would not be contaminated by silver ions in successive anodic discharges.

(A) The cell and gas purification trains were similar to those already described (Azzam, Bockris and others, 1950).

(B) Preparation of alkaline solutions: The solutions of NaOH were made from electrolytic Na amalgam. Hg was distilled three times, and the cathode was placed in a 20% solution of A.R. NaOH. The electrolysis

was continued until the amalgam was viscous, the electrolyte siphoned off and the amalgam washed in conductivity water. It was transferred by means of helium pressure into a solution preparation vessel and covered with conductivity water. During the dissolution of the amalgam, the solution was in contact with purified helium only.

The NaOH solution was preëlectrolyzed cathodically for at least two days. The c.d. for the preëlectrolysis was 10^{-2} amps cm^{-2}. The solution during preëlectrolysis was about 0.5 N and was diluted with conductivity water, distilled into the test electrode compartment of the cell, to 0.1 N NaOH (determined by titration of portions drawn through a trap from the cell).

(C) Water: This was prepared as described (Azzam, Bockris and others, 1950). It had a conductivity of $< 5.10^{-7} \Omega^{-1} cm^{-1}$. It was tested frequently for traces of permanganate.

The water was refluxed in purified He for three hours. After distillation into the cell it had a conductance of $< 2.10^{7} \Omega^{-1} cm^{-1}$.

(D) Electrodes: Spectroscopically pure Ag wire, diameter 0.2 mm, was spot welded to W as follows: 3 mm of the wire was dipped into colloidal Pt solution and heated in a small (cold) flame to form an adherent deposit of Pt. Alternatively, the Pt was deposited electrolytically from a solution of H_2PtCl_6. The Pt coated end was spot welded to 0.5 mm W wire.

Other details concerning electrode preparation resemble those of Bockris, Conway and Mehl (1956) and are detailed in Bockris and Devanathan (1957).

(E) Circuit: The circuit is shown in fig. 8. A is a conventional cathodic polarizing circuit. B consisted of a 90 V battery source with a variable high resistance in series. The auxiliary electrode for the anodic charging was the Pt plate, and the low resistance (about 10Ω) between this and the test electrode ensured that the current was controlled only by the high resistance, so that it remained constant during an anodic charging pulse.

Change-over from the cathodic to anodic circuit was affected in a time interval of about 2μsec, by means of a special switch S, described by Mehl, Devanathan and Bockris (1958).

(F) Procedure:

(1) The cell was allowed to stand in contact with chromic-sulphuric acid for 2 - 4 days. The acid was removed, the cell filled with distilled water and emptied about ten times and care was taken to wash out acid in the sintered discs by streaming distilled water through them under pressure.

(2) Before each run the cell was allowed to stand in nitric-sulphuric acid mixtures for 2 - 3 hours. The above washing procedure was repeated. The cell was thereafter rinsed three times with equilibrium water.

(3) The cell was filled with equilibrium water. The auxiliary "bridge" connections were made to the cell, the cap removed and the electrodes sealed in thin glass protecting bulbs placed in position in the cap, whereafter the latter was returned to the cell.

(4) The conductivity water was removed under de pressure and the distillation of water into the test electrode compartment and in He commenced. The distillate was allowed to fill the cell and drain away. This procedure was repeated until the water had the specific conductance of $2.10^{-7} \Omega\ cm^{-1}$. The cell was filled completely with conductance water distilled into the cell in helium and again drained.

(5) A small quantity of the preëlectrolyzed NaOH solution was admitted to the cathode compartment and diluted by distilling in more conductance water.

(6) The solution was admitted into the reference electrode and anode compartments and preëlectrolyzed on a Ag electrode at a c.d. of 10^{-1} amps cm^{-2} for 36 hours, while purified oxygen-free He was bubbled through cathode and anode compartments.

(7) The preëlectrolysis current was interrupted by raising the preëlectrolysis electrode above the level of the solution; one of the bulbs surrounding a spherical Ag electrode was broken cautiously (to avoid breaking the stem) under the solution with the aid of a glass probe in the cell, connected to the exterior by means of a slip joint lubricated with conductance water. On this electrode, H_2 overpotential measurements were carried out over the c.d. range 10^{-2} - 10^{-7} amps cm^{-2} (the sphere was positioned so as almost to touch the Luggin capillary). These measurements were unsatisfactory, the galvanostatic measurements were not carried out, or preëlectrolysis was continued for a further period, until satisfactory η-log i current density relations were obtained, indicating a satisfactory degree of removal of impurities and depolarizers from the solution.

(8) An auxiliary cylindrical Pt electrode was lowered into position around an Ag electrode.

(9) The test electrode was polarized to the desired steady cathodic potential, and the change-over switch pressed (S, Fig. 8), the anodic circuit having been previously adjusted so that the desired constant anodic current would be thereupon impressed upon the electrode.

(10) The potential-time relation was registered on an oscilloscope (Tektronix 535) with preamplifier (53-54D, Tektronix). To avoid excessive drain from the cell through the preamplifier, an attenuator probe, with an input impedance of 10 MΩ was used between the test electrode and the preamplifier.

(11) The transients were recorded on an Exakta camera with short focus attachment (f = 1.9; exposure 1/10 sec approx.). Persistence of the image made use of a synchronization device unnecessary.

(12) The transients were traced onto graph paper at a magnification of 50 times that of the oscilloscope screen size.

6. RESULTS

(A) Typical relations

The Tafel plot for the hydrogen evolution on silver in aqueous 0.1 N NaOH solution is reproduced in Fig. 9. The Tafel constants were found to be $b = 0.124 \pm 0.001$ and $i_o = 10^{-6.5 \pm 0.1}$ as mean of ten results.

In Fig. 3 are shown a typical pair of charging curves. The number of coulombs required to dissolve off the adsorbed atomic hydrogen under various conditions of polarization were obtained from each set of

curves as follows. From the curve of type (I) (transient starts from cathodic condition) the capacity C of the electrode system was calculated from the gradient of the charging curve in its linear region at low times, i.e., before the commencement of any dissolution of adsorbed hydrogen. A number of these points was measured (front silvered mirror and set square) for both curves of type I (see above) and type 2 (transient starts at a potential anodic to the reversible H_2 electrode). The currents i_F and i_{an} were calculated from equations (8) and (11) for various potentials using the previously obtained value for C which was assumed to be constant throughout the potential range. (Errors involved in this assumption are discussed below.) Fig. 4 shows these currents plotted against the potential. A plot of the difference in these values against the potential is shown in Fig. 5. The dissolution of the adsorbed atomic hydrogen is assumed to be complete when the difference of i_F and i_{an}, namely, the current function of Fig. 5, becomes insignificant. The same difference in current densities, plotted against the time required to attain the respective potentials in the case of the first type of charging curve, is shown in Figs. 6 and 7. Q_H is obtained from the area under the plots examplified by these figures (cf. Section 4, equations (13) and (14)).

(B) Q_H as a function of the anodic current density

In Table 1 is shown the results for Q_H at a constant cathodic polarizing current density of 10^{-3} A. cm^{-2} for current densities of anodic charging from 5.10^{-3} to 4.10^{-1} A. cm^{-2}. The results are presented graphically in Fig. 10. Q_H becomes constant at about 55 μC.cm^{-2} when

the anodic c.d. exceeds about 200 $A.cm^{-2}$. These results show a similar variation with anodic c.d. to that found on Pt both by the present workers and by Breiter, Knorr and Völkl (1955). As in the case of platinum, the asymptotic value at high anodic c.d., i.e. when the value of Q_H had become independent of the charging time, is taken as the amount of hydrogen on the electrode, unaffected by readsorption from the solution or from bubbles.

TABLE 1

APPARENT COULOMBS FOR REMOVAL OF H ON Ag DURING CATHODIC POLARIZATION AT 10^{-3} A. cm^{-2}

Anodic c.d. for charging	Apparent coulombs	No. of independent sets of experiments on which result based
5	152	4
20	126	6
40	117	4
60	97	3
100	68	4
150	80	2
200	103	3
250	55	2
300	45	2
350	50	3
400	60	3

(C) Q_H as a function of cathodic current density

Results obtained at various cathodic c.d.'s at a constant anodic charging c.d. of 100 mA. cm^{-2} are given in Fig. 11. Q_H varies linearly with the logarithm of the cathodic c.d.

(D) Q_H as a function of poison concentration

The cathodic c.d. was 10^{-3} A. cm^{-2} and the anodic c.d. was 200 mA. cm^{-2}. Arsenious oxide was used as the poison. The As_2O_3 concentration was varied from 10^{-6} to 10^{-4} moles per litre. Change of As_2O_3 from zero to 10^{-4} moles per litre caused a 250% increase in the surface hydrogen concentration.

7. DISCUSSION

(A) Validity and accuracy of the method

(1) Evaluation of Q_H

The hydrogen on the electrode surface is given by means of the integral

$$Q_H = \int_0^{t_\infty} i_{H,\theta}\, dt, \tag{15}$$

whereas in the above described method, the integral

$$\int_0^{t_\infty} i_{H,\theta} \left(1 - \frac{i_{an}}{i_{H,\theta}}\right) dt \tag{16}$$

is used for the evaluation. It is necessary, therefore, to analyze the error thereby introduced.

In Figures 3, 4 and 6 and 7 are shown, respectively, charging curves for Ag in 0.1 N NaOH; the derived curves of $i_{H,\theta} + (1 - \theta)i_{an}$ and i_{an} as a function of potential, and the corresponding relation of $i_{H,\theta}\left[1 - (i_{an}\theta/i_{H,\theta})\right]$ as a function of time.

Referring to the points on Fig. 4 by the number there given, it is clear that values of $i_{H,\theta}\left[1 - (i_{an}\theta/i_{H,\theta})\right]$ are effectively free of error up to point 6. At point 7, the small error introduced into the plot can be calculated as follows. The "error term" in equation (13) is:

$$\frac{i_{an\theta}}{i_{H,\theta}} = \frac{1}{1 + \Delta/i_{an}\theta}, \qquad (17)$$

where Δ is defined in Section 4.

For point 7, of Fig. 4, the error term has the numerical value: $1/(1 + 1.9/\theta_{(7)})$. Now $\theta_{(7)}$, i.e. the coverage with H corresponding to point 7, can be evaluated with negligible error because the foregoing point 6, 5, etc., yield data free from error ($i_{an} \rightarrow 0$). Subtracting the Q_H up to 7 from the total, one obtains 24 coulombs of charge which correspond to the H still to be removed from one cm^2 of the electrode (Veselovsky, 1939). The ratio of real to apparent surface area of Ag is not less than 2 (Kortüm and Bockris, 1951). Removal of one true cm^2 of H from a Ag surface requires 238 microcoulombs. Hence, the maximum fraction of Ag covered with H at point 7 is $24/476 \simeq 0.05$. Hence, the value of the error term for point 7 is $1/(1 + 1.9/0.05) = 1/38 = 2.7\%$. Similar analysis for all further points to the right of 7 in Fig. 4, shows a smaller error than this owing to the rapid decrease of θ at times greater than that of point 7. The correct value of the

current density, $i_H\left[1 - (i_{an}\theta/i_{H,\theta})\right]$, is found to be never 3% less than i_H. The fact that in, e.g., Figs. 6 and 7, the relation plotted is $i_H\left[1 - (i_{an}\theta/i_{H,\theta})\right]$ and not i_H therefore implies an error of less than 3%.

(2) Capacity

In principle, it is necessary to use in, e.g., equation (12), the value of the double layer capacity from independent measurements at the various potentials for which $i_H - i_{an}\theta$ is evaluated. In the absence of such independent values of C_v, approximate values of the capacity can be obtained from the charging curves themselves at low times, e.g., for the second type of charging curve at low times, when $i_{an} = 0$, and

$$C_v\left(\frac{\partial V}{\partial t}\right)_{t,2} = i_a \qquad (18)$$

Alternatively, for the first charging curve at sufficiently low times,

$$C_v\left(\frac{\partial V}{\partial t}\right)_{t,1} = i_a \qquad (19)$$

The latter equation is more convenient to use because the potential-time relation at the commencement of the second charging curve is obtained in the presence of an appreciable IR drop, at high anodic c.d.'s.

The error introduced by the use of a C_v value independent of potential can be estimated as follows. Let it be assumed that the maximum capacity change which occurs over the potential region investigated is 100%, i.e., the percentage change observed on a Hg electrode during the transition from the extreme negative to the extreme positive

side of the electrocapillary maximum. (This assumption represents an overestimate of the probable change in C_v with V because, in the potential range of the transients, the potential is always in a region negative to that of the e.c.m., so that, by analogy with the behavior of Hg, the probable change is likely to be $< 20\%$.) The larger part of any change in C_v would be expected to occur in the most positive potential range (cf. Hg). Reference to Fig. 4 shows that this is the region at which most of the H has already been dissolved off and the curves i_{F_1} and i_{F_2} are rapidly coming close together. Let it be assumed that the capacity becomes 75% greater over the potential range + 200 to 600 V (cf. Fig. 4). Let the capacity increase linearly with potential over this range. Numerical computation upon these assumptions utilizing equation (12) and the results of Figs. 4 and 5 show that the resulting error on the overall result arising from the capacity changes assumed is less than 4% (results reported are too small).

A further error might arise from increase in capacity in the less positive potential region, e.g., that near the reversible potential. Here, the maximum reasonable capacity change will be much less than that discussed for the positive region. However, the effect on the results will be greater than effects in the positive region because the value of $(dV/dt)_2 - (dV/dt)_1$ is greater in the more negative potential regions (cf. equation (12)). Let it be assumed, referring to the typical results in Figs. 4, 6 and 7, that the capacity increases linearly with potential by 25% between the reversible potential (V = 0) and that of V = + 200 mV. The resulting computed error is about 10% (reported results too low). The total from the reasonable maximum capacity change is hence some 14%

for the example of Figs. 4, 6 and 7. Application of a similar analysis to charging curves at other potentials shows a similar percentage error for the portion at lower potential. The total error arising from possible capacity changes may be assumed to be less than 20% (stated results too small).

(3) Partial pressure of H_2 in solution

He is bubbled through the solution in the test electrode compartment during the measurements so that the reference electrode, and the test electrodes are under different partial pressures of H_2, However, this is true only of the bulk of the solution. In the vicinity of the test electrode during anodic charging, the solution is likely to be saturated with H_2, due to the evolution of H_2 during the cathodic polarization which precedes the anodic pulse. Suppose this pressure were to fall to 1/10 of atmospheric pressure, due to presence of He. The potential of the test electrode in the absence of current would become 29 mV more positive than that in contact with H_2 at 1 A. The actual change is likely to be negligible for reason stated.

(B) Degree of coverage on silver in alkaline solution

The results for the number of coulombs required to ionize the adsorbed hydrogen present per unit area of the electrode under steady state cathodic hydrogen evolution are given in Table I as a function of anodic current density. The asymptotic value free from errors of read-sorption is some 50 μ C.cm^{-2} for an overpotential of - 400 mV, in 0.1 N

NaOH. Results at other overpotentials are given in Fig. 11. Assuming that the apparent area is twice the real area, one has some 25 μ C. cm^{-2}. This (see above) indicates a θ value of about 10% under the stated conditions.

8. STUDIES ON NICKEL

Ni electrodes find extensive application in strongly alkaline solutions and therefore this system was selected for study.

(A) Ni electrode

B.D.H. nickel rod fitted with a polythene sleeve was used as the test electrode. A polythene rod 1/2 in. diam. and 2 in. long was drilled axially to an int. diam. of 3/32 in. A nickel rod 4 in. long and 1/8 in. diam. was then forced through the hole in the polythene rod to obtain a water-tight fit. The polythene-covered end was machined flat so as to expose only the area of cross-section (0.083 sq. cm.).

(B) Cell and Auxiliary Electrodes

The cell (see fig. 12) was made of Pyrex glass and had three compartments. The test electrode was a B34 test-tube and was connected on either side to B14 test-tubes, which served as the anode in the reference electrode compartments. The diffusion of oxygenated anolyte into the test chamber was prevented by means of a sintered disc inserted between the compartments. The Luggin capillary from the reference electrode compartment was centered vertically upwards in the test chamber.

Provision was made to admit purified hydrogen into the test and reference electrode compartments through capillary tubes.

The anode compartment was fitted with a bright sheet of platinum and this was used for the cathodic polarization of the test electrode. The reference electrode was the hydrogen electrode prepared in the conventional manner. In the test electrode compartment were two electrodes; the polythene-sleeved nickel electrode was surrounded by a platinum cylinder 3/4 in diam. and 2 in. long. The platinum cylinder was used as the cathode, first during the pre-electrolysis and later, for the anodic polarization of the test electrode. These two electrodes were mounted on a polythene stopper which fitted tightly the B34 cone. The B34 cone and the reference electrode had bubblers containing distilled water to prevent diffusion of air into the cell.

(C) Electrolyte

Sodium hydroxide solution (2 N) was used as the electrolyte. Merck's pellets (extra pure quality) of sodium hydroxide were dissolved in conductivity water, which was prepared by alkaline permenganate oxidation of distilled water, followed by two distillations from an all-glass well-seasoned Bara still. The specific conductivity of this water was 0.4μ mhos.

(D) Purification of Hydrogen

Commercial electrolytic hydrogen was deoxygenated by passage through a palladized asbestos furnace. The gas was bubbled through water

and fed by polythene tubing to the test and reference electrode compartments. The rate of bubbling of hydrogen was easily controlled using plastic aquarium-type regulator valves.

(E) Electrical Circuit

The circuit used is given in Fig. 13. There were two polarizing circuits - one to polarize the Ni electrode cathodically and the other to polarize it anodically. The Ni electrode was first polarized cathodically and the change to anodic polarization effected instantaneously. This was achieved by using a special relay with a rise time of 10^{-7} sec. The cathodic polarizing circuit was never shut off. On switching on the anodic current by means of this relay, the test electrode became anodically polarized. Since the anodic current was at least a hundred times larger than the cathodic current the effect of the latter is negligible when calculating the anodic c.d. Leakage of the anodic pulse into the cathodic polarizing circuit was prevented by including a high-capacity choke.

For cathodic polarization, a conventional battery-powered circuit was used. The current through the circuit was measured by a Cambridge unipivot multirange microammeter. For very small currents, the potential across a standard 10 x 1 megohm resistor was measured with a Doran valve potentiometer, and the current calculated.

For anodic polarization the current source was a high-capacity 90 V battery. The current through the circuit was varied by adjusting the resistance in a resistance box. Since the resistance between the platinum cylinder and the test electrode was negligibly small the anodic current was controlled only by the resistance box.

(F) The Relay

A Western electric relay using mercury-wetted contacts in high-pressure nitrogen (type 2758) was used. It was operated by a 90 V battery and a microswitch with a suitable filtering circuit.

(G) Measuring and Recording Apparatus

(a) Potentiometer: Doran pH meter reading to $\pm$ 0.0005 V;

(b) Oscilloscope: Tektronix type 535 with 53/54 D high-gain differential d.c. amplifier;

(c) Camera: Exakta Varex IIA fitted with Makro Kilar D 1:2.8/4 cm.

(H) Procedure

The cell was cleaned with dichromate + sulphuric acid mixture and washed thoroughly with distilled water. It was rinsed several times with sodium hydroxide before introducing the solution. The exposed area of the nickel electrode was scraped with a clean grease-free blade to give a bright surface. The solution was pre-electrolyzed at 25 mA (power pack) for 3 - 4 hrs. using the bright platinum sheet as anode and the platinum cylinder as cathode. During pre-electrolysis as well as during measurements, a steady stream of hydrogen was bubbled through the test and the reference electrode compartments.

After pre-electrolysis, hydrogen overpotential measurements were carried out over the c.d. range 10^{-1} to 10^{-6} A. cm^{-2}, the test electrode being fitted so as almost to touch the Luggin capillary. Galvanostatic anodic charging was then carried out. The test electrode was polarized

cathodically at any desired c.d. An anodic pulse of predetermined magnitude was then passed through the nickel electrode by pressing the microswitch. The Ni electrode immediately became anodic and the rate of change of potential from cathodic to that of oxygen evolution was registered on the oscilloscope. The oscilloscope trace was photographed on a fast green-sensitive recording film using the Exakta camera fitted with the close-up lens (exposure for about 3 sec at B). For any combination of cathodic and anodic c.d., 2 oscilloscope traces, the normal and the compensation, were obtained. The normal curve was that obtained starting from the equilibrium overvoltage at any cathodic c.d. The compensation curve was obtained immediately after the normal curve. When the microswitch was released, there was only cathodic polarization of Ni and the potential of the electrode gradually changed from the anodic towards the cathodic side. The compensation curve was produced by switching on the anodic polarization circuit when the potential of the Ni electrode had fallen from + 25 to 50 mV, as measured by the potentiometer. The compensation curve obtained starting at + 25 mV was nearly identical with that obtained starting at + 50 mV, indicating the absence of adsorbed hydrogen on the surface between these potentials. This is also supported by the low values for the capacity (20 μ F), calculated from the compensation curve. The film was placed in an enlarger and the oscilloscope trace was drawn on cm. graph paper at a linear magnification of four times the oscilloscope screen size. The gradients of the normal and compensation curves were found at various points by graphical differentiation using a front-silvered mirror and set square. All measurements were carried out at room temperature (26 - 28° C).

9. RESULTS

(A) Overpotential Results

Overpotential measurements on Ni cathodes in alkaline solutions have been published only for dilute solutions (Bockris and Thacker, 1959). These results, which were obtained with hydrogen-saturated wire electrodes, show that overpotential decreases with increase in alkali concentration. Our results are for electrodes which had not been previously heated in a hydrogen atmosphere. Hence, one would expect lower energies of activation for the discharge of H^+ ion. This, consequently, is another factor causing low overpotential values. Our results are in accordance with expectations and are shown in Fig. 14. The reproducibility was $\pm$ 2 mV at low c.d.'s rising to $\pm$ 10 mV at high c.d.'s.

(B) Calculation of q_H

In Fig. 15 are shown a typical pair of galvanostatic charging curves. The term $(i_H - i_{an}\theta)$ at any potential was calculated from the gradients of the normal and the compensation curves using eqn. (16). A plot of $(i_H - i_{an}\theta)$ against t_N, where t_N is the time required to reach this potential on the normal curve, is given in Fig. 16. The area under the curve gives the quantity of electricity (q_H) required to dissolve all the adsorbed atomic hydrogen which was present on the cathodically polarized surface.

(C) Variation of q_H with Anodic c.d.

This variation at a constant cathodic c.d. of 10^{-4} A. cm^{-2} is given in Fig. 17. It is seen that q_H has a constant value of about 55μC $cm.^{-2}$ at anodic c.d.'s exceeding 0.6 A cm^{-2}. This shows that re-adsorption of hydrogen is negligible at anodic c.d.'s above 0.6 A. $cm.^{-2}$. The results were reproducible to $\pm$ 5μC except in the regions where there was re-adsorption.

(D) Variation of q_H with Cathodic c.d.

To study this variation, the anodic c.d. was kept constant at 1 A. $cm.^{-2}$. At this value there is no re-adsorption of hydrogen. The results given in table 2 show that q_H values at cathodic c.d.'s exceeding 10^{-3} were very large and variant. This is evidently due to re-adsorption from hydrogen bubbles sticking to the electrode. This phenomenon has also been observed on noble metals by Breiter, Knorr, and Völkl (1955), and on Ag by Devanathan, Bockris and Mehl (1959/60).

(E) Degree of Coverage

For this calculation the roughness factor (r.f.) should be first obtained. This was calculated from the capacity of the electrode. The average value obtained for the capacity was 20μ F. Since the capacity of the Hg electrode under cathodic polarization has been shown by various workers to have a value of 16μ F, the roughness factor of our nickel electrode was 1.25.

TABLE 2

VARIATION OF q_H AND θ WITH CATHODIC c.d.

ANODIC c.d. = 1 A. cm.$^{-2}$

Cathodic c.d. (Acm^{-2})	η (mV)	q_H (μC)	θ
1.00×10^{-6}	10	18	0.045
1.00×10^{-5}	30	26	0.065
1.80×10^{-5}	37	26	0.066
3.00×10^{-5}	52	29	0.072
5.65×10^{-5}	70	42	0.104
1.00×10^{-4}	90	49	0.122
1.80×10^{-4}	121	72	0.179
3.00×10^{-4}	140	100	0.250
5.65×10^{-4}	166	121	0.303
1.00×10^{-3}	186	155	0.386
3.00×10^{-3}	242	1,050	2.62
1.00×10^{-2}	802	3,040	7.60
1.00×10^{-1}	460	10,440	25.55

Calculations show that the charge required to dissolve the hydrogen adsorbed on 1 sq. cm. of Ni assuming a 1:1 H:Ni ratio is 326 μC. Hence, the charge required to dissolve a monolayer of hydrogen from 1 sq. cm. of apparent area is equal to $326 \times 1.25 = 400 \mu C$.

Values of θ calculated in this way are recorded in column 4 of Table 2.

10. STUDIES ON COPPER

Some experiments were carried out on copper in 0.2 N NaOH using the same technique and apparatus used for silver. As expected the number of coulombs for the dissolution of hydrogen decreased asymptotically as the anodic current increased. The results are given in Table 2.

TABLE 3

Anodic cd. $mA/cm.^2$	Q_H $C/cm.^2$
5	300
250	180
400	40

11. MECHANISM OF THE HYDROGEN EVOLUTION REACTION ON SILVER

(A) Dissolution of H at Cathodic Potentials

According to Figs. 4 and 5, the dissolution of H commences at potentials of about -150 mV with respect to the reversible H_2 electrode. This is not a thermodynamic anomaly because the electrode during anodic charging is not under reversible conditions. Consideration of this potential of dissolution gives information concerning the rate-determining reaction for the hydrogen evolution reaction at Ag in 0.1 N NaOH.

Suppose that this step is the rate of proton discharge from water molecules (the following desorption step being combination of adsorbed H atoms). Then, if θ_η is the degree of coverage at the overpotential corresponding to the cathodic current density obtaining before anodic charging commenced, and θ_R that corresponding to the reversible potential,

$$i_c = i_o\left[\frac{1-\theta_\eta}{1-\theta_R}\,e^{-\alpha\eta F/RT} - \frac{\theta_\eta}{\theta_R}\,e^{(1-\alpha)\eta F/RT}\right], \qquad (20)$$

where i_c is the steady cathodic current density before anodic charging, i_o is the exchange current density, and η is the steady state overpotential corresponding to time t = o, i.e., the time of commencement of anodic charging.

When the steady cathodic current is replaced by the anodic charging current, this is at first used largely to bring about rapid change to the potential of the electrode, i.e. as a capacitative current. During this early part of the anodic sweep, it may be assumed that the value of θ lags behind the steady state coverage corresponding to the (rapidly changing) η_t. Let it be assumed as an approximation that, in the period of the anodic pulse referred to, $\theta = \theta_{t=o}$. From (20), the current, i_c, becomes anodic when (assuming θ_η and θ_R are not near to I),

$$\frac{\theta_{t=o}}{\theta_R}\,e^{(1-\alpha)\eta_t F/RT} > e^{-\alpha\eta_t F/RT} \qquad (21)$$

i.e.

$$\eta_{t,\text{dissolution}} = \frac{RT}{F}\ln\frac{\theta_R}{\theta_{t=o}} \qquad (22)$$

where $\eta_{t,\text{dissolution}}$ is the electrode potential, with respect to the

corresponding thermodynamically reversible potential, at which dissolution of H commences during the anodic sweep.

From Fig. 11,

$$Q_{H,R} \triangleq 10^{-.75};\ Q_{H,\eta} = 10^{2.1} \qquad (23)$$

Hence, $\eta_{t,dissolution} = -80$ mV, in reasonable agreement with the - 100 to - 200 mV observed.

Assumptions concerning the rate-determining step other than that suggested (see above) are not consistent with the potential at which dissolution becomes appreciable.

(B) Variation of Coverage with Potential

On the basis of the above stated rate-determining step, it can be shown that:[8]

$$\theta_\eta = Ke^{-\eta F/4RT} \qquad (24)$$

where K is a constant, i.e.:

$$\frac{\partial \eta}{\partial \log \theta_\eta} = -4 \times 2.303\ RT/F \triangleq -0.24 \text{ at } 25^\circ C \qquad (25)$$

The results of Fig. 9 are qualitatively in agreement with this equation and yield $\partial\eta/\partial \ln \theta = -0.31$. The results at the highest overpotentials show a tendency to decrease in slope, i.e., for θ_η to become decreasingly dependent upon potential. If the electrochemical mechanism were the rate-controlling step in the h.e.r. (Bockris, 1954) on Ag, $\theta_\eta \neq f(\eta)$. The tendency observed may, therefore, indicate the commencement of partial control by the $H^+ + H_{ads} + e_o \rightarrow H_2$ reaction at the highest overpotentials examined.

The results of Fig. 11 are inconsistent with a rate-determining step on Ag other than that of porton discharge, followed by non rate-determining desorption by means of combination of adsorbed atomic H. Thus, were the desorption step the non rate-determining reaction $H^+ + H_{ads} + e_o^- \rightarrow H$, θ_η would be independent of potential (Bockris, 1954). Were the rate-determining step $2H_{ads} \rightarrow H_2$.

$$\theta_\eta = K' e^{-\eta F/RT} \qquad (26)$$

at low coverages, i.e. $\partial \eta / \partial \log \theta = -2.303\ RT/F \simeq 0.06$ at 25°C, in marked disagreement with the results of Fig. 11.

These observations hence support a rate-determining discharge, followed by atomic combination as the mechanism of the evolution of H_2 on Ag in 0.1 N NaOH. This observation supports the mechanism suggested from determination of the stoichiometric number (Pentland, Bockris and Shelden, 1957).

A rate-determining electrochemical desorption reaction has been indicated for the hydrogen evolution reaction in acid solutions (Pentland, Bockris and Shelden, 1957; Conway and Bockris, 1957). (However, as a result of potentiostatic studies in acid solutions a rate-determining discharge with descrption by the electrochemical reaction has also been reported (Gerischer and Mehl, 1955)). A change from a rate-determining step of electrochemical desorptien to that of slow discharge upon passage from acid to alkaline solution has been indicated as a probably general tendency (Pentland, Bockris and Shelden, 1957), because discharge from water molecules would be expected to be associated with a heat of activation considerably greater than the corresponding discharge from protons

(Parsons and Bockris, 1951; cf. also Frumkin, 1952).

12. MECHANISM OF THE HYDROGEN EVOLUTION REACTION ON COPPER

The Tafel slope, stoichiometric number and the order of magnitude of the coverage with hydrogen atoms suggest that the mechanism on copper is also the same as that on silver, namely slow discharge followed by recombination.

13. MECHANISM OF THE HYDROGEN EVOLUTION REACTION ON NICKEL

Our measurements of θ at various c.d.'s on Ni in alkaline solutions enables us to determine the stages involved in the cathodic evolution of hydrogen. The first step in the evolution of hydrogen must be the discharge of a hydronium ion (path A), or a water molecule (path B), to yield adsorbed atomic hydrogen on the Ni surface:

(A) $$H_3O^+ + Ni + e = NiH + H_2O,$$

(B) $$H_2O + Ni + e = NiH + OH^-.$$

In strongly alkaline solutions (2 N.) path A is unlikely as the concentration of hydrogen ions is negligibly small and it appears that the discharge of a water molecule is the first step in the formation of adsorbed atomic hydrogen.

The removal of this adsorbed atomic hydrogen from the surface could proceed either by electrochemical desorption (path C), or by Tafel recombination (path D):

(C) $$NiH + H_3O^+ + e = H_2 + H_2O + Ni,$$

(D) $$NiH + NiH = H_2 + 2Ni.$$

14. RATE-DETERMINING STEP

Since for reasons already given, path A is unlikely, any one of the steps B, C or D could be rate-determining. It has been shown that when discharge is the rate-determining step the stoichiometric number is 2. This number v can be determined using the equation,

$$v = 2i_o \frac{RT}{F} \left(\frac{d\eta}{di_c}\right)_{\eta \to o}, \qquad (27)$$

or, approximately, from the point at which the overpotential deviates from the Tafel line due to the ionization of hydrogen. v is then given by the equation,

$$v = V'/0.038, \qquad (28)$$

where V' is the potential at which there is the break in the overpotential curve. We have calculated v by both methods and found the stoichiometric number to be 2. Therefore, the rate-determining step in the evolution of hydrogen on nickel in strongly alkaline solutions is slow discharge from a water molecule. If slow discharge is the rate-determining step, it is reasonable to expect small values for θ. Fig. 18 shows θ plotted as a function of log c.d. It will be seen that the values indicate low coverage up to a c.d. of 5×10^{-4} A. cm^{-2}. Thereafter, there is an extremely rapid rise which we attribute to re-adsorption from hydrogen bubbles sticking to the electrode surface.

15. DESORPTION MECHANISM

The desorption of adsorbed hydrogen atoms can proceed through Tafel recombination or by an electrochemical mechanism. If Tafel recombination is the desorption step, then

$$i_c = k_T \theta^2 \tag{29}$$

Electrochemical desorption can be fast, or slow and rate-determining. For the latter case,

$$i_c = K_E \theta. \tag{30}$$

For fast electrochemical desorption, θ should be independent of the c.d. A plot of log i against log θ would therefore give a gradient of zero for fast electrochemical desorption, 1 for slow electrochemical desorption and 2 for Tafel recombination. Our results plotted in this way are given in Fig. 19. The gradient is two, thus proving that Tafel recombination is the desorption step. It should also be noted that this result is not affected by the value of roughness factor assigned in the calculation of θ. For a different value only the intercept is changed.

The value, $10^{-2.2}$ A. cm^{-2} of i_c at log $\theta = 0$ gives the rate constant in A, for the recombination step.

16. THE TAFEL EQUATION

The Tafel equation is based on the formula

$$i = i_o \exp(-\alpha \eta F/RT). \tag{31}$$

In this equation, i_o is the rate of discharge of hydrogen ions on 1 sq. cm. of the electrode surface when $\eta = 0$. It is apparent that this i_o, commonly called the exchange current, is only a partial current, since even at the reversible potential there is some coverage with atomic hydrogen. In order to get the rate constant for the discharge of hydrogen ions it is necessary to correct for the coverage. We therefore modify the Tafel equation to read

$$i_c = \vec{i}_o(1 - \theta) \exp(-\alpha \eta F/RT), \tag{32}$$

where θ is the coverage at the overpotential η. Here i_c is the current through 1 sq. cm. of apparent area, the fraction θ being blocked for the discharge of H^+ ions (except, of course, for an electrochemical desorption process); $\vec{i}_o$ is the c.d. for the discharge process on a hydrogen-free surface when $\eta = 0$. For this reason, we have not calculated the Tafel constants from the graph of η against log i_c (Fig. 14). A true value for the constants could be obtained only after correction for the degree of coverage. We have therefore plotted η against log $\left[i_c/(1 - \theta) \right]$ (Fig. 20). It will be seen that above 75 mV the graph is a straight line giving $\vec{i}_o = 10^{-4}$ A cm.$^{-2}$ and b = 38 mV.

The deviation from the Tafel line at low cathodic c.d.'s has been attributed to the reverse reaction (i.e. ionization) becoming appreciable. If, therefore, a quantitative correction could be applied for this ionization current, then all the points should fall on a straight line when η is plotted against log $\left[i_c(\text{corr.})/(1 - \theta) \right]$.

The measured cathodic current is the difference between the discharge and the ionization currents, i.e.,

$$i = \vec{i} - \overleftarrow{i}. \qquad (33)$$

$\overleftarrow{i}$ must depend on θ and the overpotential. It may be expressed in terms of $\overleftarrow{i}_o$ by the equation

$$\overleftarrow{i} = \overleftarrow{i}_o \theta \exp\left[(1 - \alpha)\eta F/RT \right]. \qquad (34)$$

Hence, the complete equation for the cathodic current is obtained from eqn. (32), (33) and (34) and is given by

$$i_c = \vec{i}_o(1 - \theta) \exp(-\alpha\eta F/RT) - \overleftarrow{i}_o \theta \exp\left[(1 - \alpha)\eta F/RT \right]. \qquad (35)$$

This equation may be contrasted with an equation by Breiter, Knorr and Völkl (1955),

$$i_c = i_o \left(\left(\frac{1 - \theta}{1 - \theta_R} \right) \exp \left(\frac{\alpha \eta F}{RT} \right) - \frac{\theta}{\theta_R} \exp \left[\frac{(1 - \alpha) \eta F}{RT} \right] \right). \quad (36)$$

If one puts $\theta = \theta_R$ and $\eta = 0$ in this equation, $i_c = 0$, which means that $\vec{i} = \overleftarrow{i} = i_o$. As we have pointed out earlier, i_o cannot be the true c.d. as it is only a partial current on 1 sq. cm. of a partly covered surface. In contrast, our equation reduces to

$$0 = \vec{i_o}(1 - \theta_R) - \theta_R \overleftarrow{i_o}. \quad (37)$$

$\overleftarrow{i_o}$ can be equal to $\vec{i_o}$ only if $\theta_R = \frac{1}{2}$. However, if θ_R is known, it is possible to calculate $\overleftarrow{i_o}$ from $\vec{i_o}$ by using the above equation. θ_R is determined by extrapolating a graph of θ against η to $\eta = 0$. A straight line was obtained for overpotential values less than 50 mV and θ_R was found to have a value of 0.04.

Therefore,

$$\overleftarrow{i_c} = \vec{i_o}(1 - 0.04)/0.04 = 240 \mu A \text{ cm.}^{-2}. \quad (38)$$

We can check the validity of eqn. (35) in the following manner. We write our equation in the form,

$$\frac{i_c + \overleftarrow{i_o} \theta \exp \left[(1 - \alpha) \eta F / RT \right]}{1 - \theta} = \vec{i_o} \exp \left(- \frac{\alpha \eta F}{RT} \right), \quad (39)$$

and plot the log of the left-hand term against overpotential (Fig. 20). It will be seen that all the points lie on the same line with $\vec{i_o} = 10^{-5}$ A cm.$^{-2}$ and the slope b = 88 mV (as before). The data used in this calculation are recorded in Table 4.

A perusal of column 5 shows that the ionization current is approximately 10μA throughout the range covered. At a c.d. of 10^{-4} A cm.$^{-2}$ it forms 10% of the total current, thus confirming Bockris and Potter's observation that departure of the Tafel line from linearity is due to the

ionization current. The results and the graph confirm the validity of eqn. (35).

Up to a c.d. of 10^{-3} A cm.$^{-2}$, desorption proceeds by Tafel recombination. The double charging method cannot be applied to determine θ at higher c.d.'s because of errors arising from re-adsorption of hydrogen.

TABLE 4

I	II	III	IV	V	VI	VII
η(mV)	θ	$\frac{(1-\alpha)\eta F}{RT}=x$	e^{-x}	$\overleftarrow{i}_o\theta e^{-x}$	$\frac{i_c+\overleftarrow{i}_o\theta e^{-x}}{1-\theta}$	$\log\frac{i_c+\overleftarrow{i}_o\theta e^{-x}}{1-\theta}$
10	0.045	0.123	0.887	9.60	11.1	1.045
30	0.065	0.355	0.705	11.00	22.5	1.352
37	0.066	0.453	0.636	11.20	30.2	1.480
52	0.072	0.600	0.549	9.45	42.5	1.628
70	0.104	0.833	0.436	10.80	75	1.875
90	0.122	1.09	0.336	9.82	125	2.097
121	0.179	1.45	0.237	10.18	232	2.365
140	0.250	1.70	0.183	11.0	414	2.617
166	0.303	2.03	0.131	9.5	824	2.916
186	0.386	2.30	0.100	9.32	1630	3.212

17. THE CONDITIONS NECESSARY FOR THE SUCCESSFUL APPLICATION OF THE GALVANOSTATIC METHOD

A detailed analysis (ref. ONR Report No. 3) showed that the following conditions must be fulfilled.

(A): The reversible potential of the metal must occur at a potential more positive than 100 mV referred to the reversible hydrogen potential in the same solution in order to avoid the presence of H on the surface at potentials anodic to that of the reversible H_2 electrode.

(B): The time of the sweep must be long enough so that the hydrogen has sufficient time to dissolve off. This is at least $0.3 \frac{dt}{dV}$ sec.

(C): On the other hand, the sweep time must be less than $10^{-5}/i_c$ sec., where i_c is the cathodic current density existing before the sweep, in order to avoid appreciable loss of H by combination during the sweep.

(D): The anodic c.d. must be sufficiently high so that the effect of the readsorption of hydrogen is negligible. Approximately the order of the lowest values in 100 ma. $cm.^{-2}$

Consideration of these conditions in respect to the known kinetic and thermodynamic parameters for a range of metals indicates that the galvanostatic method may successfully be applied only to Ag, Cu, in acid and alkaline solutions, and to a wide range of transition metals in alkaline solutions; and the noble metals. (For these latter the oxide formation occurs at a potential much more positive than that of the reversible H_2 electrode and determinations can be made by a simple (non double pulse) coulometric method.

The main disadvantage of this method is, of course, its restricted applicability in acid solutions.

18. POTENTIOSTATIC METHOD

In the potentiostatic method (Slygin and Frumkin, 1935, 1936), the cathodic potential during the steady state evolution of hydrogen is changed in about one microsecond to an anodic potential which is sufficiently noble to correspond to the complete absence of H. The dissolution of adsorbed hydrogen will be complete in a time less than 1 millisec., and will be uninfluenced by passivation of the metal, which would not commence, in most practical solutions, until after 1 sec. or more.

However, when the anodic pulse is passed, it causes not only the dissolution of the adsorbed hydrogen, but also the dissolution of the substrate, so that it is necessary to ascertain the conditions of i_H, P_{H_2}, c.d., and order of concentration of atomic hydrogen on the surface, whereby a measurable anodic pulse of H, clearly separated from the pulse for the metal dissolution, would be expected.

After the switching in of the anodic potential V, let i be the total current at any instant, i_H the current for the dissolution of adsorbed H, i_{an} that for dissolution of the metal which takes place at a potential V, C the capacity of the double layer, and t the time.

Then:

$$i = i_H + i_{an} + C \frac{dv}{dt} \qquad (40)$$

After charging of the double layer is complete,

$$i = i_H + i_{an} \qquad (41)$$

If $(\theta_H)_t$ is the fraction of the surface covered with adsorbed

hydrogen at time t:

$$i_H = (i_o)_H \frac{(\theta_H)_t}{(\theta_{rev})_H} e^{\frac{\alpha \eta F}{RT}} \tag{42}$$

and

$$i_{an} = (i_c)_{an} \left[1 - (\theta_H)_t\right] e^{\frac{\alpha_{an} \eta_{an} F}{RT}} \tag{43}$$

The potential terms are constant, whereupon:

$$i_H = I_H (\theta_H)_t \tag{44}$$

where

$$I_H = \frac{(i_o)_H}{(\theta_{rev})_H} e^{\frac{\alpha_H \eta F}{RT}} \tag{45}$$

and

$$i_{an} = I_{an} \left[1 - (\theta_H)_t\right] \tag{46}$$

where:

$$I_{an} = (i_o)_{an} e^{\frac{\alpha_{an} \eta_{an} F}{RT}} \tag{47}$$

also

$$i_H = - FZ \frac{d(\theta_H)_t}{dt} = I_H (\theta_H)_t \tag{48}$$

From (44)

$$\therefore (\theta_H)_t = - \frac{FZ}{I_H} \frac{d(\theta_H)_t}{dt} \tag{49}$$

Or:

$$\frac{d(\theta_H)_t}{(\theta_H)_t} = - \frac{I_H}{FZ} dt \tag{50}$$

Hence,

$$(\theta_H)_t = (\theta_H)_o e^{\frac{-I_H t}{FZ}} \tag{51}$$

where $(\theta_H)_{t=o}$ is the coverage during the cathodic polarization.

Thus,

$$i_t = I_H(\theta_H)_o \, e^{\frac{-I_H t}{FZ}} + I_{an}\left[1 - (\theta_H)_o \, e^{\frac{-I_H t}{FZ}}\right] \tag{52}$$

$$= \left[I_H - I_{an}\right](\theta_H)_o \, e^{\frac{-I_H t}{FZ}} + I_{an} \tag{53}$$

$$\therefore \quad \frac{i_t}{I_{an}} = \left(\frac{I_H}{I_{an}} - 1\right)(\theta_H)_o \, e^{\frac{-I_H t}{FZ}} + 1 \tag{54}$$

The quantity I_H contains θ_{rev} (cf. equation (43)), and this can be expressed in terms of $\theta_{t=o}$, e.g., for a mechanism of hydrogen evolution

$H^+ + e_o \xrightarrow{\text{slow}} H_{ads}$; $2H_{ads} \xrightarrow{\text{fast}} H_2$ by means of the equation:

$$\frac{(\theta_H)_{t=o}}{\theta_{rev}} = e^{\frac{-\eta F}{4RT}} \tag{55}$$

If the cathodic overpotential during the cathodic polarization before the application of the anodic pulse is η_H then it can be shown (Bockris and Devanathan, 1959) that:

$$\eta = \left|\eta_H\right| + 0.1 \tag{56}$$

where η is the minimum allowable for the anodic overpotential in the anodic pulse.

Further,

$$\eta_{an} = \eta - e_{rev,M} \tag{57}$$

where $e_{rev,M}$ is the reversible potential of the metal in the given solution. Making the relevant substitution in (54), one obtains:

$$\frac{i_t}{I_{an}} = \left[\frac{(i_o)_H}{(i_o)_{an}} 10^{\frac{\eta}{0.059}\left\{\alpha_H + \frac{1}{4} - \alpha_{an}\left(1 - \frac{\theta_{rev,M}}{}\right)\right.} \left. - (\theta_H)_o \right] 10^{\frac{-(i_o)_H t}{2.303 F Z (\theta_H)_o}} \cdot 10^{\frac{\eta}{01.059}(\alpha_H + \frac{1}{4})} + 1 \qquad (58)$$

The nature of the plot of i_t against time for the cases $\frac{I_H}{I_{an}} > 1$, $\frac{I_H}{I_{an}} < 1$ are shown in Figs. 21 and 22 respectively. The area bounded by the exponential curve and the abscissae $i_t = I_{an}$ in both Figs. 21 and 22 is a measure of the dissolved atomic hydrogen (which is equivalent to the area under the curve).

To test whether the method would work for a particuler metal, a useful criterion is that $\frac{i_t}{I_{an}} \geqslant 10$ when $\frac{I_H}{I_{an}} > 1$, or $\frac{i_t}{I_{an}} \leqslant \frac{1}{10}$, when $\frac{I_H}{I_{an}} < 1$, at an arbitrary time of 10^{-5} sec. By fixing one of the variables $(\theta_H)_o$, η, t in equation (58) it is possible to express $\frac{i_t}{I_{an}}$ in terms of the remaining two in a three dimensional drawing. For a particular metal the values of $\frac{i_t}{I_{an}}$ for suitable combinations of η and $(\theta_H)_o$ are evaluated and the results may be plotted. Such a plot for nickel is shown in Fig. 23. The surface ABCDEF represents values of $\frac{i_t}{I_{an}}$ for any combination of η and $(\theta_H)_o$, when η ranges from 0.15 - 1.00 v. and (θ_H) from 10^{-3} - 1. The area ABF which lies below the surface $(\frac{i_t}{I_{an}} = \frac{1}{10} (\theta_H)_o, \eta)$ gives values of η and $(\theta_H)_o$, which fulfill the second criterion (i.e., $i_t/i_{an} \leqslant \frac{1}{10}$) and of course fixes the conditions under which the method would give results.

Construction of three dimensional diagrams (such as that of Fig. 3, ONR Report No. 3) showed that the following conditions exist for a satisfactory ratio of $\frac{i_t}{I_{an}}$ for $t < 10^{-5}$ sec. (Table 5).

It can be seen from these theoretical results that even for metals which appear to be possible very restrictive assumptions have to

TABLE 5

EXAMINATION OF POTENTIOSTATIC METHOD

FOR EVALUATION OF ADSORBED H

Ni	$\frac{i_t}{I_{an}} \leqslant 1/10$	when $(\theta_H)_o$ = 0.89 - 1.0 and η = 0.15 - 0.26 v.
Cu, Fe, Ag	No values of $(\theta_H)_o$ and η in chosen ranges, give $\frac{i_t}{I_{an}} \leqslant 1/10$	or $\frac{i_t}{I_{an}} \geqslant 10$
Pt	$\frac{i_t}{I_{an}} \geqslant 1/10$	when $(\theta_H)_o$ = 0 and η = 0.15 - 0.48
Au	$\frac{i_t}{I_{an}} \geqslant 10$	when $(\theta_H)_o$ = 0 - 1.0 and η 0.15 - 0.48 v.

be made for a successful application. Similar results appear likely for other metals, and the chances of success with the potentiostatic method are therefore not good (principally because of the difficulty of obtaining suitable $(\theta_H)_o$ - η combinations in practical ranges).

19. EXAMINATION OF OTHER POSSIBLE METHODS OF MEASURING SURFACE COVERAGE

(A) Direct measurement of the Adsorbed Hydrogen by Transfer from a continuous Rotating Wire Passing through Two Vessels

Consider a continuous wire which passes through two vessels, as shown in Fig. 24. Vessel A contains a solution in which the wire is cathodically polarized. B is a vessel containing a solution of identical composition, initially free from H_2. The wire is moved continuously

through A and B and through a "cleaning process" section, C. The speed of passage of the wire is such that there is (a) enough time for the wire to attain a steady state hydrogen evolution, and (b) insufficient time for significant evaporation to occur between the vessels A and B. The time to reach a steady state is given by the rise time of the circuit, i.e., 4 CR, where C is the double layer capacity and R the differential resistance of the electrode reaction, i.e., $\partial i / \partial \eta$, where $i = i_o e^{-\frac{\alpha \eta F}{RT}}$ for $\eta > 20$ mvs. The rise time at current densities of 10^{-3} amp. $cm.^{-2}$ can thus be shown to be about 1 μ sec. If the gap between the vessels is 0.1 cms. the speed of passage of the wire has to be about 50 ft. $sec.^{-1}$.

The orifices at D, D^1, E and E^1 are prevented from spillage by enclosing the arrangement in a compartment with variable pressure. At D and E, the wire passes through a capillary (or is subjected to jets of H_2) which limits the amount of electrolyte swept out to about one thousand layers (see below).

The originally H_2-free compartment B, contains a Ag cathode and sufficient Ag salt so that when the cathode is working Ag is deposited.

(B) Variation of the Permeation Rate with Current Density

The variation of the electrolytic permeation rate of H through a metal with current density can lead to a knowledge of the mechanism of the H_2 evolution reaction, and hence qualitatively the coverage. The corresponding experimental data can also be used to obtain a quantitative estimate of the coverage.

Consider electrochemical desorption to be the slow step in the H_2

evolution reaction. The relevant steps are (Bockris, 1954):

$$M + H^+ + e^- \underset{\overleftarrow{k_A}}{\overset{\overrightarrow{k_A}}{\rightleftharpoons}} M - H \qquad (59)$$

$$MH + H^+ + e^- \xrightarrow[\overrightarrow{k_c}]{\overleftarrow{k_A}} H_2\uparrow + M \qquad (60)$$

where the k's are the appropriate rate constants. Let V_1, V_2, V_3 be the rates of (59) in the forward direction, (59) in the backward direction, and (60) in the forward direction respectively. Then:

$$V_1 = \overrightarrow{k_A}\, a_{H^+}\, (1 - \theta)\, e^{\frac{-\eta F}{2RT}} = a_1(1 - \theta) \qquad (61)$$

$$V_2 = \overleftarrow{k_A}\, \theta\, e^{\eta F/2RT} = a_2\, \theta \qquad (62)$$

$$V_3 = \overrightarrow{k_c}\, a_{H^+}\, e^{-\eta F/2RT} = a_3\, \theta \qquad (63)$$

a_{H^+} is the activity of H^+ in solution in the double layer.

Assuming that the back reaction rate of (60) is negligible,

$$V_1 = V_2 + V_3 \qquad (64)$$

i.e.

$$a_1(1 - \theta) = a_2\, \theta + a_3\, \theta \qquad (65)$$

and

$$\theta = \frac{a_1}{a_1 + a_2 + a_3} \qquad (66)$$

If (60) is the rate-determining step then:

$$a_3 < a_1 + a_2 \qquad \text{and} \qquad a_2 > 10a_1$$

Hence,

$$\theta = a_1/a_2 \qquad (67)$$

i.e.

$$\theta = a_{H^+} \frac{\overrightarrow{k_A}}{\overleftarrow{k_A}} \frac{e^{-\eta F/2RT}}{e^{\eta F/2RT}} \qquad (68)$$

For the conditions corresponding to (67),

$$\eta = \frac{2}{3}\frac{RT}{F} \ln i_o - \frac{2RT}{3F} \ln i \tag{69}$$

$$\theta = K\, a_{H^+}\, e^{-2/3(\ln i_o - \ln i)} \tag{70}$$

$$\ln \theta = C + 2/3 \ln i \tag{71}$$

$$\therefore \frac{\partial \ln \theta}{\partial \ln i} = \frac{2}{3} \tag{72}$$

We make the assumption that the permeation rate is proportional to the surface coverage. This basic assumption was proved explicitly by Ward for H diffusion through Cu from the gas phase. It appears to be a reasonable assumption that either the surface reaction or the bulk diffusion is the rate-determining step in the permeation process.

Thus, from these assumptions and (72),

$$P \propto i^{2/3} \tag{73}$$

The Tafel slope which would be associated with (73) is:

$$\frac{\partial \eta}{\partial \ln i} = \frac{-2RT}{3F} = -\frac{b}{2.303}$$

$$= -0.04 \text{ at } 25^{\circ}C \tag{74}$$

In a similar way, the current dependence of permeation rate for other possible mechanisms can be worked out. The results are summarized in the Table 6 below.

It can be seen from Table 6 that the dependence of P on i, together with the Tafel slope, distinguishes among mechanisms except B and E. As the mechanism is associated with characteristic coverages, information on θ can thus be obtained.

TABLE 6

PERMEATION OF ELECTROLYTIC H AS A FUNCTION OF CURRENT DENSITY

DEPENDENCE ON MECHANISM

Slow Step	Tafel Slope at 25°C	Permeation - Current Relation	Qualitative Coverage
A Slow discharge followed by rapid combination	0.12	$P \propto i^{1/2}$	<0.1
B Slow discharge followed by rapid electrochemical desorption	0.12	P independent of i	<0.1
C Rapid discharge followed by slow combination desorption	0.03	$P \propto i^{1/2}$	<0.1
D Fast discharge followed by slow electrochemical desorption (low potentials)	0.04	$P \propto i^{2/3}$	<0.1
E Fast discharge followed by slow electrochemical desorption (high potential)	0.12	P independent of i	$\gtrsim 1$

The successful development of the low pressure vacuum systems and pressure measurement to 10^{-10} mm. Hg was followed by development of techniques for the permeation measurements. During this work,

higher pressure (10^{-7} mm. Hg) were used, and the metal was SAE 1010 steel. In the course of this development, it was found possible to make crude exploratory measurements with U, Ta, Ti, Cu, Ni.

20. TECHNIQUE OF EXPLORATORY PERMEATION MEASUREMENTS

(A) Vacuum System

The vacuum system consisted of a manifold 3 cm. diameter tube, 1.5 meter long, which could be evacuated to 10^{-7} mm Hg. by a two stage mercury diffusion pump, backed by a rotary oil pump. The high pressure side of the diffusion pump is connected to a 5 l. bulb which could be used as a fore pump instead of the rotary oil pump. Such a system works well for long periods so long as the pressure on the 5 l. bulb remains at least a power of ten less than the minimum pressure (0.1 mm Hg) required to back the diffusion pump. (This eliminates pump wear.) Pressures down to 10^{-7} mm Hg on the manifold were measured on a PMG 09 ionization gauge. Continuous evacuation of the manifold during the period of this work was found to be necessary to avoid the possibility of readsorption of gases by the walls of the system, and by the grease.

(B) Electrodes

The material under consideration was fabricated in the form of a disc 1.3 cm diameter, 0.5 mm thickness which was silver soldered to a Kovar tube of the same diameter. The tube was joined to a Kovar glass tube by a housekeeper seal, which was in turn joined to a pyrex glass tube by a graded seal. The cathode assembly was tested for vacuum tightness by incorporating it in a system of approximately 100 cc.

capacity (A in Fig. (25)) which could be evacuated through a greased vacuum stopcock. The pressure in the volume A was measured by a Stokes TP5 vacuum gauge. After several hours of evacuation, A was isolated from the line, and the pressure was measured at five minute intervals. The nature of the plot of p against t clearly indicates whether the pressure increase with time is due to a leak or to outgassing of the walls of the system. (A linear plot of p against t indicates a leak). This can be confirmed by enclosing the suspected area of the leak in an atmosphere of H_2 gas, which results in a sudden increased rate of change of p with t. An expotential change of p with t indicates outgassing of the walls. The two types of behavior are shown in Fig. 26.

Electrical contact with the disc is made with Pt wire wrapped round the Kovar tube. The Kovar tube and Pt wire are coated with Apiezon wax such that only the metal disc is available for contact with the solution.

Metals, such as Ti, Ta, and U, which are difficult to silver-solder to Kovar metal, can be waxed directly to a glass tube. It was found that the seal was able to withstand satisfactorily a vacuum of 10^{-7} mm. Hg with practice. Before final connection of the electrodes to the volume A, the internal surfaces were cleaned mechanically by the use of an abrasive, and finally pickled in concentrated HCl, washed with water, and then carefully dried. The external surface of the metal disc was polished with fine emery paper just before use.

(C) Cell

The cell Fig. (25) consisted of 1 l. beaker to which has been attached an anode compartment, and a cooling coil. The anode compartment

was connected to the rest of the cell through two holes at the lower end. The anode consisted of a piece of Pt foil 1 cm. square, which was connected to an electrical circuit by a Pt lead. The electrolyte was sitrred by a glass propeller. The H_2 overpotential at the cathode was measured against a saturated calomel electrode.

(D) Procedure

The electrode compartment A was assembled as described in section (B), and evacuated to 10^{-7} mm. Hg for 24 hours. Tap T was closed to isolate A from the line, and the pressure change at 5 min. intervals recorded. If the rate of outgassing was negligibly small, the cathode surface was polished, and the cell raised into position. The cell was then filled with N/10 HCl solution and the current is switched on. Pressure readings are recorded at 2 min. intervals, until the steady state permeation conditions have been attained. Experiments were carried out over the current density range 10^{-4} amp. cm^{-2}. At the lower current densities, where there is little evolution of hydrogen, vigorous agitation of the electrolyte was necessary to facilitate the removal of gas bubbles from the metal surface. At current densities between 0.5 and 1 amp. cm^{-2} there was a marked heating of the electrolyte. The temperature was kept down by circulating ice water through the cooling coil. The simple anode compartment used in the cell described here was effective in removing cathode depolarization.

21. RESULTS

In Fig. 27 is shown a typical plot of increasing H_2 pressure as recorded on the vacuum gauge on the electrode assembly A in Fig. 25. Such

plots were preceded by a test of pressure constancy over a time of 2 - 3 hours.

Fig. 28 gives a summary of the permeation data for H_2 on SAE 1010 steel, in 0.1 N HCl (without decontamination) as a function of current density. The data comprise the results from some thirty-five independent runs. The least square analysis shows:

$$\frac{\log P}{\log I} = 0.52 \pm 0.07 \qquad (75)$$

In Fig. 29, similar data is summarized for Pd in 0.1 N HCl. The least squares analysis shows:

$$\frac{\log P}{\log I} = 0.6 \pm 0.04 \qquad (76)$$

Measurements of hydrogen overpotential on Fe (Fig. 30) show an exchange c.d. of 6.10^{-6} A. cm.$^{-2}$ is in excellent agreement with the recent measurements of D. F. A. Koch.

Figs. 31 and 32 give the p - t date for Ni and Cu; and Fig. 16 gives the change of pressure with time on the diffusion side after charging Ta, Ti and U for some 4 hours. (Parameters, and derived diffusion coefficients are given in Table 7.)

TABLE 7

VALUE OF DIFFUSION COEFFICIENTS

Metal	D (cm^2 sec^{-1})	Lit. values
Fe	1.5×10^{-6}	2×10^{-6} (Davis and Butler, 1958)
Pd	7.3×10^{-7}	2×10^{-6} (Barrer, 1951)
Ni	7.6×10^{-9}	
Cu	1×10^{-8}	

A sample calculation of p is given: the plot of p with time shown in Fig. 27 was obtained for a cylindrical cathode (6.35 length, 1.3 cm diameter and 0.38 mm wall thickness) of 1010 steel immersed in the electrolyte to a depth of 1 cm. Thus, the change in the number of moles of H_2 in the electrode assembly A with time is given by

$$\frac{dn}{dt} = \frac{V}{RT}\frac{dp}{dt} \tag{77}$$

where T is the absolute temperature, R the gas constant and V the volume of electrode assembly A (Fig. 25). $\frac{dp}{dt}$ is the change of pressure in the volume A with time in the steady state.

The permeation rate P is given by

$$P = \frac{dn}{dt} \times \frac{1}{a} \tag{78}$$

where l is the thickness, and a is the area of the electrode immersed in the electrolyte.

Volume of section A in Fig. 25 = 109.7 cc

Area of immersion = 6.14 sq. cm.

Slope = 3μ/min.

T = 300°C

R = 82.05 cal deg^{-1} $mole^{-1}$

Thickness = 0.38 mm.

Permeation rate

$$P = \frac{108.7 \times 3 \times 10^{-3} \times 0.38}{82.05 \times 300 \times 760 \times 60 \times 4.76}$$

$$= 0.18 \times 10^{-10} \text{ mole mm } sec^{-1} \text{ } cm^{-2} \tag{79}$$

In the contaminated solutions used, Fig. 28 indicates that $P = KI^{1/2}$ for SAE 1010 steel. Reference to Table 6 shows that this result is consistent only with a mechanism for the hydrogen evolution

reaction on Fe for 0.1 n HCl of slow proton transfer followed by rapid combinative desorption. This conclusion indicates qualitatively that the coverage of adsorbed H on the metal is low (i.e., about one tenth).

22. INVESTIGATION OF PERMEATION UNDER HIGH PURITY CONDITIONS

It has been shown that the rate of permeation of electrolytic H through metals is highly sensitive to small traces of surface contaminants. It is therefore necessary to obtain a state in which the electrode surface is "clean." This necessity arises not only because of the need to make investigations in a standard state but also to find a "zero position" in the investigation of the effect of capillary active substances on the permeation rate.

23. TECHNIQUE OF PERMEATION EXPERIMENTS CARRIED OUT UNDER CONDITIONS OF HIGH PURITY

(A) Vacuum System

The vacuum system is substantially the same as that described in (ONR Report No. 3).

(B) Electrodes

The two essential requirements (a) that the surface of the metal must be cleaned in H_2 at 600° and (b) only the metal under investigation should come into contact with the highly purified solution.

Investigations were carried out on electrodes fabricated in the form of a closed cylinder of the material (length 6 to 10 cm. diameter 0.7 cm. and wall thickness 0.038 cm.). Connection of this electrode tube

to the evacuable volume B, Fig. 33, is made by a Kovar seal, the vacuum joint being made with silver solder. Possible contamination of the electrolyte with Ni, Co, Ag and Cu from the Kovar and the silver solder is minimized by immersion of the lower end of the cylinder in the electrolyte. In this case it is only necessary to subject the end of the electrode tube to high temperature H_2 treatment, thus reducing the possibility of breakdown of the silver soldered joint. Vacuum testing of the electrode assembly B (Fig. 33) is carried out in a similar manner to that described in ONR Report No. 3. Electrical contact to the electrode tube is made with a nickel wire inside the tube at the silver soldered joint. The nickel wire passes up the glass slide and is welded to a W wire which is vacuumatically sealed through the glass bulb (Fig. 33).

(C) The Cell

The considerations which resulted in the cell design described below are:

(a) For purposes of determining the diagnostic criteria it is necessary to have the permeation rates at a minimum of five values of the current density. (b) For each measurement of the permeation rate at a particular current density the electrode tube must be in the same initial standard state. (c) The electrode surface must be cleaned by reduction in hydrogen at 800°C. (d) The electrode assemblies must be thoroughly outgassed by continuous evacuation for several hours. (e) Electrolysis must be carried out in highly purified solutions. (f) Final purification of the electrolyte by pre-electrolysis must be carried out in the cathode compartment. (g) The volume of electrolyte must be kept down to a minimum to facilitate speedy purification.

It emerges from these considerations that the cell must be provided with at least five electrode assemblies. An arrangement, similar to the standard type of electrolytic cell for studying the mechanism of the hydrogen evolution reaction on metal wires was found to be impractical because of the difficulty of producing a small enough cathode compartment to house all the electrodes. As a result of this it was concluded in order to fulfill condition (g) each electrode assembly should have a separate cathode compartment. The possibility of seven such compartments having a common anode compartment was considered, but was ruled out because of overheating which would take place during simultaneous pre-electrolysis in all of the seven cathode compartments. (Total current $\approx$ 10 amps) to avoid the difficulty each cathode compartment was fitted with a separate anode compartment.

A typical unit cell is depicted in Fig. 33. The electrode assembly B is essentially the same as A in Fig. 25 (ONR Report No. 3). In the upper position the electrode tube is contained in a furnace, where the high temperature hydrogen pretreatment can be carried out, and the bulb B can be connected to a vacuum line. The height of the electrode assembly can be adjusted by a ground glass slide, and on disconnection from the vacuum line can be moved to a lower position such that the tip of the electrode tube reaches almost to the base of the cathode compartment. The cathode compartment is provided with a pre-electrolysis electrode attached to a ground glass slide so that it can be moved clear of the electrolyte. The anode compartment is connected through a glass sintered disc and a ground glass stopcock to the cathode compartment. Seven such unit cells are banked together side by side as depicted in Fig. 34. The two outer

cells are used for potential measurements against a saturated calomel electrode which has a salt bridge of purified electrolyte terminating in a Luggin capillary. The height of the electrolyte in the outer compartment is adjusted so the tip of the Luggin capillary is 1 mm. below the level of the electrolyte. For the potential measurements the electrode tube is lowered so that only the lower surface touches the surface of the electrolyte thus keeping the ohmic drop to a minimum. The initial preparation of HCl solution is carried out in a separate vessel which is connected to the cells by a manifold.

24. PROCEDURE IN THE HIGH PURITY MEASUREMENTS

(A) Cleaning of Components

At the termination of each experiment, the entire cell sections, in their seven parts, were subject to emptying and washing with tap water, with particular reference to the removal of the previous solution from the sintered discs. The cells were then immersed in the Beckmann solution and allowed to remain therein for two hours. A fresh Beckmann solution was made up about every five runs.

After removing the Beckmann solution, the cells were washed with a number of (about six) rinses of equilibrium water and then allowed to stand in equilibrium water (filling the whole cell) overnight. Thereafter, the cells were once more rinsed with six changes of conductance water (conductivity 10^{-7} mhos cm^{-1}) and preserved out of contact with air, filled with conductance water.

(B) Preparation of the electrodes

Electrodes were mechanically polished, electropolished, and then introduced into the H_2 atmosphere at 800°C, and maintained in this for 20 minutes when they became bright.

(C) Procedure

At the commencement of the run, the hydrogen overpotential was measured on two independent Fe electrodes in the compartments M and N (Fig. 34) in order to establish the overpotential c.d. relation for the given condition of solution, etc.

Thereafter, the purified electrodes, after H_2 treatment, were lowered in the H_2 atmosphere, into the electrolyte, and electrolysis commenced at a series of c.d.'s. The lower limit of c.d. is set by the rate of corrosion of Fe, the higher limit by the heating effects in the solution. The pressure increase with time was measured on the Stokes TP 3 gauges. Measurements were carried out in parallel on five electrodes.

25. NEW TECHNIQUE FOR PERMEATION STUDIES

It was apparent in the above studies that the experimental technique of permeation into a vacuum was extraordinarily complex and exacting in its demands. It was therefore essential to devise a simpler technique of permeation measurements in order that it may be used in routine measurements. The following purely electrochemical technique was devised, and tested with palladium membranes before being applied to iron membranes. A study of the behavior of electrolytic hydrogen in palladium was necessary for the following reasons. The application of this electrochemical technique

of measuring the permeation rate in corrodible metals requires the use of thin coetings of palladium. Consequently the diffusion behavior in palladium membrane had to be investigated first. Anomalies in the thickness dependence of the permeation of hydrogen through palladium have been reported (Wahlin and Naumann 1953, Silberg and Bachman 1958). Hence it is necessary to find out whether such anomalies exist with electrolytic hydrogen in palladium. Further the easy permeation of hydrogen in palladium make this metal a first choice for verifying the diffusion formulae deduced below.

26. THEORY OF THE NEW METHOD

(A) Diffusion Theory Relevant to the Method

Consider unit area of a membrane of thickness L and diffusion constant for hydrogen D (see Figure 35) where the diffusion is in the direction of decreasing x. Let the concentration of hydrogen at x = 0 and x = L be maintained at C_1 and C_2 respectively. In the steady state the through-put of hydrogen is given by

$$P = D \frac{dc}{dx} = \frac{D(C_2 - C_1)}{L} \qquad (80)$$

For the non-stationary state the general solution of the Fick's Law equation

$$\frac{\partial c}{\partial t} = \frac{\partial}{\partial x}\left(D \frac{\partial c}{\partial x}\right) = D \frac{\partial^2 c}{\partial x^2} \text{ (if D is constant)} \qquad (81)$$

for this problem is

$$C_{xt} = C_1 + (C_2 - C_1)\frac{x}{L} + \frac{2}{\pi}\sum_{n=1}^{n=\infty}\frac{(C_2\cos n\pi - C_1)}{n}\exp\left(-\frac{Dn^2\pi^2 t}{L^2}\right)\sin\frac{n\pi x}{L}$$

$$+ \frac{4C_o}{\pi}\sum_{n=o}^{m=\infty}\frac{1}{(2m+1)}\sin\frac{(2m+1)\pi x}{L}\, e^{-\frac{D(2m+1)^2\pi^2 t}{L^2}} \qquad (82)$$

where C_{xt} is the concentration at any point x at time t, and C_o is the initial constant concentration of hydrogen in the membrane. On dropping the term in C_o for membranes initially free of hydrogen, differentiating with respect to x and multiplying by D, the equation obtained is

$$D\left(\frac{dc}{dx}\right)_t = \frac{D(C_2 - C_1)}{L} + \frac{2D}{L}\sum_{n=1}^{n=\infty}(C_2\cos n\pi - C_1)\exp\left(-\frac{Dn^2\pi^2 t}{L^2}\right)\cos\frac{n\pi x}{L} \qquad (83)$$

For the plane x = 0 (83) yields

$$P_{(x=o)t} = \frac{D(C_2 - C_1)}{L} + \frac{2D}{L}\sum_{n=1}^{n=\infty}(C_2\cos n\pi - C_1)\, e^{-\frac{Dn^2\pi^2 t}{L^2}} \qquad (84)$$

where $P_{(x=o)t}$ is the permeation rate at x=o times t. In the steady state, $t \to \infty$, the exponential term is zero and reduces to

$$P_{(x=o)t_\infty} = \frac{D(C_2 - C_1)}{L} \qquad (85)$$

Similarly for the plane x = L (83) gives

$$P_{(x=L)t} = \frac{D(C_2 - C_1)}{L} + \frac{2D}{L}\sum_{n=1}^{n=\infty}(C_2\cos n\pi - C_1)\exp\left(-\frac{Dn^2\pi^2 t}{L^2}\right)\cos n\pi \qquad (86)$$

which for $t \to \infty$ becomes

$$P_{(x=L)t_\infty} = \frac{D(C_2 - C_1)}{L} \qquad (87)$$

The diffusion constant, D, may be evaluated from permeation transients in the following ways:

(1) Time lag method

This is the method used hitherto, when only the quantity of hydrogen permeating was measurable as a function of time, i.e. $\int_0^t P_{(x=o)t}\,dt$ which is denoted Q_t. For this purpose integration of (84) from o to t yields

$$Q_t = \frac{D(C_2 - C_1)t}{L} - \frac{2L}{2}\sum_{n=1}^{n=\infty}\frac{(C_2 \cos n\pi - C_1)}{n^2}\left(1 - e^{-\frac{Dn^2\pi^2 t}{L^2}}\right) \qquad (88)$$

It is well known that the intercept T_{lag} (time lag) on the time axis of a Q_t - t plot for large t is given by

$$T_{lag} = \frac{L^2}{6D} \qquad (89)$$

When $C_2 >> C_1$ this yields thus permitting the calculation of D. Formula (89) has been extensively used, but as we shall show elsewhere a correction to the experimentally determined time lag is required in order to apply (89).

(2) Rise time constant

When the permeation rate can be continuously recorded, the diffusion constant can be calculated as follows. From equations (84) and (85) the following is obtained.

$$\left(\frac{P_t - P_\infty}{P_\infty}\right)_{x=o} = \frac{2}{C_2 - C_1}\sum_{n=1}^{n=\infty}(C_2 \cos n\pi - C_1)\, e^{-\frac{Dn^2\pi^2 t}{L^2}} \qquad (90)$$

For $C_2 >> C_1$ (90) reduces to

$$\left(\frac{P_t - P_\infty}{P_\infty}\right)_{x=0} = 2\sum_{n=1}^{n=\infty} (-1)^n e^{-\frac{Dn^2\pi^2 t}{L^2}} \qquad (91)$$

On substituting $1/t_o$ for $\frac{Dn^2\pi^2}{L^2}$, and expanding (91) the series form (92) is obtained

$$\left(\frac{P_t - P_\infty}{P_\infty}\right)_{x=0} = 2\left[-e^{-\frac{t}{t_o}} + e^{-\frac{4t}{t_o}} - e^{-\frac{9t}{t_o}} - - - -\right] \qquad (92)$$

This may be written as:

$$\left(\frac{P_t - P_\infty}{P_\infty}\right)_{x=0} = -2\left[1 - e^{-\frac{3t}{t_o}} + e^{-\frac{8t}{t_o}} - - - -\right]e^{-\frac{t}{t_o}} \qquad (93)$$

The term within the brackets is indeterminate when t=o for it could be unity or zero, depending on whether an odd n or even n is considered. On taking logarithms.

$$\log_e\left(\frac{P_t - P_\infty}{P_\infty}\right)_{x=0} = \log_e\left[1 - e^{-\frac{3t}{t_o}} + e^{-\frac{8t}{t_o}} - - - -\right] - \log_e 2 - \frac{t}{t_o} \qquad (94)$$

The log of the term within the brackets, though indeterminate at t=o, rapidly becomes zero at t increases. Hence a plot of $\log_e\left(\frac{P_t - P_\infty}{P_\infty}\right)_{x=0}$ versus t yields as gradient $1/t_o$ and intercept $\log_e 2$. Thus from the gradient of this graph D can be calculated, using the formula

$$\text{gradient} = \frac{1}{t_o} = \frac{D\pi^2}{L^2} \qquad (95)$$

(3) Time lag from rise transient

The time lag is obtained by a linear extrapolation of the Q_t vs t plot when t is large, i.e. after steady state has been established (point A of Figure 15). Therefore the time lag T_{lag} given by equation

(89) represents the time at which the diffusion process (if it could proceed always at steady state value) should start in order that the amount permeating will be the same as that for the ordinary diffusion process in the steady state for large t. An inspection of figure 36 shows that this time is that which makes the area of the rectangle ABCD equal to that under the rise curve OECD. That is, the vertically hatched area EBF should be equal to the horizontally hatched region EAG. Equation (94) shows that for $b > o$ the rise of the permeation is approximately exponential since the term $\left[1 - e^{-3t/t_o} + e^{-8t/t_o} - - - -\right]$ rapidly reaches unity at for $t > o$. It is easy to show that for an exponential curve of time constant t_o this point E corresponds to a permeation rate of 0.6299 times the steady state value. Thus the interval from zero time to the time the permeation rate is 0.6299 times the steady state value is T_{lag}. Hence

$$T_{lag} = \frac{L^2}{6D} = t_{0.6299} \tag{96}$$

(4) Break through time t_b

For an exponential curve the time taken to obtain 0.6299 times the steady state value is the time constant. Hence, if t_b represents the time at which the permeation rate begins to rise from zero, the connection between these quantities as shown by Figure (36) is

$$T_{lag} = t_b + t_o \tag{97}$$

Therefore from t_b the diffusion constant can also be obtained with the formula

$$t_b = \frac{L^2}{D}\left(\frac{1}{6} - \frac{1}{\pi^2}\right) = \frac{L^2}{D\ 15.3} \tag{98}$$

(5) Decay time constant

Equation (82) is the general solution when an initially uniform concentration exists in the membrane. If the concentration were some function of x in the membrane, the general solution is given by

$$C = C_1 + (C_2 - C_1)\frac{x}{L} + \frac{2}{\pi}\sum_{n=1}^{n=\infty}\frac{(C_2 \cos n\pi - C_1)}{n}\exp\left(-\frac{Dn^2\pi^2 t}{L^2}\right)\sin\frac{n\pi x}{L}$$

$$+ \frac{2}{L}\sum_{n=1}^{n=\infty}\exp\left(-\frac{Dn^2\pi^2 t}{L^2}\right)\sin\frac{n\pi x}{L}\int_0^L f(x')\sin\frac{n\pi x'}{L}\,dx' \qquad (99)$$

Where $C = C_1$ at $x = o$ for all t

$C = C_2$ at $x = L$ for all t

$C = f(x)$ at $t = o$ for $0 < x < L$

If the steady state has been established in a membrane initially free of hydrogen, then the concentration gradient is linear, and the concentration is C_1 at x=o and C_2 at x=L. If now the source of hydrogen is suddenly stopped and the time reckoned from this point, it follows that the initial distribution function required in the second term of equation (99) is simply

$$f(x') = \frac{(C_2 - C_1)x}{L} + C_1 \simeq f\frac{c'x}{L} \qquad (100)$$

since $C_1 \simeq 0$. The decay of the permeation at x=o may then be described by equation (99) with the boundary conditions

$C = C_1 \simeq 0$ at $x = o$ for all t

$C = C_2 = 0$ at $x = L$ for all t

$C = f(x) = \frac{c'x'}{L}$ at $t = o$ for $0 < x' < L$

Under these conditions, (99) reduces to

$$C = \frac{2}{L} \sum_{n=1}^{n=\infty} \exp\left(-\frac{Dn^2\pi^2 t}{L^2}\right) \sin\frac{n\pi x}{L} \int_0^L ax' \sin\frac{n\pi x'}{L}\, dx' \qquad (101)$$

where $a = \frac{c'}{L}$.

Integration by parts of (101) yields

$$C = \frac{2}{L} \sum_{n=1}^{n=\infty} \exp\left(-\frac{Dn^2\pi^2 t}{L^2}\right) \sin\frac{n\pi x}{L} \left\{ \left[-\frac{ax'L}{n\pi} \cos\frac{n\pi x'}{L} \right]_0^L + \frac{aL}{n\pi} \int_0^L \cos\frac{n\pi x'}{L} \right\} \qquad (102)$$

where the last term is zero. Substituting for the limits, differentiating with respect to x and multiplying by D, we get for the permeation at x=o

$$P_{x=o,t} = 2aD \sum_{n=1}^{n=\infty} (-1)^{n+1} e^{-\frac{Dn^2\pi^2 t}{L^2}} \qquad (103)$$

Using the symbol t_o for $\frac{L^2}{D\pi^2}$ as before and expanding (103) may be written as

$$P_{x=o,t} = 2aD\, e^{-t/t_o} (1 - e^{-et/t_o} + e^{-8t/t_o} - - -) \qquad (104)$$

For t=o, let the permeation be $P_{(x=o)t=0}$. For reasons already given only the first term of the series is important and hence (104) can be transformed into the simple exponential decay form

$$P_{x=o,t} = P_{(x=o)_{t=o}}\, e^{-t/t_o} \qquad (105)$$

Hence a plot of log, $(\frac{P_t}{P_o})_{x=o}$ against time has a gradient $1/t_o$ and thus the diffusion constant can be calculated from the decay time constant with the aid of equation (95). The above analysis shows that the diffusion constant may be evaluated by five different methods when transients can be recorded.

(B) Formulae for the Determination of Coverage

When the above equations are to be used difficulties arise, for the concentrations C_1 and C_2 refer to the concentrations within the membrane at $x = 0$ and $x = L$ whereas only the concentrations outside the membrane are amenable to control. As shown by Barrer (1939) and Ash and Barrer (1960) large discontinuities in concentration exist at phase boundaries and these have to be considered in the application of these formulae to real systems. A detailed analysis of this problem has been given by Barrer (1959) and what we give here is a simple treatment adapted for the electrochemical systems which interest us.

Consider the same membrane but let some electrochemical reaction produce a steady state coverage with adsorbed atomic hydrogen θ_H at the interface at $x = L$. Let the opposite interface at $x = o$ be maintained at some anodic potential sufficient to cause rapid ionization of any hydrogen atoms on the surface, thereby producing a steady coverage of zero. Let the rate constant for the transfer of hydrogen from the surface into the metal be $k^{s \to b}$ and for the reverse process, $k^{b \to s}$. In the absence of any diffusion process within the membrane, let the equilibrium concentration of hydrogen in the metal at $x = L$ be C_e. This equilibrium is represented by the equation

$$k^{s \to b} \theta_H = k^{b \to s} C_e \qquad (106)$$

when θ_H is small, and C_e is much less than the saturation concentration c_s. If due to a diffusion process within the membrane, the concentration at $x = o$ is altered from C_e to C_c, then the permeation of hydrogen into the membrane is given by

$$\left({}^{b\rightarrow s}_{k}\, C_e - {}^{b\rightarrow s}_{k}\, C_2 \right) = P \qquad (107)$$

For steady state diffusion within the membrane, the concentration gradient is uniform, and if the concentration in the membrane at x = o is C_1 the rate of permeation is given by

$$\frac{D(C_2 - C_1)}{L} = P \qquad (108)$$

At the interface at x = o the equilibrium is

$$ {}^{b\rightarrow s}_{k}\, C_1 = P \qquad (109)$$

From (106), (107), (108) and (109) the following equation is obtained:

$$\frac{1}{P} = \frac{L}{D\theta} \frac{{}^{b\rightarrow s}_{k}}{{}^{s\rightarrow b}_{k}} + \frac{2}{{}^{s\rightarrow b}_{k}\ \theta} \qquad (110)$$

The gradient of a plot of $\frac{1}{P}$ against L is given by

$$g = \frac{{}^{b\rightarrow s}_{k}}{{}^{s\rightarrow b}_{k}\ D\theta} \qquad (111)$$

and its intercept by

$$I = \frac{2}{{}^{s\rightarrow b}_{k}\ \theta} \qquad (112)$$

The minimum values of g and I are reached with $\theta \longrightarrow 1$, hence

$$g_m = \frac{{}^{b\rightarrow s}_{k}}{{}^{s\rightarrow b}_{k}\ D} \qquad (113)$$

and

$$I_m = \frac{2}{{}^{s\rightarrow b}_{k}} \qquad (114)$$

Hence θ can be calculated using the equation

$$\theta = \frac{g_m}{g} = \frac{I_m}{I} \qquad (115)$$

In the above deduction it has been assumed that diffusion is the rate controlling process, i.e., $k^{s\rightarrow b}$, $k^{b\rightarrow s}$ D. Under these conditions, the formulae previously deduced for the evaluation of D apply, and hence D can be obtained independently. Therefore, with the aid of (113) and (114) both rate constants can be evaluated with a knowledge of D obtained from an analysis of the transients. When diffusion is rate controlling, the permeation rate will depend on the thickness of the membrane used according to equation (80). When $k^{s\rightarrow b}$ and $k^{b\rightarrow s}$ are both smaller than D, then, the surface reaction is rate controlling. In this case the permeation rate will be independent of the thickness of the membrane.

In the event of it being impossible to realize a surface completely covered with atomic hydrogen (i.e. $\theta_H = 1$) but only one of a certain maximum coverage θ_M, then equation (115) gives the coverage as a fraction of this maximum coverage only. An independent determination of the absolute coverage at one point will then enable the calculation of the absolute coverage at all potentials.

27. PRINCIPLE OF THE METHOD

Diffusion theory requires that the coverage of the membrane with adsorbed atomic hydrogen on one side be maintained at a certain fixed level, while on the opposite side it should be always zero. These conditions are easily satisifed by cathodic polarization of one side and anodic polarization of the opposite side using potentiostatic circuits. The simplicity of this technique is due to the fact that the current in the anodic potentiostatic circuit which maintains zero

coverage on one side of the membrane, is by Faraday's Laws a direct measure of the instantaneous rate of permeation of hydrogen. It is thus possible to obtain a continuous record of the instantaneous rate of permeation of hydrogen with all the sensitivity associated with current measurement. Thus with a current recorder of sensitivity 0.003 μA/mm. commonly used in polarographs in the anodic circuit, and a membrane of one square centimeter area, a permeation rate of 3×10^{-14} gram atoms per secondor 3×10^{-9} ml. of hydrogen per second can be detected. The sensitivity of this method reveals details in the permeation not detectable by previous methods especially with metals susceptible to hydrogen embrittlement, as we shall show in a later communication.

28. EXPERIMENTAL

(A) Cell

The electrochemical cell used is shown diagrammatically in figure 37. It consisted of two identical units terminating in standard half inch pyrex pipe flanges. Each flange carried its teflon gasket with the side facing the membrane polished flat. The assembly was then bolted on with the membrane in between the gaskets. The "give" of the gaskets ensured a water tight seal with the thickest membranes used. Each unit carried a bright platinum auxiliary electrode and a Luggin capillary-calomel reference electrode system as shown in Figure 37. Facilities for bubbling nitrogen were also provided. The combination of float and sintered disc shown in the figure isolated the auxiliary electrode without increasing the electrical resistance appreciably.

(B) Materials

Palladium membranes of various thicknesses were obtained from E. Bishop & Co. They were degreased with benzene in a Soxhlet extractor before use.

Sodium hydroxide solutions were prepared from Baker Analytical Reagent grade pellets with conductivity water. The solutions were pre-electrolysed in an external cell before admission into the cell.

Nitrogen was deoxygenated by active copper and passed through cooled charcoal traps before admission into the cell. Standard procedures were used in cleaning the cell and auxiliary glassware.

(C) Electrical Circuit

This is shown in figure 38. The cathodic polarization was effected by a Wenking electronic potentiostat and the current read on the ammeter of the instrument. When necessary the output of the instrument was fed to a Sargent S. R. recorder to monitor the cathodic polarization current. The anodic circuit was similar but the potentiostat output was fed to a Sargent XXI polarograph with its bridge set at zero. This enabled the wide sensitivity range control of the polarograph to be used to record the current on a suitable scale. Small residual currents could also be opposed with the zero shifting control of the polarograph.

(D) Procedure

A 0.1 N. solution of sodium hydroxide pre-electrolysed for 24 hours in a separate cell, was admitted into both compartments. The solution in each compartment was again pre-electrolysed for a further

period of 1-1/2 hours with the system of auxiliary electrodes while nitrogen was being bubbled on both sides to promote stirring. Cathodic polarization was then commenced at a potential corresponding to a cathodic current density of 10^{-4} A cm^{-2}. The anodic potential applied to the membrane was then varied over a wide range and the steady values of the anodic current measured. A plot of anodic current against the applied potential with respect to the saturated calomel electrode revealed a plateau between -600 mv and -300 mv. In order to ensure rapid ionization of the hydrogen the anodic potentiostat was set at the highest permissible anodic potential namely -300 mv on the calomel scale for all subsequent experiments.

The cathodic polarization potential was next set also to -300 mv thus ensuring the complete absence of hydrogen and the small residual current in the anodic circuit compensated by means of the zero shift. The cathodic potential was now switched from -300 mv to a fixed value of -850 mv on the calomel scale which resulted in cathodic polarization of the palladium to a current density of about 10^{-5} amps. cm^{-2}. The instant of switch-on was marked on the recorder chart. The arrival of the first traces of hydrogen on the anodic side of the membrane was registered by the recorder as an increase in the current. This current continued to increase and reached the steady value. Several minutes after steady state had been reached the cathodic polarization was switched back to -300 mv thus stopping the production of electrolytic hydrogen. The recorder thereupon showed a decrease in the current which soon decayed to zero after some time. Reproducibility was very good when precautions were taken to avoid contamination by traces of surfactants.

In this manner records were obtained for various thicknesses of palladium maintaining the same polarization conditions. Several runs were carried out for each thickness. All experiments were made at room temperature which was 25 ± 2°C.

29. RESULTS

Figure 39 shows a drawing of a typical record. Starting from zero time the point marked t_b represents the breakthrough time. The time required for the permeation to reach 0.6299 times the steady state value is marked T_L, since as previously shown it is also the time lag.

30. CALCULATIONS

The diffusion formulae previously deduced (Devanathan 1961, 1962) were verified as follows.

(A) Time Constants

According to equation (94) a plot of $\log \left(\frac{P_t - P_\infty}{P_\infty}\right)_{x=0}$ versus time should yield a straight line of gradient $\frac{1}{t_o}$, where t_o is $\frac{L^2}{\pi^2 D}$, for the rising transient. Similarly for the decay transient according to equation (105), a plot of $\log \left(\frac{P_t}{P_\infty}\right)_{x=0}$ versus time should give the same slope. In figure 40 a typical plot is shown, for the rise and decay transients. The straight lines are parallel indicating the indentity of their gradients. This identity has not been previously demonstrated. At large times the decay rate is somewhat different. This is due to the fact that when the cathodic potential is switched from -950 mV to -300 mV, anodic dissolution occurs on both sides. Hence with time the linear

concentration profile which existed at the early stages of the decay will be altered by additional diffusion to the originally cathodic side. The decay formula will therefore not apply for long times. Frank and Thomas (1960) obtained continuous records of the permeation of gaseous hydrogen through cylindrical single crystal germanium, but used the classical time lag plot for the rise transient, while using a logarithmic plot for the decay transient.

(B) Intercepts and Relaxation Time

According to equation (105) the logarithmic plot has a zero intercept, but figures 39 and 40 show that even when the cathodic potential is switched to a potential representing zero coverage, the permeation current continues at its steady value, for a period of time marked t_r, and only then does it start to decay. The reason for this behavior is clear when one considers the derivation of these diffusion equations, all of which refer to concentrations within the membrane and not surface concentrations on the membranes. When the potentiostat is switched to a different potential, the surface coverage changes in a time interval of the order of microseconds. But the concentration of hydrogen just inside the surface will require a much longer time for adjustment to a value corresponding to equilibrium with the new surface coverage. This time of relaxation can be regarded as due to finite rate constant for the transfer of hydrogen atoms from the surface into the metal phase. However, why this relaxation time is thickness dependent according to an approximately cubic law, as will be shown later, is not clear. This appears to be general phenomena, and has also been

observed in decay transients for gaseous diffusion by Frank and Thomas (1960). Since the equations apply only to membrane concentrations, it is reasonable to subtract, t_r from the switch-on time and the switch-off time, to obtain the transients on a time scale which refers to concentrations in the membrane. When this is done it is found that equations (105) and (94) are obeyed with respect of the intercepts, which should be zero and $\log_{10}2$ or 0.301 respectively. This can be seen in figure 40 where the corrected time scale is shown as the dashed line while the electrical time scale is shown as a continuous line.

(C) Time Lag T_1

The classical method (Daynes 1920, Barrer 1939) of obtaining the diffusion constant is by evaluating the time lag. This was done by integration of the rising transient. As shown previously (Devanathan 1961, 1962) the same value can be readily obtained by spotting the time at which the permeation is 0.6299 times the steady state value. When the time lag was evaluated by both methods the agreement was always within 2%. However the time lag obtained by either method will be in error by an amount equal to the relaxation time. Thus particularly for larger thicknesses, the diffusion constant was as much as 20% smaller than the value calculated from the time constant t_o. But when a correction was made for the relaxation time agreement was very good, as shown in Table 8.

TABLE 8

Thickness cm.	t_b (sec.)	T (sec.)	t_o (sec.)	t_o (sec.)	t_v (sec.)	t_b (corr.) (sec.)	T (corr.) (sec.)	D_{t_b} (10^{-7} cm^2 sec^{-1})	D_T (10^{-7} cm^2 sec^{-1})	D_{t_b} (10^{-7} cm^2 sec^{-1})	D_T (corr.) (10^{-7} cm^2 sec^{-1})	$D_{t_o}^{rise}$ (10^{-7} cm^2 sec^{-1})	$D_{t_o}^{decay}$ (10^{-7} cm^2 sec^{-1})
0.0055	12.5	36.5	23.3	25.4	6.5	6.	30.0	1.58	1.38	----	1.68	1.31	1.27
0.014	115.6	339.7	180.3	139.8	37.0	78.6	302.7	1.11	0.96	1.63	1.08	1.10	1.42
0.021	238.3	563.5	271.0	279.7	81.3	157.0	482.2	1.21	1.30	1.84	1.52	1.65	1.60
0.027	433	1159	678.7	552.7	177.1	256.0	981.9	1.10	1.05	1.86	1.24	1.09	1.34
0.039	1019	2415	1264	1195	483.0	536.0	1932	0.97	1.05	1.85	1.31	1.22	1.29
0.051	1900	4540	1678	1965	1050	850.0	3490	0.89	0.96	2.00	1.24	1.57	1.34
						Average		1.06 ± 0.20	1.12 ± 0.20	1.84 ± 0.20	1.34 ± 0.30	1.32 ± 0.20	1.37 ± 0.15
D from the slopes of plots t_b, t_o and T_v against L^2 found graphically from the Fig. 41.										1.88	1.25	1.27	1.27

Mean value for D $1.30 \pm 0.20 \times 10^{-7}$

(D) Breakthrough Time, t_b

Since the time lag is the sum of the breakthrough time t_b and the time constant t_o as shown previously, a similar correction has to be made in the breakthrough time in order to obtain concordant values. In Table 8, the corrected and uncorrected breakthrough times are compared with t_c. The consistency of the results proves the validity of the diffusion equations previously deduced for these transients. Since t_b is the smallest value measured, it is more subject to error in subtracting the time of relaxation. Hence in the final value for the diffusion constant, only the time lag and the rise and decay time constants have been used in obtaining the mean.

(E) Thickness Dependence

In the derivation of these equations, it has been assumed that the permeation is controlled by diffusion in the bulk of the metal. If this is so, then the diffusion constant should be independent of thickness. This can be easily verified by plotting T_{lag}, or t_o against L^2. Straight lines of gradient $\frac{1}{6D}$ and $\frac{1}{\pi^2 D}$ should be obtained. Such plots are shown in figure 41. The points, which cover a thickness range of 0.0035 to 0.055 cm corresponding to an L^2 variation by a factor of 250, fall clearly on straight lines passing through the origin. This provides conclusive proof for the first time that the diffusion constant is indeed independent of the thickness under non-stationary conditions. The points for the uncorrected time lag fall on a straight line for small thickness and then curve away as the thickness is increased (see also Table 8).

(F) Variation of Permeation

For steady state permeation, even though the diffusion constant is independent of thickness, the permeation rate could change irregularly if the coverage of the cathodic side of the membrane changes for any cause, e.g., adsorption of impurities. According to the simple theory developed the a plot of $\frac{1}{P}$ against the thickness should be a straight line. Such a plot is shown in Figure 42. The points are clearly seen to be on a straight line. The intercept as shown previously is related to the rate constant for the transfer of hydrogen from the surface to the bulk of the metal.

(G) Diffusion Constant

The mean diffusion constant calculated from the uncorrected time lag points in figure 41 was found to be about 1.05×10^{-7} cm^2 sec^{-1} while that from the corrected time lag was 1.25×10^{-7} cm^2 sec^{-1}. From the gradient of the t_o line the diffusion constant was 1.27×10^{-7} cm^2 sec^{-1}, in harmony with the corrected time lag value. The data of Frank and Thomas (1960) presented in Figure 41 of their paper also shows a considerable difference between the classical time lag and the decay transient diffusion constant. But they computed the mean of these two sets of values without applying a correction for the relaxation time. Thus it appears that the classical time lag method may be in error depending on the ratio of the time of relaxation to the true time lag. This aspect is further discussed, later in this paper.

The mean value for the diffusion constant for hydrogen in α-palladium at room temperature can therefore be taken as $1.30 \pm .20$

x 10^{-7} cm^2 sec^{-1}. Values obtained by other authors by a variety of methods have been discussed by Barrer (1941) and the best value calculated for 25°C is 1.56 x 10^{-7} cm^2 sec^{-1} in good agreement with our result.

31. DISCUSSION

(A) Consistency of the Results

The consistency of the results in respect of the various methods of calculation of the diffusion constant from the recorder traces shows that the equations previously deduced are correct. The fact that the time lag is directly proportional to the square of the thickness shows that the quantity being measured is the diffusion constant of hydrogen in the bulk of the metal. The linear variation of the reciprocal of the permeation with thickness then shows that the surface coverage is constant and that transport processes across the surfaces are not rate controlling. This consistent behavior of electrolytic hydrogen is in contrast to the behavior of gaseous hydrogen when diffusing through palladium membranes. As is well known despite the variety of methods used to measure the diffusion constants in palladium, no concordant values are reported in the literature (Barrer 1941). Furthermore the permeation has not been found to be inversely proportional to the thickness (Wahlin and Naumann, 1953) nor has it followed the expected $p^{1/2}$ law for diffusion from the gas phase (Silberg and Bachman 1958).

(B) Anomalies in Diffusion

It is unlikely that the diffusing species at room temperatures is different from that in the range 200-600°C which is the usual range for

studies of diffusion from the gas phase. It is generally accepted that gaseous hydrogen dissociates into atoms on adsorption. Hence the migrating species must be same whether the hydrogen atoms are produced electrolytically or from molecular hydrogen. The anomalous behavior reported for the diffusion of hydrogen must therefore arise from a failure of the experimental set up to maintain conditions required by theory. Provided the diffusion constant is invariant, the permeation should be directly dependent on the surface coverage with atomic hydrogen as shown previously. But the possibility of alteration of surface coverage, from experiment to experiment due to adsorption of trace impurities in diffusion studies, cannot be excluded. In our experiments, the use of potentiostats and purified solutions is a simple method of maintaining constant coverage, and it is probably this one fact which has led to consistent results.

(C) Non-stoichiometric Phase Formation

One significant difference in the two methods is in the extent of hydrogen absorption during the experiment. At the cathodic potentials used the current density was about 10^{-5} amps cm^{-2} or only 10^{-10} gram atoms of hydrogen per second. Even during an experiment lasting an hour the total quantity of hydrogen produced will be only about 10^{-6} gram atoms. This quantity is insignificant compared to the number of gram atoms of palladium in the thinnest membranes used. Thus the palladium membranes cannot absorb hydrogen in significant amounts to form any β-phases. But with gas phase diffusion studies it is very likely that a hydrogen rich β-phase forms. The movement of such concentration discontuities may

then account for the anomalous diffusion behavior as suggested by Ash and Barrer (1959, 1960). Our attempts to investigate the diffusion of gaseous hydrogen by passing hydrogen gas into the dry cathode polarization unit gave very large currents. Whenever the permeation currents were large the anodic side of the palladium showed a tendency to passivate with formation of visible oxide films. The current time curves, nevertheless were of the same type given in figure 39. A calculation of the diffusion constant gave values which were as low as 0.02×10^{-7} cm^2 sec^{-1} for membranes of thickness 0.0035 cm gradually rising to about 0.58×10^{-7} cm^2 sec^{-1} to membranes of thickness 0.014 cm. Although no systematic experiments were carried out on gas phase diffusion the trend suggests that with thin membranes significant amounts of β -phase with a presumably smaller diffusion constant are formed thus leading to anomalies. Norberg (1952) found a diffusion constant about one-tenth smaller than our values, in palladium wires charged with hydrogen thereby forming presumably a β - phase. This result would tend to confirm our data with hydrogen rich palladium. However the formation of visible oxide films on the anodic side of the membrane suggests that perhaps this film is responsible for reducing the apparent diffusion constant. Hence our results cannot be regarded as giving unambiguous support to the view that the diffusion constants in α and β palladium are different. On the contrary the agreement of our results with the extrapolated values from high temperature measurements seem to suggest that both α and β forms may have the same diffusion constant despite the difference in hydrogen content.

The results which we have obtained for the permeation of electrolytic hydrogen are, in contrast to permeation from the gas phase, consistent in the dependence on the thickness. The linearity of the t_o and T_L versus L^2 and the $\frac{1}{P}$ versus L plots shows that the criteria for non-stationary and steady state diffusion are satisfied. Hence we can conclude that for small cathodic current densities no β-phase moving boundaries are produced, and that the diffusion constant obtained is that for the hydrogen poor α-palladium.

(D) Errors in Classical Time Lag Method

It appears that measurements based on the time lag method may be in error to about 15% in the absence of any correction for the relaxation time. As already shown relaxation times are easily measured when a continuous record of the permeation is made. Our results on thickness variation show that the relaxation times increase approximately as the cube of the thickness of the membrane. Thus a spurious thickness dependence will be noticed in the determination of diffusion constant by the classical time lag method. The reason for the variation of the time of relaxation with thickness is not easy to explain. One should expect this to be a constant if indeed it represents the time required for the concentration in the membrane to adjust itself to equilibrium with the surface coverage, and hence the explanation advanced earlier must be regarded as inadequate. The correction nevertheless is important for the calculation of the time lag and must be applied in this empirical way in order to get results concordant with the rise and decay time constants.

Frank and Thomas' (1960) results (Figure 41) for the temperature dependence indicate that the time of relaxation may also be temperature dependent to a different degree from the diffusion constant. Thus the decay constant points (t_o) seem to be less temperature dependent than the time lag points. It therefore appears that the time lag method may also give rise to a spurious temperature dependence of the diffusion constant. In view of these drawbacks in the time lag method it seems necessary to apply this continuous recording method in order to study the diffusion of hydrogen in metals. It will then be possible to apply a correction for the time of relaxation in the time lag, in the manner described, or the rise and decay transients can be used without any correction.

32. EXPERIMENTS WITH ARMCO IRON MEMBRANES

(A) Permeation Measurements

Details of the cell and auxiliary apparatus used in these experiments have already been described (Devanathan and Stachurski, in press). For these investigations Armco iron sheets prepared in the following way were used. Sheets of various thickness were degreased in benzene and treated to 700°C in an atmosphere of pure hydrogen and allowed to anneal. The membranes were then mounted in the cell as described elsewhere (Devanathan and Stachurski, in press). The anodic compartment contained N NaOH and to reduce the possibility of passivation, this side was coated with a thin electrodeposit of palladium. This thin coating did not materially affect the rate of permeation of atomic hydrogen which was rate controlled only in the iron membrane (Devanathan (1961).

Attention was paid to purification of the solution and pre-electrolysis was carried out in an external cell, before admitting the solution in to the cell. In the permeation studies, the transients were recorded as described earlier for various cathodic potentials and various thicknesses of the membrane.

(B) Capacity Determinations

The capacity of the iron electrode at various potentials was measured by using single sweep galvanostatic cathodic pulses. The electrode was polarised at a low cathodic current density about 10^{-5} amp cm^{-2} with a simple galvanostatic circuit consisting of two decade power resistors in series and a 120 v dry battery (Figure 43). Across one decade box a fast rise time mercury relay was connected so that on closing the contacts the decade resistance box was shorted. Thus, it was possible to obtain a rapid change of current density from a low value to the required high value. The attendant change in potential measured with respect to calomel reference electrode was registered by a Tektronix 535 A oscilloscope with a type D preamplifier. The trace was recorded on polaroid 46-C film with a Tektronix C12 camera. Calculations were made from tracings on graph paper at a magnification of 4 per cm of oscilloscope screen. The electrolyte solutions used were sulphuric acid, sodium hydroxide and acetate buffer solutions. All measurements were carried out at room temperature which was about $25 \pm 2^{o}C$.

33. RESULTS AND DISCUSSION

(A) Anomalies in the Permeation

A typical permeation transient is shown in Figure 44. As shown elsewhere the diffusion constant can be calculated from this curve in as many as five different ways (Devanathan, 1961, 1962). Since the identity of the diffusion constant evaluated by the various methods has already been established, we have calculated D by measuring the time taken for the permeation to reach 0.6299 of its limiting value. Thus time is the same as the classical time lag related to the diffusion constant by

$$T_{P=0.6299\ P_{\infty}} = T_{lag} = \frac{L^2}{6D} \qquad (116)$$

Hence a plot of $T_{P=0.6299\ P_{\infty}}$ vs. L^2 should be a straight line whatever the cathodic polarization conditions. Such a plot is shown in Figure 45, and thus linearity is proof of the constancy of the diffusion constant. A summary of these determinations for various thicknesses is presented in Table 9. In the first place we may note that the diffusion constant is independent of thickness. Several investigators have reported a variation of the diffusion constant with thickness, when calculated according to the classical time lag method. Thus Paleczewska and Ratajczyk (1961) find that for diffusion from the gas phase the diffusion constant increases from about 3.8×10^{-7} cm^2 sec^{-1} for Armco iron membranes of thickness 0.02 cm to about 3.1×10^{-6} cm^2 sec^{-1} for a thickness of 0.12 cm. They concluded that above a thickness of about 0.078 cm the diffusion constant is almost independent of thickness. It appears likely that this

TABLE 9

DIFFUSION COEFFICIENTS MEASURED FOR VARIOUS THICKNESSES

	t_o(sec)		
L(cm)	-1000 mV	-1400 mV	$D(\frac{cm^2}{sec})$
0.129	33.0	----	8.4×10^{-5}
0.129	----	33.7	8.2×10^{-5}
0.104	20.1	----	8.9×10^{-5}
0.104	----	21.0	8.6×10^{-5}
0.079	16.0	----	6.5×10^{-5}
0.079	----	12.4	8.4×10^{-5}
0.059	8.7	----	6.6×10^{-5}
0.059	----	7.0	8.3×10^{-5}
0.026	3.2	----	3.5×10^{-5}
0.026	----	2.6	4.3×10^{-5}
0.010	1	----	2×10^{-5}
0.010	----	1	2×10^{-5}
	Average D taken from Figure 45 is:		8.3×10^{-5}

effect is due to the surface exerting a controlling influence on the diffusion. In our experiments in acid solutions we observed a black film of finely divided iron depositing on the cathode if the solution was not adequately pre-electrolyzed and if the corrosive solutions were allowed to be in contact with the electrode without a cathodic protection current. Whenever such a film was formed the permeation current

dropped to about 3μ amp. Thus only membranes of sufficient thickness which have an overall permeation rate much less than 3μ amp will be unaffected by this film. All thinner membranes will show a constant permeation of 3μ cm whatever the thickness because the film controls the overall rate of permeation. With careful purification and pre-electrolysis complications due to surface control by this film can be avoided and reliable permeation transients can be recorded. As shown earlier, the plot of the reciprocal of the permeation rate against the thickness should be a straight line. In Figure 46 (Devanathan, 1961, 1962) we show such a plot for film free iron. The corresponding plot for membranes covered by film is also shown for comparison as dashed lines. It is seen that since the permeation rate is constant and controlled by the film, its equivalent thickness apparently depends on the slope of the line so that only for a higher thickness can any rational thickness dependence be observed. The above results and those obtained with palladium show that attention must be paid to removing films which can control permeation when at the surface (Devanathan and Stachurski, in press). It also appears that complex theories developed for explaining apparent anomalies in permeation must be revised.

It has been shown earlier that the rate of permeation of hydrogen under these experimental conditions should follow the equation (Devanathan, 1961, 1962)

$$\frac{1}{P} = \frac{L}{D\,\theta} + \frac{k^{s\rightarrow b}}{\theta} + \frac{2}{k^{b\rightarrow s}} \qquad (117)$$

where P is the permeation rate through a membrane of thickness l and

diffusion constant D. $k^{s \to b}$ and $k^{b \to s}$ are the rate constant for the transfer of hydrogen across the metal solution boundary. Under potentiostatic control the coverage of the cathode with hydrogen atoms θ will be constant. Hence at constant η, equation (117) predicts a linear plot for 1/P vs. L. The gradient $\frac{k^{s \to b}}{k^{b \to s} D \theta}$ and the intercept $\frac{2}{\theta \, k^{b \to s}}$ are both dependent on the reciprocal of 6. Since in general θ is larger the higher the η value, for high overpotentials, both the gradient and the intercept should be smaller.

Such plots for iron in 0.1 N sulphuric acid solutions and in an acetate buffer of pH 3.6 are given in figures 46 and 47. It is evident that the predictions of equation (117) are borne out and thus proof of the validity of the assumptions used in its derivation. One of these is that the rate constants $k^{s \to b}$ and $k^{b \to s}$ be large compared to the diffusion constant. From these plots it is possible to evaluate $k^{s \to b}$ since $\theta \, k^{b \to}$ is known from the intercept and D is also known independently. The order of magnitude of $k^{b \to s}$ has been found to be 10^{-2} cm^2 sec^{-1}, which is larger than the value of D. It will not be possible to evaluate $k^{s \to b}$ until the value of θ is obtained by independent methods.

3b. MECHANISM OF THE HYDROGEN EVOLUTION REACTION ON IRON

The following stages are possible for the hydrogen evolution reaction on iron.

$$Fe + H^+ + e_o \longrightarrow FeH \qquad (A)$$

$$FeH + FeH \longrightarrow 2Fe + H_2 \qquad (B)$$

$$FeH + H^+ + e_o \longrightarrow 2Fe + H_2 \qquad (C)$$

The results of the permeation plots are shown in Figures 46 and 47. The gradient of the 1/P vs. 1 plot at constant η is according to (117) given by

$$g = \frac{\overset{s \rightarrow b}{k}}{\underset{D \quad k \quad \theta}{b \rightarrow s}} \tag{118}$$

Hence

$$\frac{d \log \theta}{d\eta} = - \frac{d \log g}{d\eta} \tag{119}$$

In order to evaluate $\frac{d \log \theta}{d\eta}$ it suffices to plot - log g against η. Since the gradients of these lines are proportional to the surface coverage of the membrane with atomic hydrogen θ, the gradient of a plot of log g against η yields the ratio $\frac{d \log \theta}{d\eta}$. This ratio has characteristic values for certain mechanism sequences.

Thus if the reaction sequence is rate determining slow discharge (A), followed by rapid Tafel recombination (B), then in the steady state we have

$$i_c = \vec{k}_D (1 - \theta) e^{- \frac{\alpha \eta F}{RT}} = k_T \theta^2 \tag{120}$$

Since when discharge is rate-determining θ is usually small we may write the approximate form

$$\vec{k}_D e^{- \frac{\alpha \eta F}{RT}} = k_T \theta^2 \tag{121}$$

Therefore the expression for θ as a function of η from (121)

$$\theta = \frac{\vec{k}_D}{k_T} e^{- \frac{\alpha \eta F}{2RT}} \tag{122}$$

Noting that α is 0.5, since the Tafel plot has a gradient of $\frac{2RT}{F}$,

logrithmic differentiation of (122) yields,

$$\frac{d \log \theta}{d \eta} = \frac{F}{4RT} \qquad (123)$$

If the reaction sequence is rate-determining discharge (A) followed by fast electrochemical desorption (C) then for the steady state we have

$$i_c = \vec{k}_D (1 - \theta) e^{-\frac{\alpha \eta F}{RT}} = k_E \theta e^{-\frac{\alpha \eta F}{RT}} \qquad (124)$$

Hence

$$\frac{\theta}{1 - \theta} = \frac{k_E}{\vec{k}_D} = \text{constant} \qquad (125)$$

That is θ is potential independent, i.e.

$$\frac{d \log \theta}{d \eta} = 0 \qquad (126)$$

We show in Figure 48 such plots for the various solutions. The curves consist of two linear sections. The first has a gradient of about 0.36 ($volt^{-1}$) compared to $\frac{F}{2.3 \times 4RT}$ which is 0.42, the second has zero gradient. Hence in the above solutions the mechanism of the hydrogen evolution reaction must be slow discharge always; followed by Tafel recombination at low overpotentials, and electrochemical desorption at high overpotentials.

(A) Pseudo Capacity

With iron in acid solutions, the view that electrochemical desorption might be rate-determining has also been suggested. Should this be the case then the preceding step (A) must be in equilibrium

unless A is irreversible. In this case as shown by Bockris and Kita (1961) a pseudo capacity should be observed. A typical transient used in evaluating the double layer capacity is shown in Figure 49. The capacity in the early stages when the faradaic current is negligible is found to be about - 40 μF (See Figure 50). These values are much too close to the double layer values, and it is reasonable to conclude the absence of pseudo capacity. This result also confirms the mechanisms suggested all of which involve discharge as the rate-determining step.

35. CONCLUSIONS

From the above it is clear that the mechanism of the hydrogen evolution reaction is rate-determining discharge followed by Tafel recombination at low overpotential, and electrochemical desorption at high overpotentials (> 600 mv). These conclusions are also in harmony with the findings of Frumkin (1957), who used a qualitative method of establishing the mechanism, by observing the increase or decrease of overpotential at constant current when additional amounts of hydrogen are introduced by permeation.

REFERENCES

Ash, R. and Barrer, R. M., Phil. Mag. 4, 1197, 1959.

Ash, R. and Barrer, R. M., J. Phys. Chem. Solids, 16, 246, 1960.

Barrer, R. M., Trans. Faraday Soc., 35, 628, 1939.

Barrer, R. M., Diffusion in and through Solids, Cambridge University Press, p. 220, 1941.

Bockris, J. O'M., et al., Trans. Faraday Soc. 46, 918, 1950.

Bockris, J. O'M., Modern Aspects of Electrochemistry, Elsevier Publ. Co., Amsterdam, 1951.

Bockris, J. O'M. and Parsons, R., Trans. Faraday Soc., 47, 914, 1951.

Bockris, J. O'M. and Devanathan, M. A. V., O.N.R. Tech. Rep. No. ONR 551(22), No. 1 (Aug. 31, 1957).

Bockris, J. O'M. and Conway, B. E., J. Chem. Phys., 26, 532, 1957.

Bockris, J. O'M., Pentland, N. and Sheldon, E. J., Electrochem. Soc. 104, 182, 1957.

Bockris, J. O'M. and Thacker, R., O.N.R. Tech. Rep. No. 3 ONR 551(22) (Dec. 31, 1959)

Bockris, J. O'M., Devanathan, M. A. V., and Mehl, W., J. Electroanal. Chem. 1, 143, 1959/60.

Bockris, J. O'M. and Kita, H., J. Electrochem. Soc., 108, 676, 1961.

Bowden, F. P., Proc. Roy. Soc., A125, 440, 1929.

Breiter, M., Knorr, C. A., and Volkl, V., Z. Elektrochem., 59, 681, 1955.

Daynes, H. A., Proc. Roy. Soc. A97, 286, 1920.

Devanathan, M. A. V., and Selvaratnam, M., Trans. Faraday Soc. 56, 1, 1960.

Devanathan, M. A. V., O.N.R. Tech. Rep. No. 3, ONR 551(22) NR036-028 (Feb. 28, 1961)

Devanathan, M. A. V., In course of publication, 1962.

Devanathan, M. A. V. and Stachurski, Z., Proc. Roy. Soc. (London) A1962 (In press).

Devanathan, M. A. V., Trans. Faraday Soc., 1962 (In press).

Devanathan, M. A. V. and Stachurski, Z., J. of Electrotechnology, 1962 (In press).

Frank, R. C. and Thomas, J. E., J. Phys. Chem. Solids, 16, 144, 1960.

Frumkin, A. N., and Slysin, Acta Physicochimica, U.S.S.R.,

3, 791, 1935.

4, 911, 1936.

5, 819, 1936.

Frumkin, A. N. et al., Kinetika Elektrodnokh, Protsessov, Izdatel'stuo Moskov, Univ. Moscow, pp. 45-46, 1952.

Frumkin, A. N., Z. Physik. Chemie, 207, 321, 1957.

Kortum, G. and Bockris, J. O'M. Textbook of Electrochemistry, Elsevier Publ. Co., Amsterdam, p. 362, 1951.

Norberg, R. E., Phys. Rev. 86, 745, 1952.

Palezewska, W. and Ratajczyk, I., Bull, De L'Acad. Polon. des Sciences, IX. 267, 1961

Parson, J. and Butler, J. A. V., Trans. Faraday Soc., 34, 1163, 1939.

Silberg, P. A. and Bachman, C. H., J. Chem. Phys. 29, 777, 1958.

Velselovsky, V., Acta Physicochim., U.R.S.S., 11, 815. 1939.

Wahlin, H. B. and Nauman, V. O., J. Appl. Phys. 24, 42, 1953.

MILLISECONDS

FIG. 2

PLATINUM GALVANOSTATIC

SOLUTION 1 M. H_2SO_4
ROOM TEMP.
AREA OF Pt. 0.304 cm^2
CATHODIC c.d = 10^{-} amp/cm^2
ANODIC c.d. = 0.61 amp/cm^2

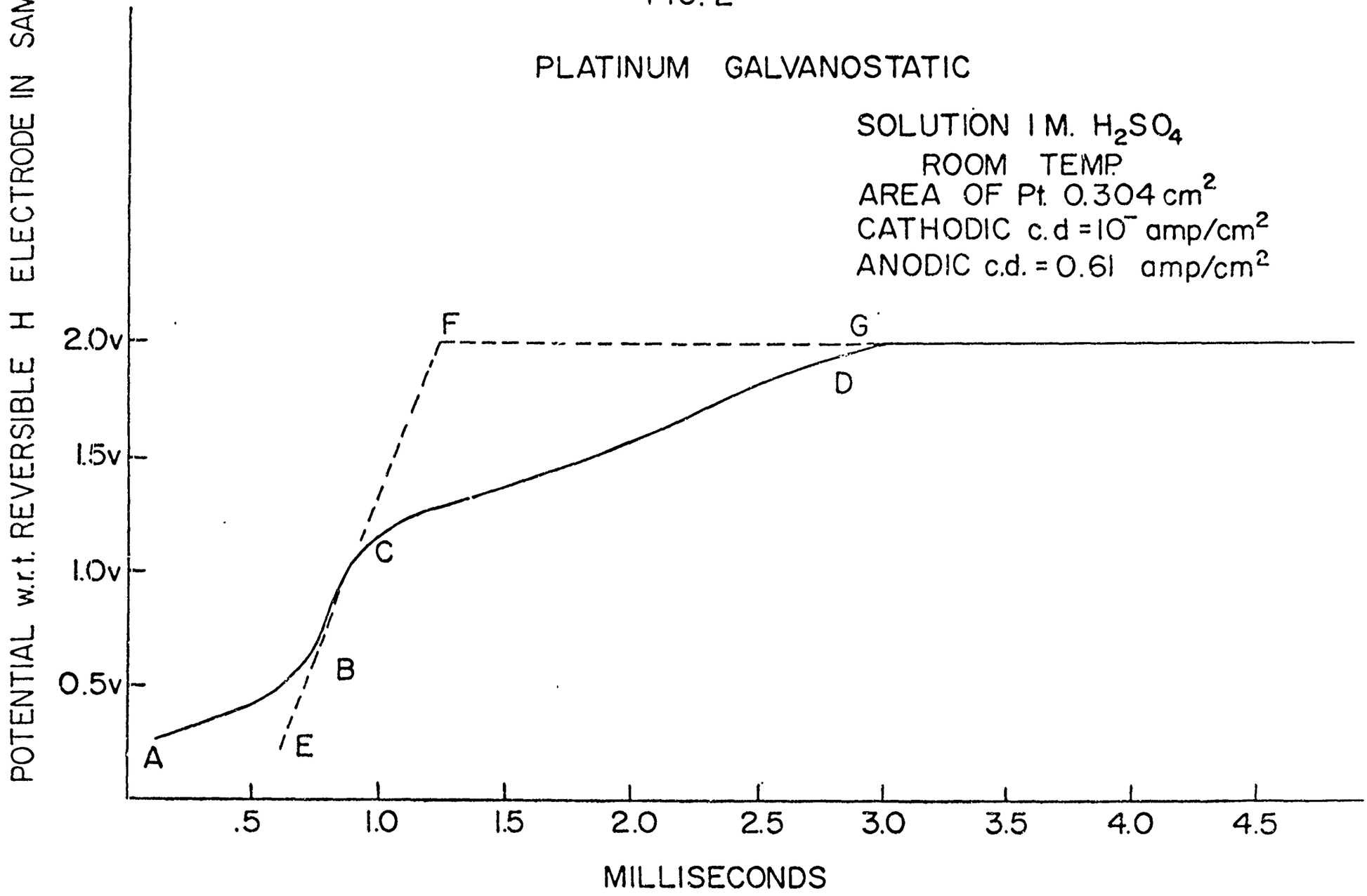

FIG. 3

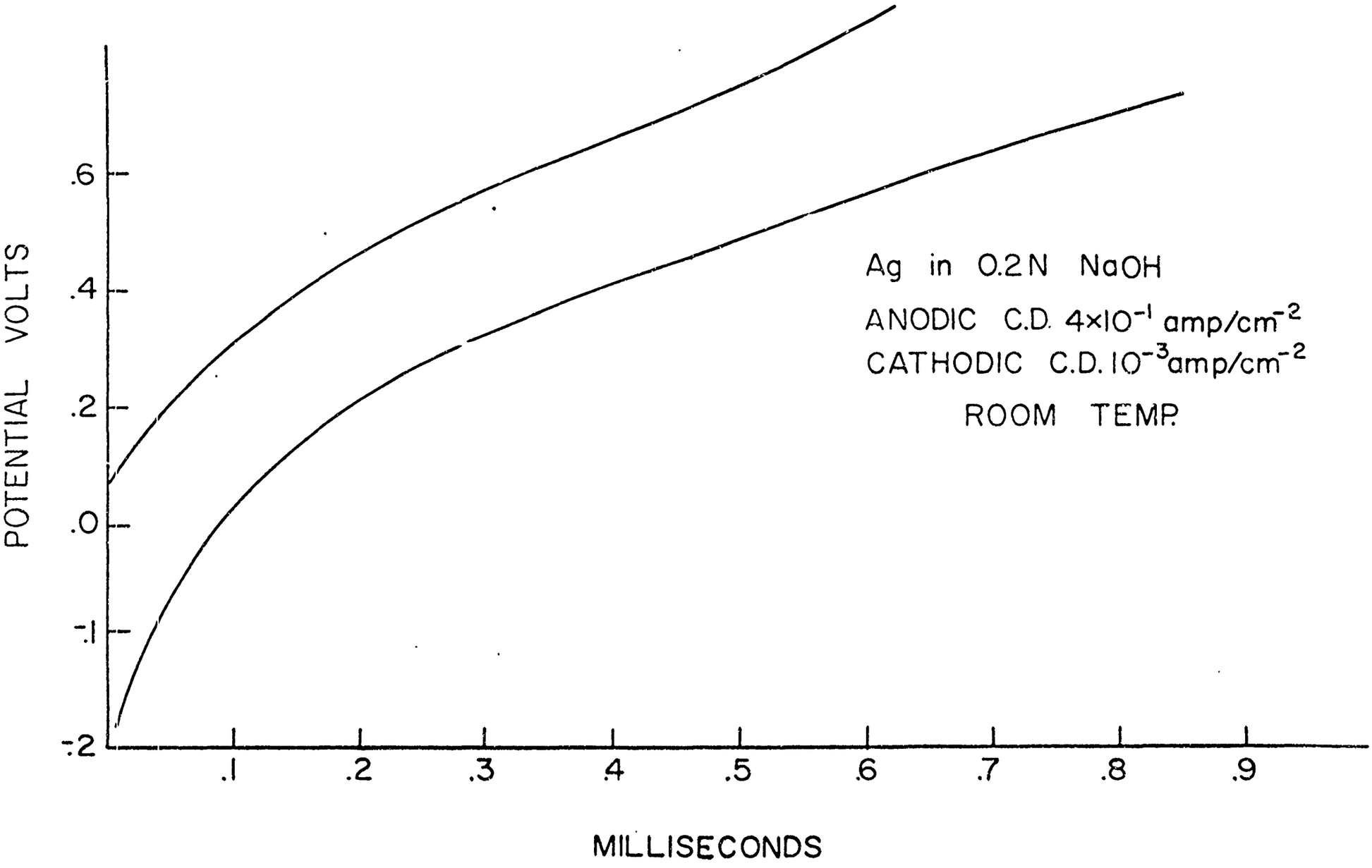
POTENTIAL VOLTS
.6
.4
.2
.0
-.1
-.2
.1
.2
.3
.4
.5
.6
.7
.8
.9
MILLISECONDS
Ag in 0.2N NaOH
ANODIC C.D. 4×10^{-1} amp/cm^{-2}
CATHODIC C.D. 10^{-3} amp/cm^{-2}
ROOM TEMP.

FIG. 4

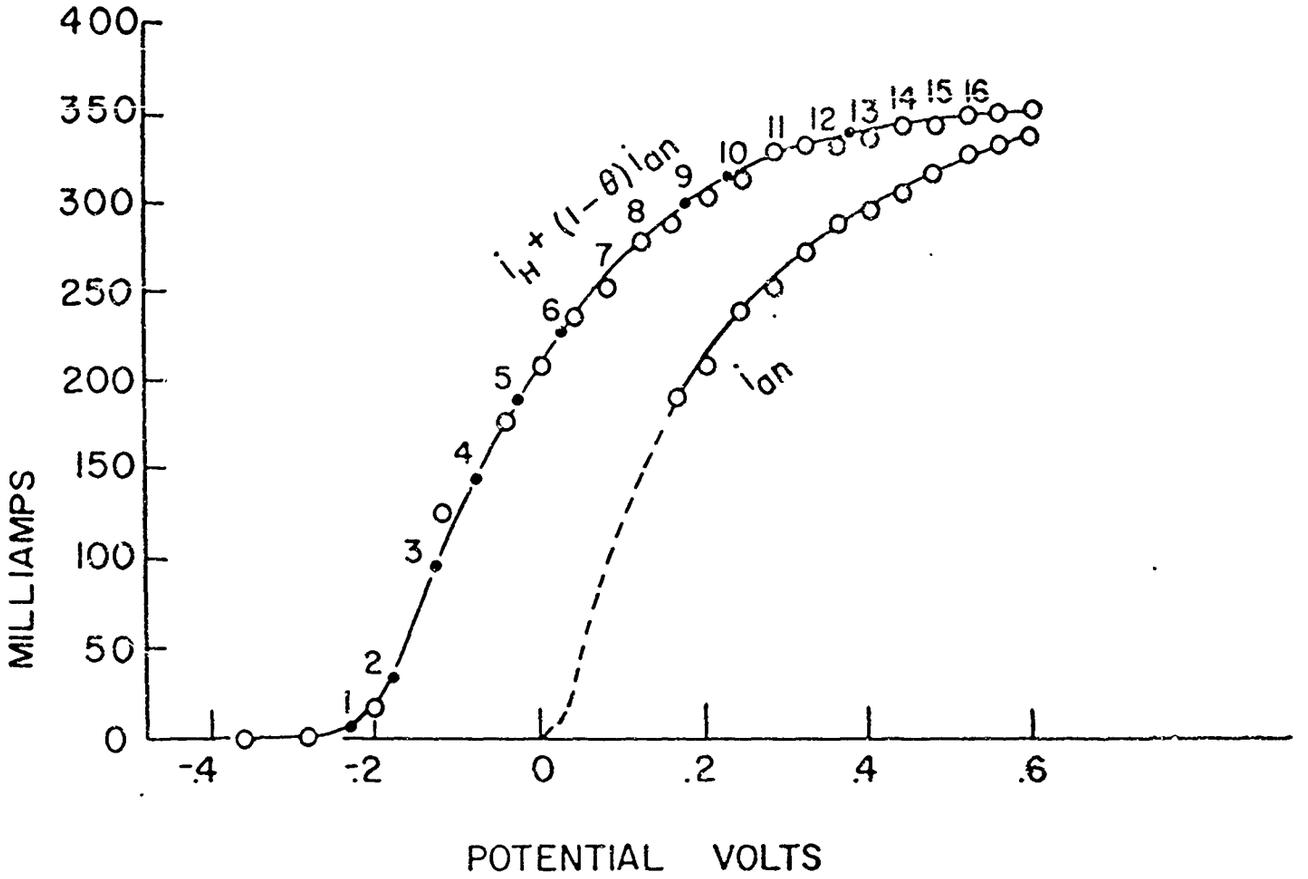
400
350
300
250
200
150
100
50
0
MILLIAMPS
-.4
-.2
0
.2
.4
.6
POTENTIAL VOLTS
$i_H + (1-\theta) i_{an}$
i_{an}
1
2
3
4
5
6
7
8
9
10
11
12
13
14
15
16

FIG. 5

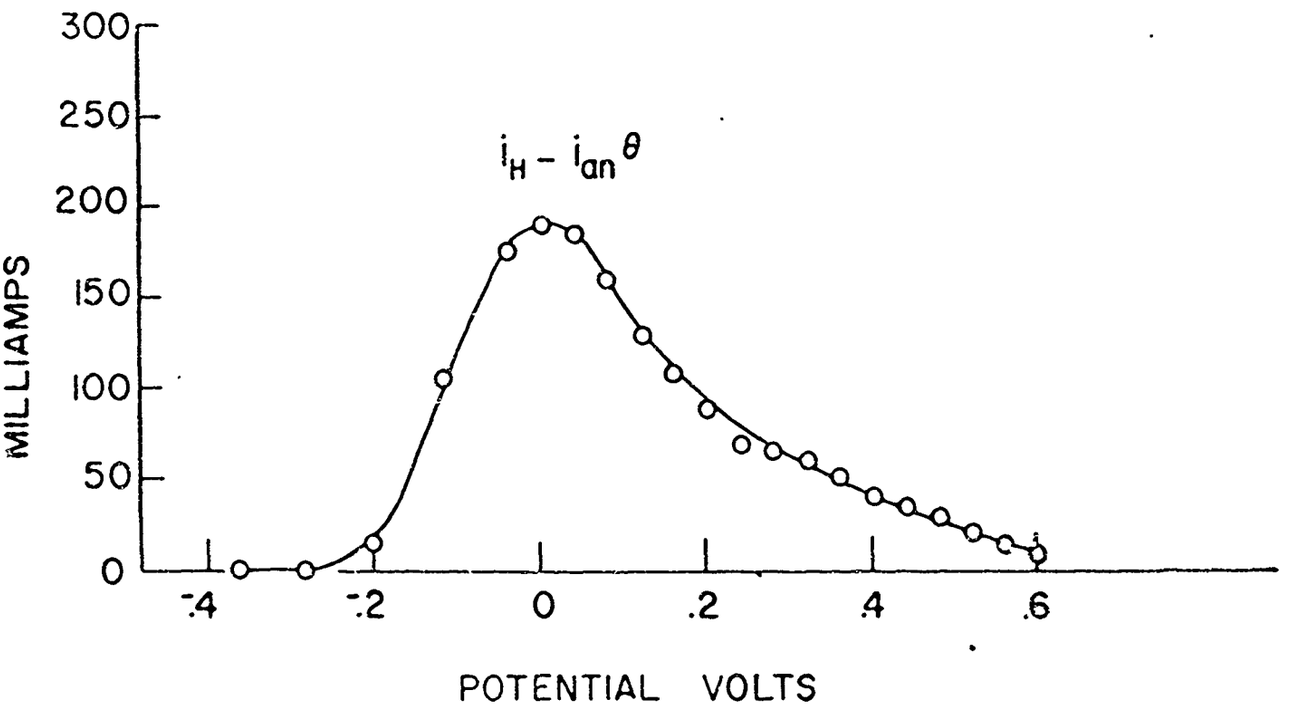
300
250
200
150
100
50
0
MILLIAMPS
-.4
-.2
0
.2
.4
.6
POTENTIAL VOLTS
$i_H - i_{an}\theta$

FIG. 7

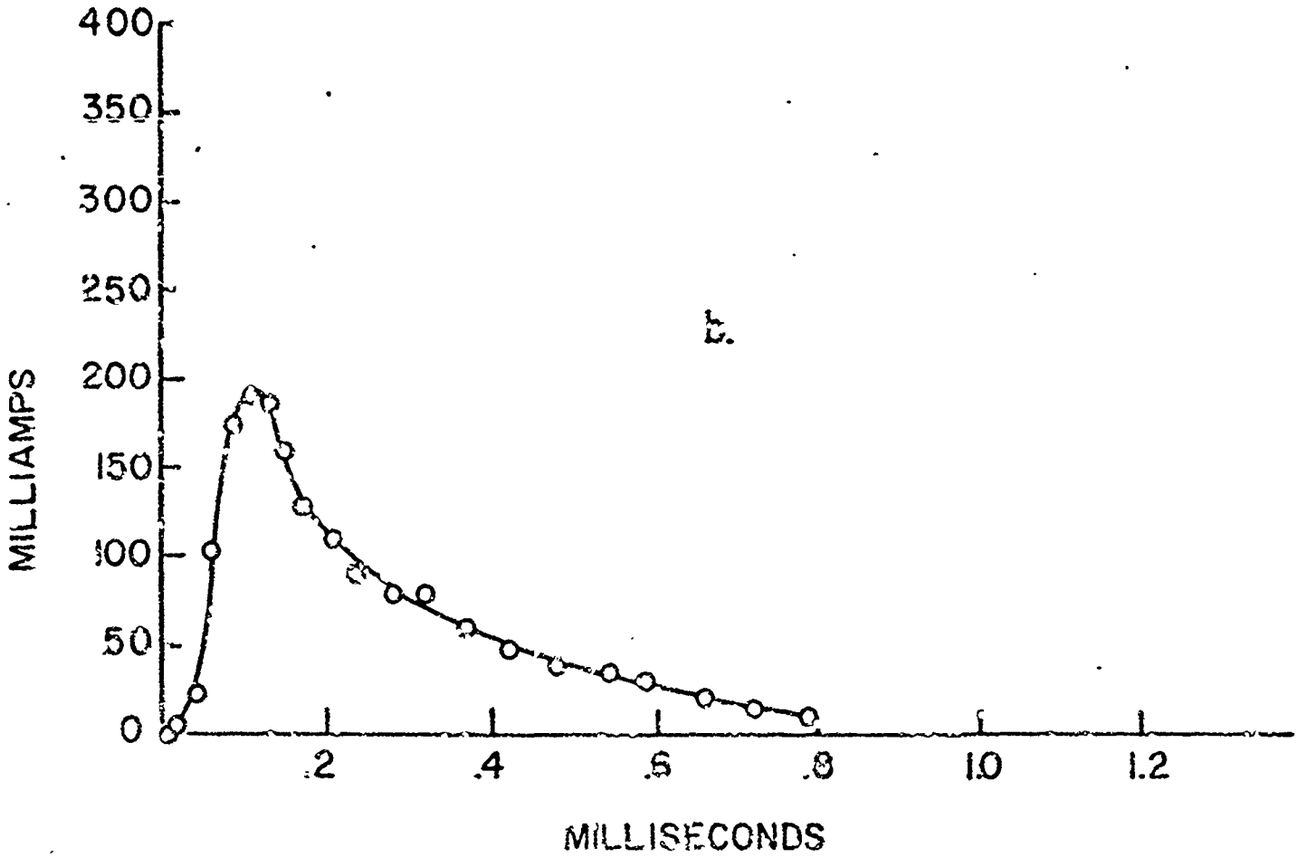

b.

Fig 2

FIG. 6

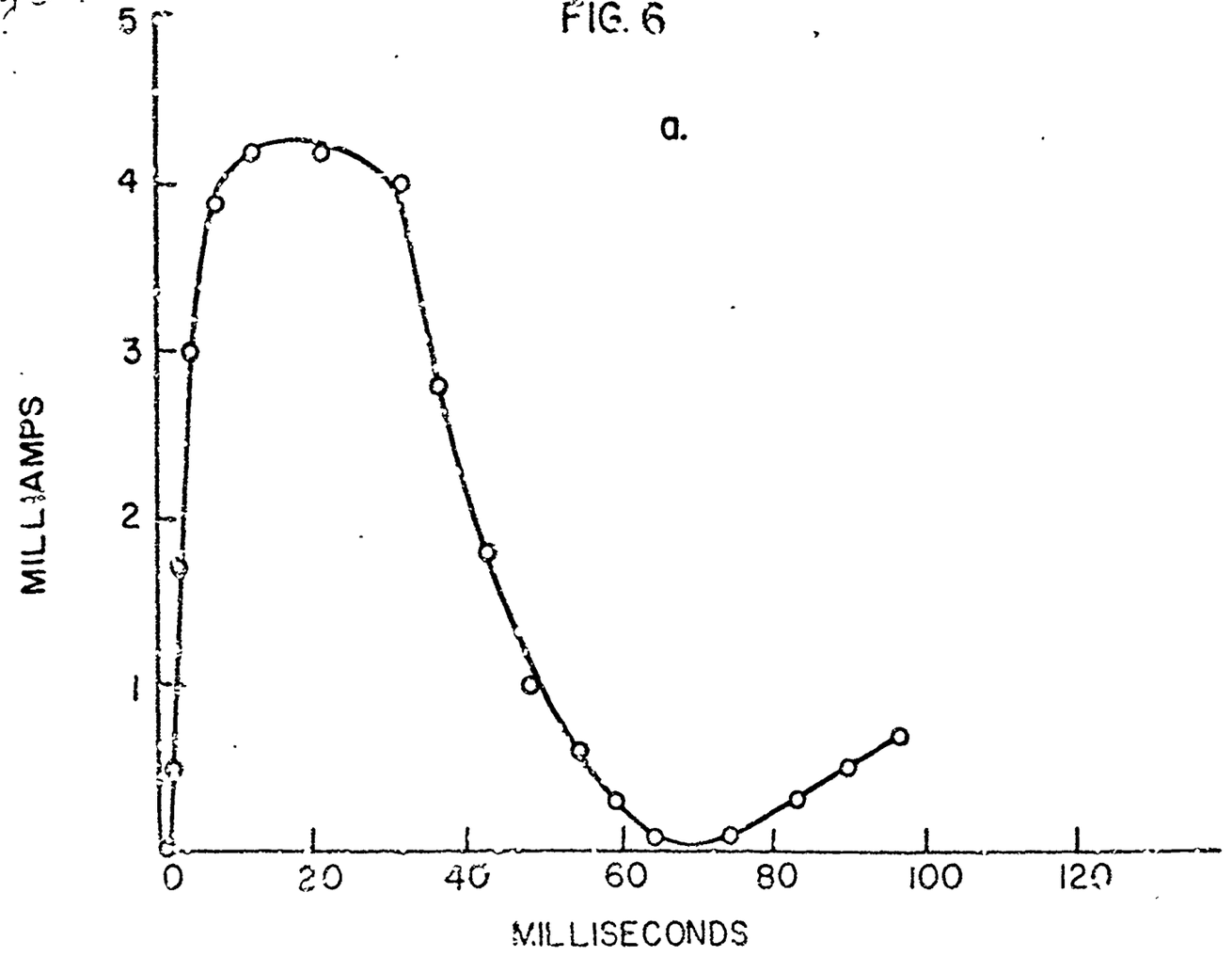

a.

FIG. 8

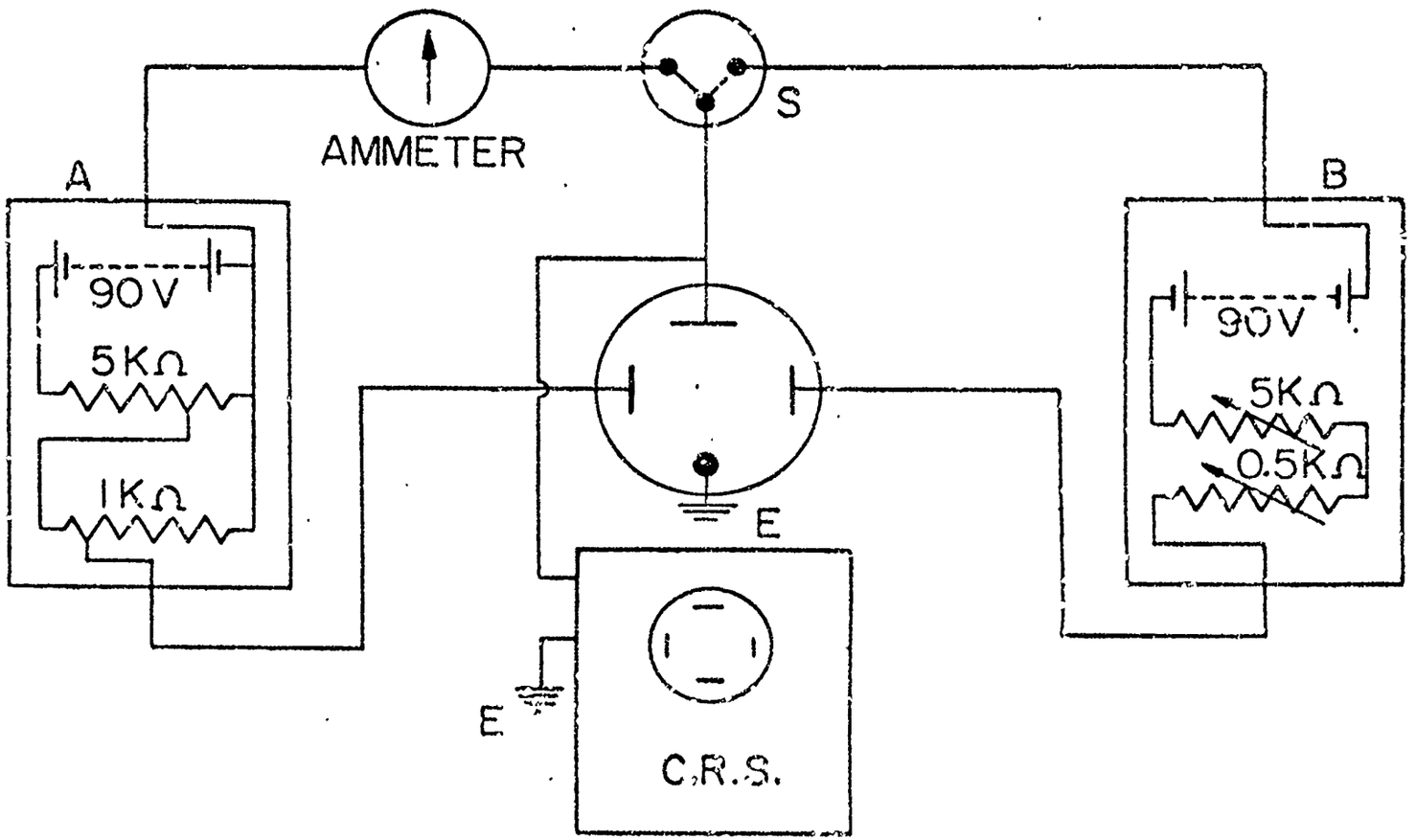

ANODIC C.D. (SCALE ACTUAL c.d./20)

FIG. 9

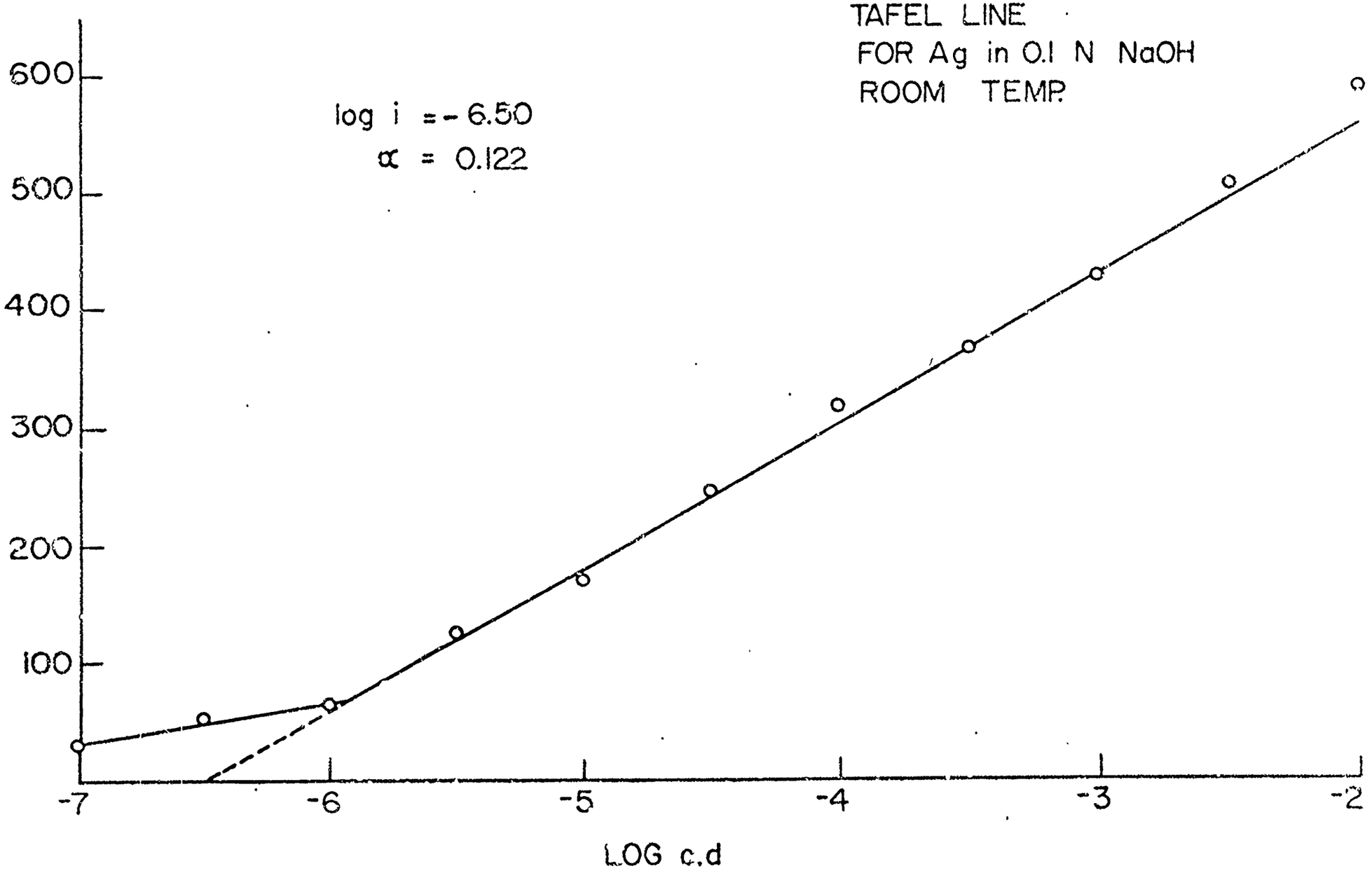

FIG. 10

VARIATION OF COULOMBS
ON Ag in 0.1 N NaOH
WITH ANODIC CHARGING c.d.

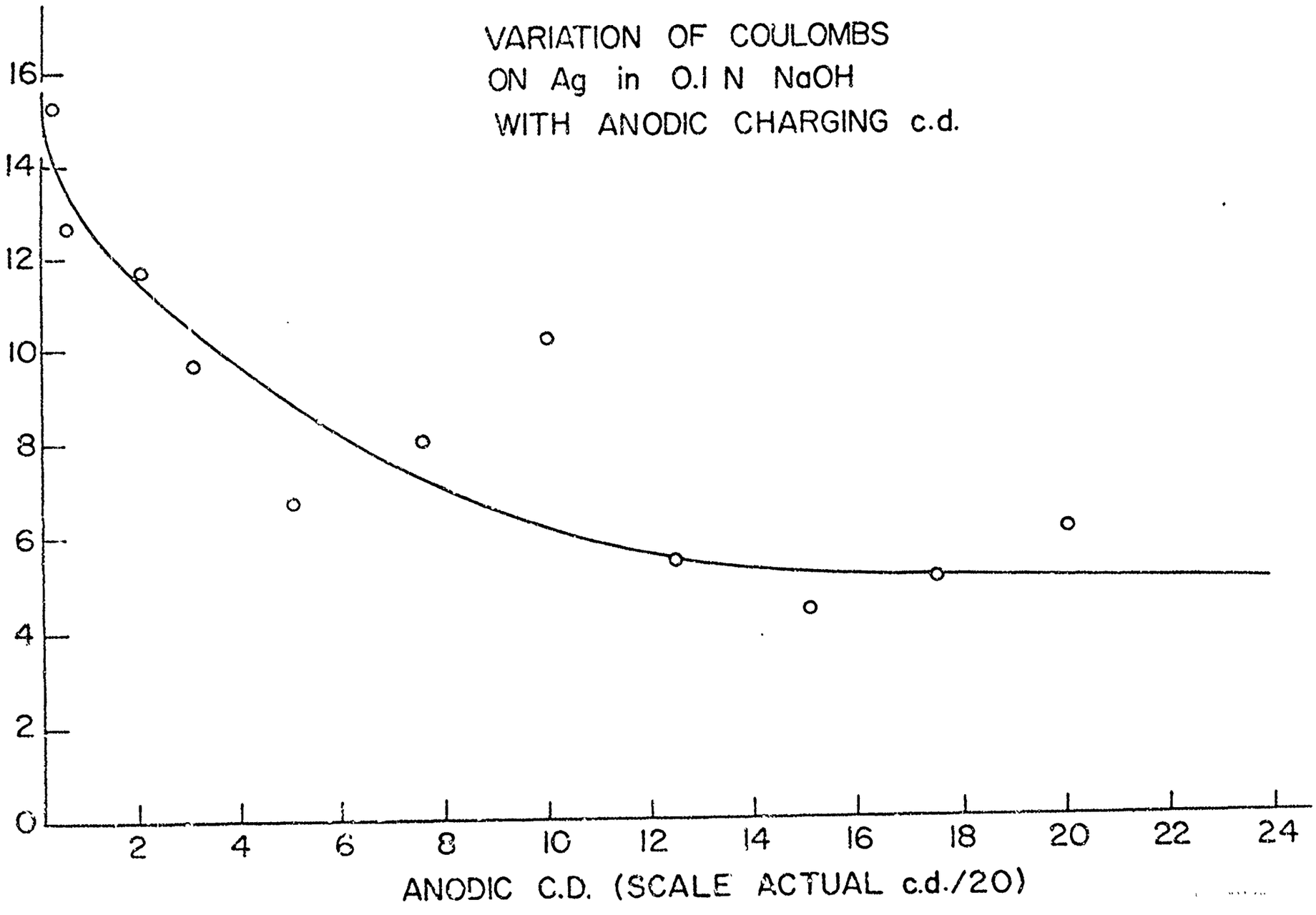

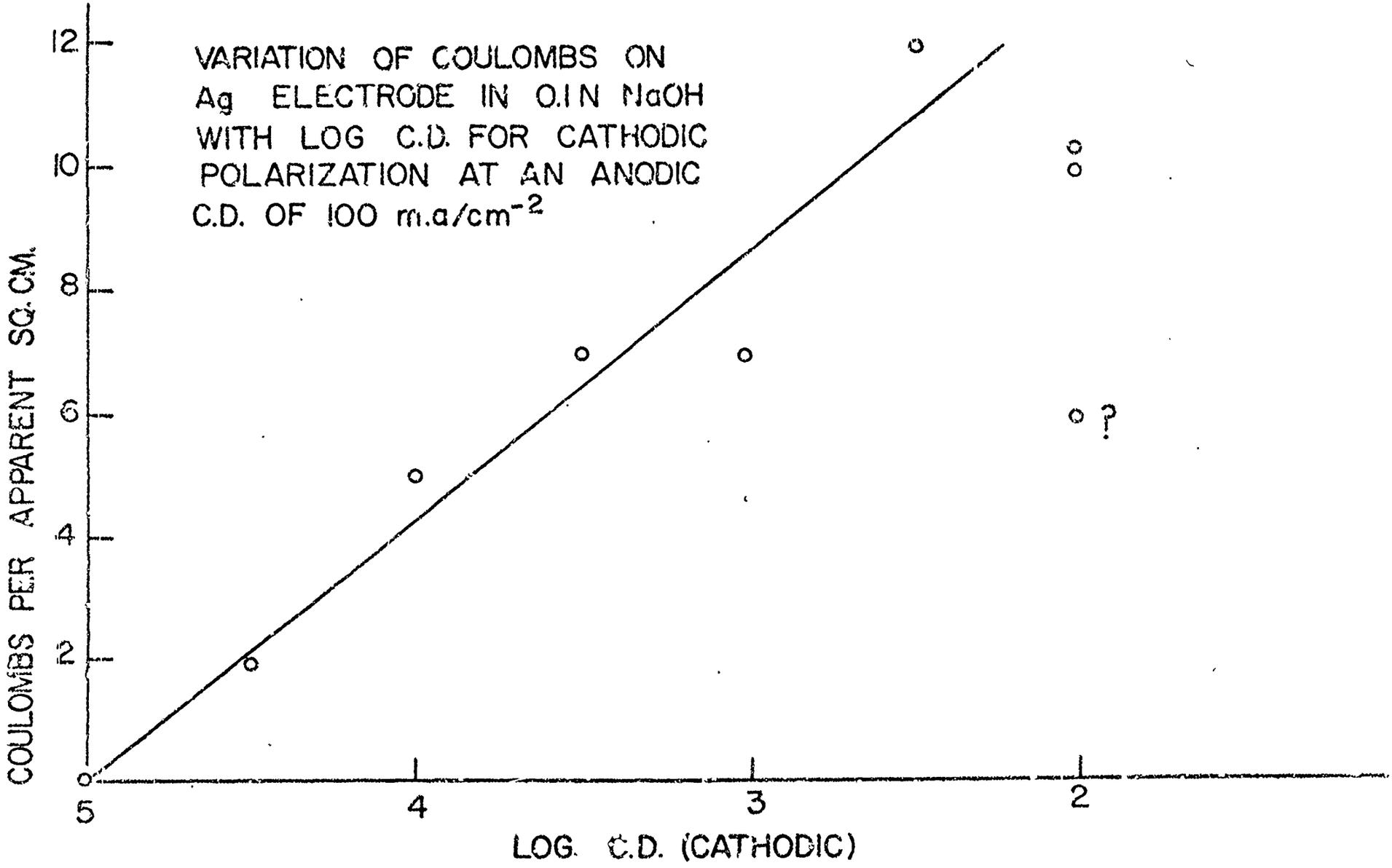
VARIATION OF COULOMBS ON
Ag ELECTRODE IN 0.1 N NaOH
WITH LOG C.D. FOR CATHODIC
POLARIZATION AT AN ANODIC
C.D. OF 100 m.a/cm^{-2}
COULOMBS PER APPARENT SQ. CM.
0
2
4
6
8
10
12
5
4
3
2
?
LOG. C.D. (CATHODIC)

FIG.11

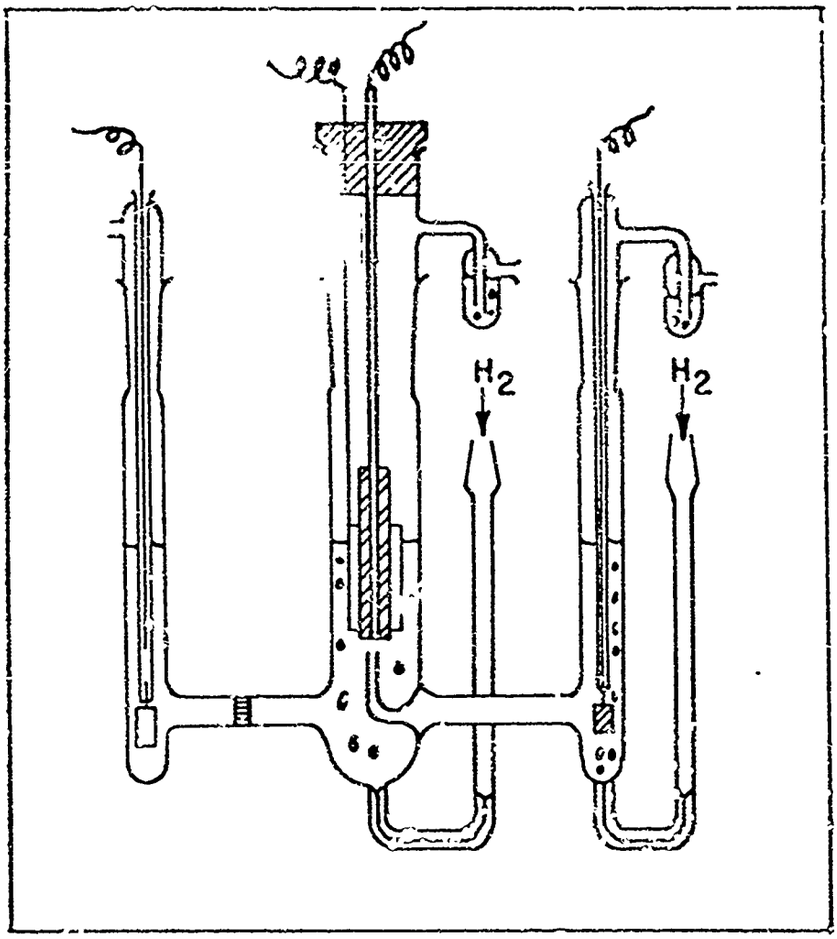
H2
H2

FIG. 12

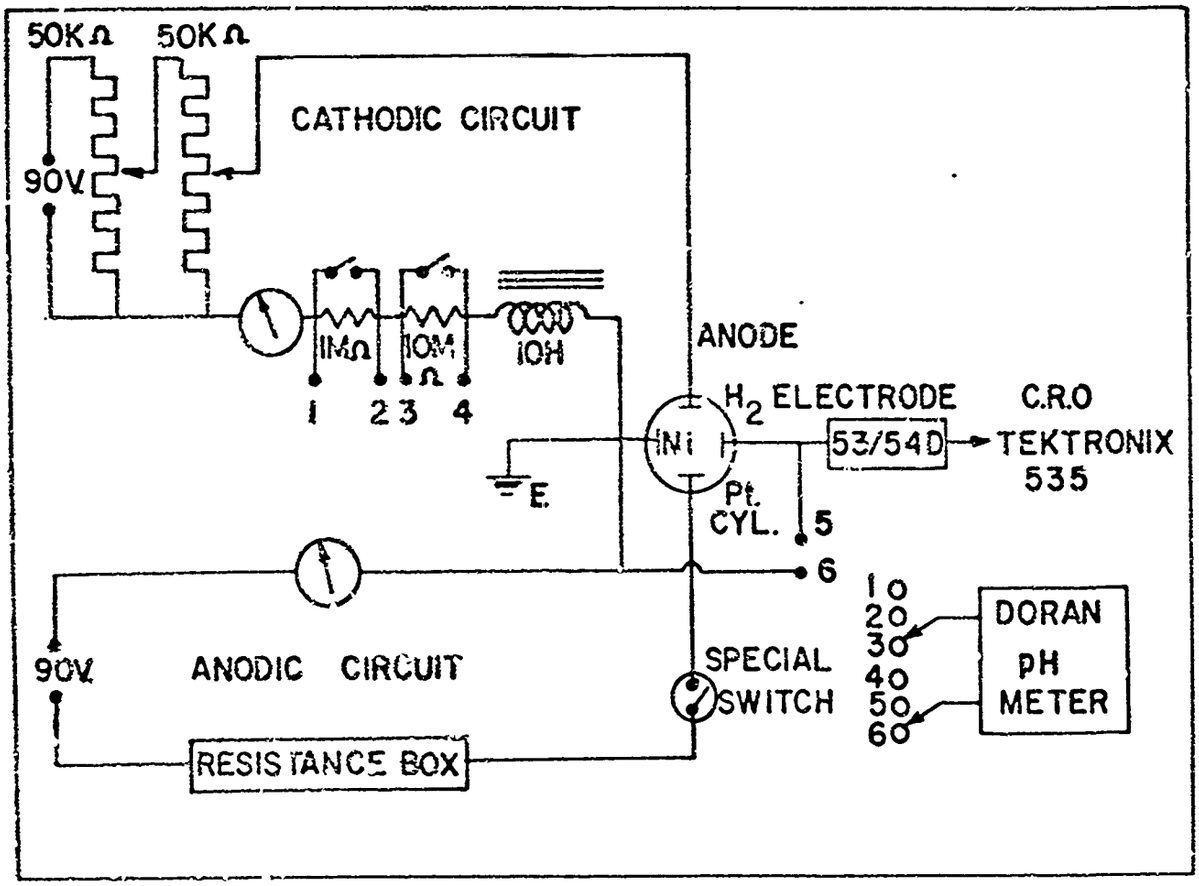
50KΩ
50KΩ
CATHODIC CIRCUIT
90V
1MΩ
10MΩ
10H
1
2
3
4
ANODE
H2 ELECTRODE
C.R.O
TEKTRONIX
535
53/54D
Ni
E
Pt.
CYL.
5
6
90V
ANODIC CIRCUIT
SPECIAL
SWITCH
10
20
30
40
50
60
DORAN
pH
METER
RESISTANCE BOX

FIG. 13

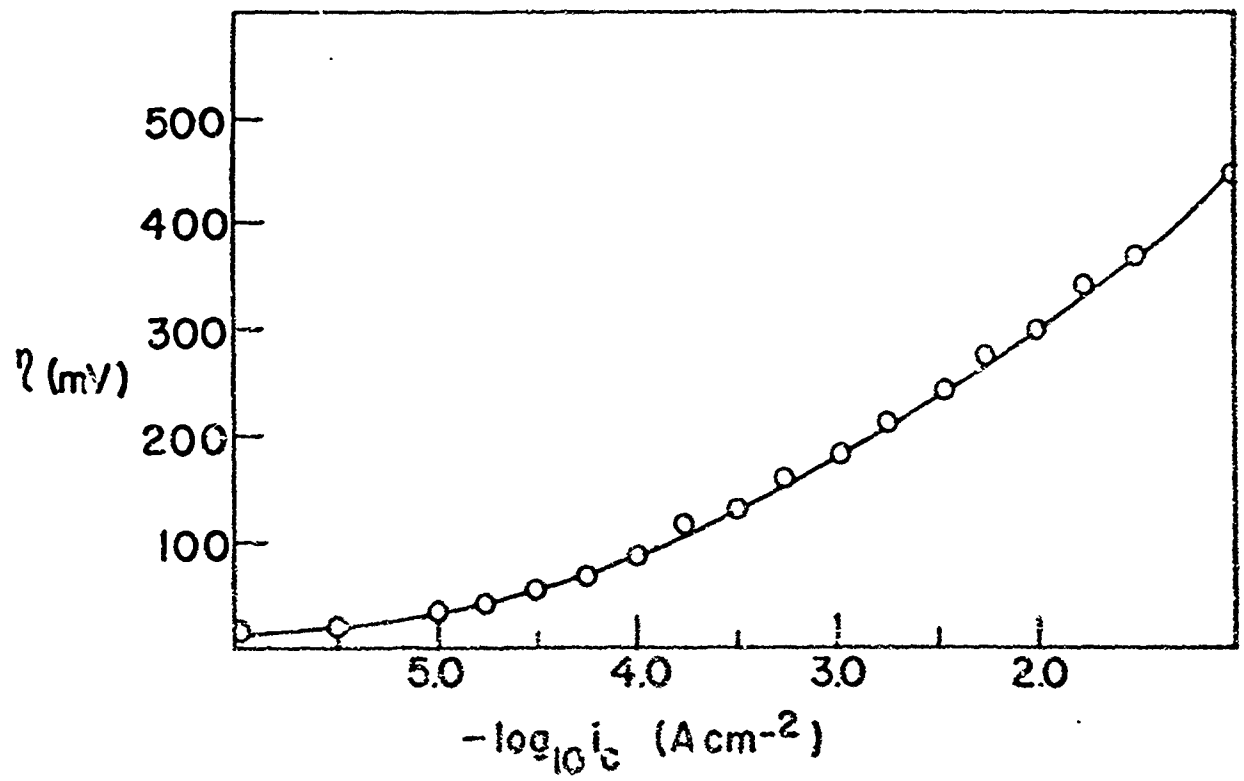

FIG.14

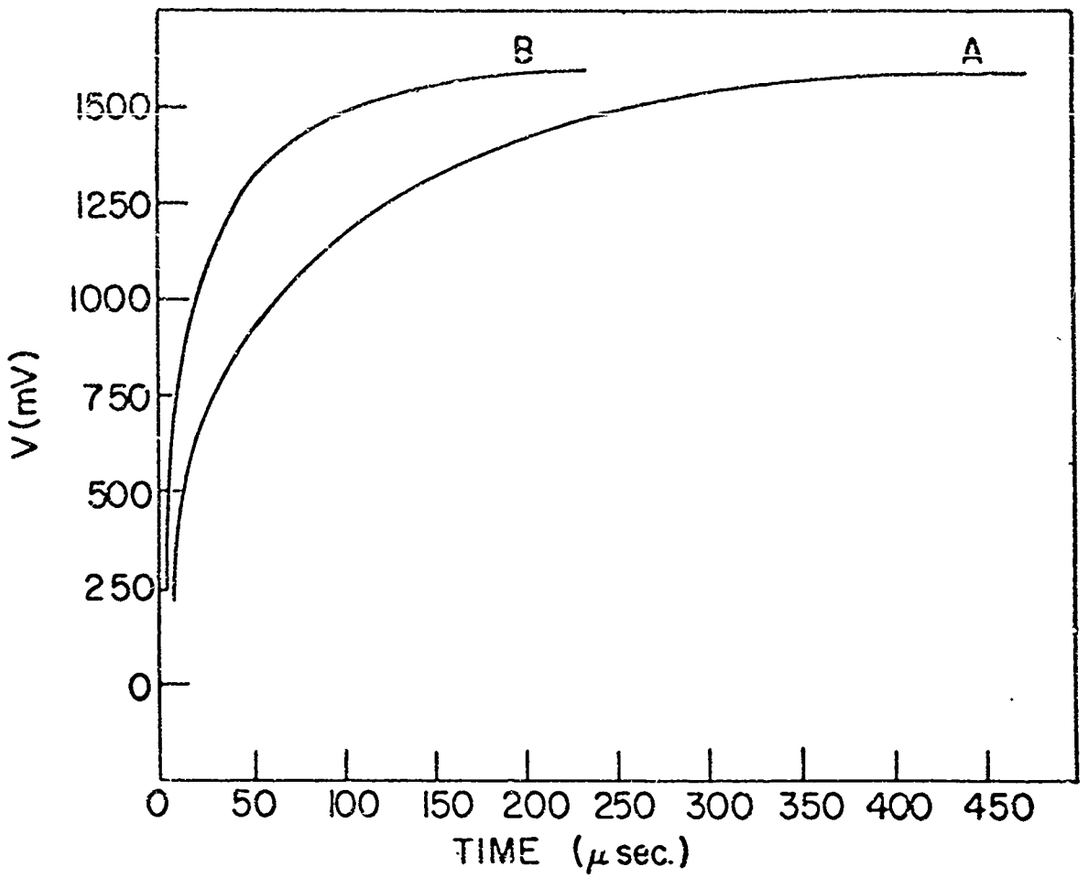
B
A
1500
1250
1000
750
500
250
0
V(mV)
0
50
100
150
200
250
300
350
400
450
TIME (μ sec.)

FIG. 15

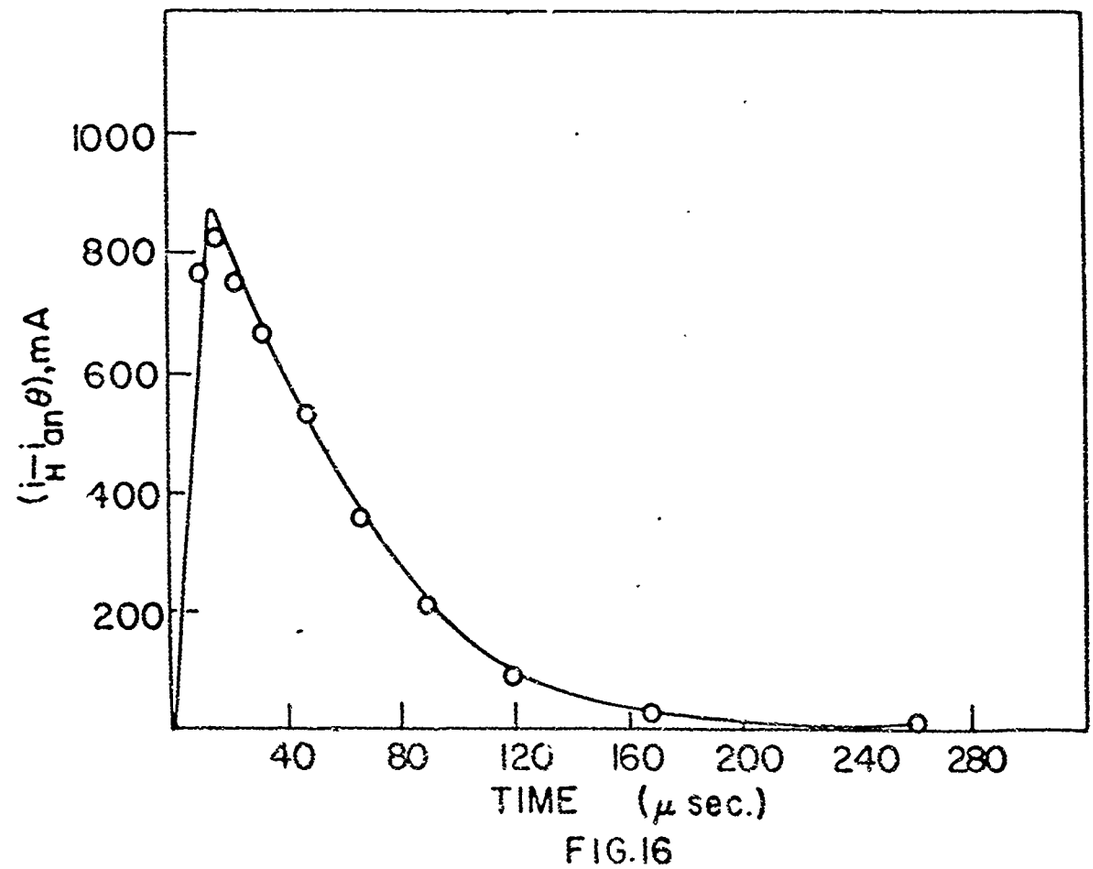
1000
800
600
400
200
$(i-i_H i_{an}\theta)$, mA
40
80
120
160
200
240
280
TIME (μ sec.)

FIG. 16

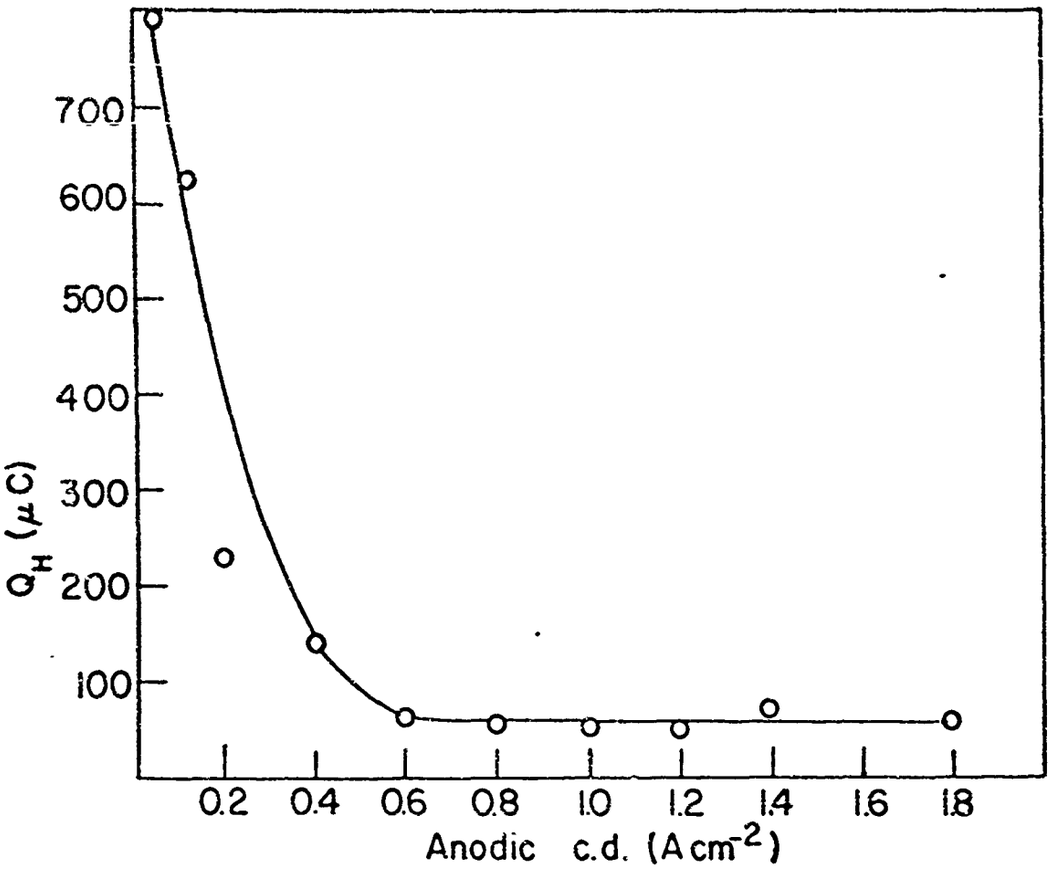
700
600
500
400
300
200
100
Q_H (μC)
0.2
0.4
0.6
0.8
1.0
1.2
1.4
1.6
1.8
Anodic c.d. (A cm^{-2})

FIG. 17

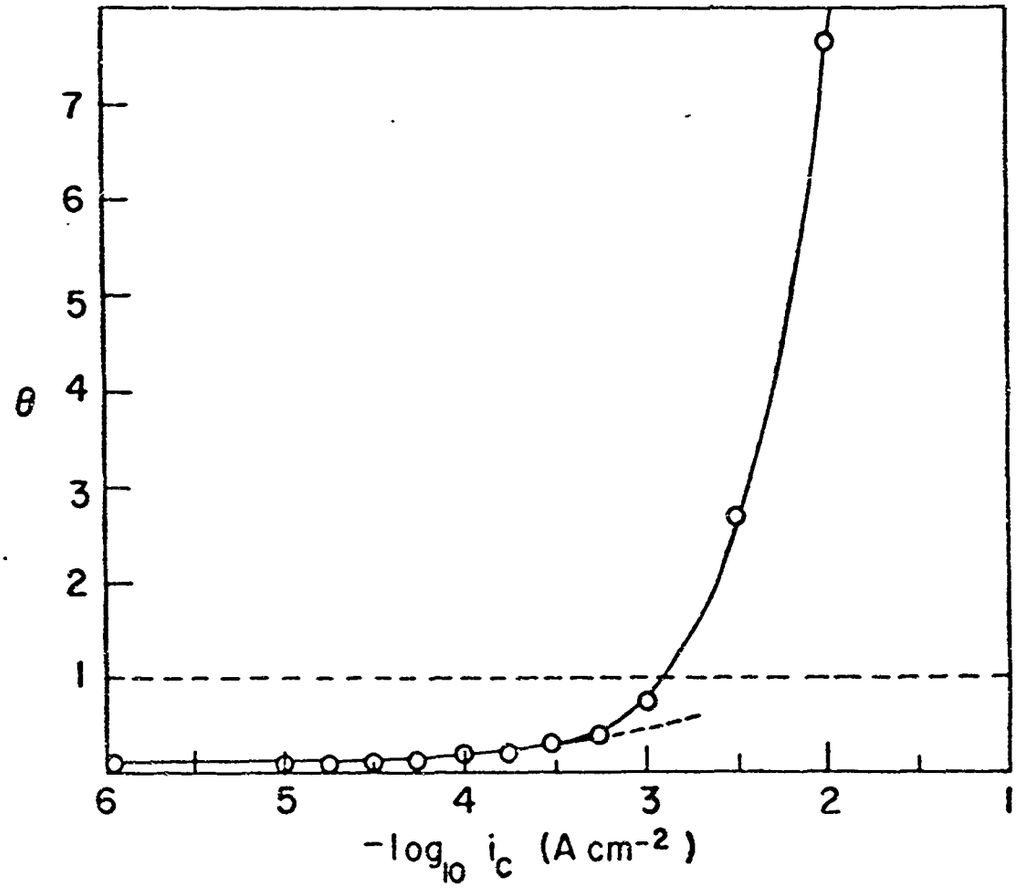
7
6
5
4
3
2
1
θ
6
5
4
3
2
1
$-\log_{10} i_c$ (A cm^{-2})

FIG. 18

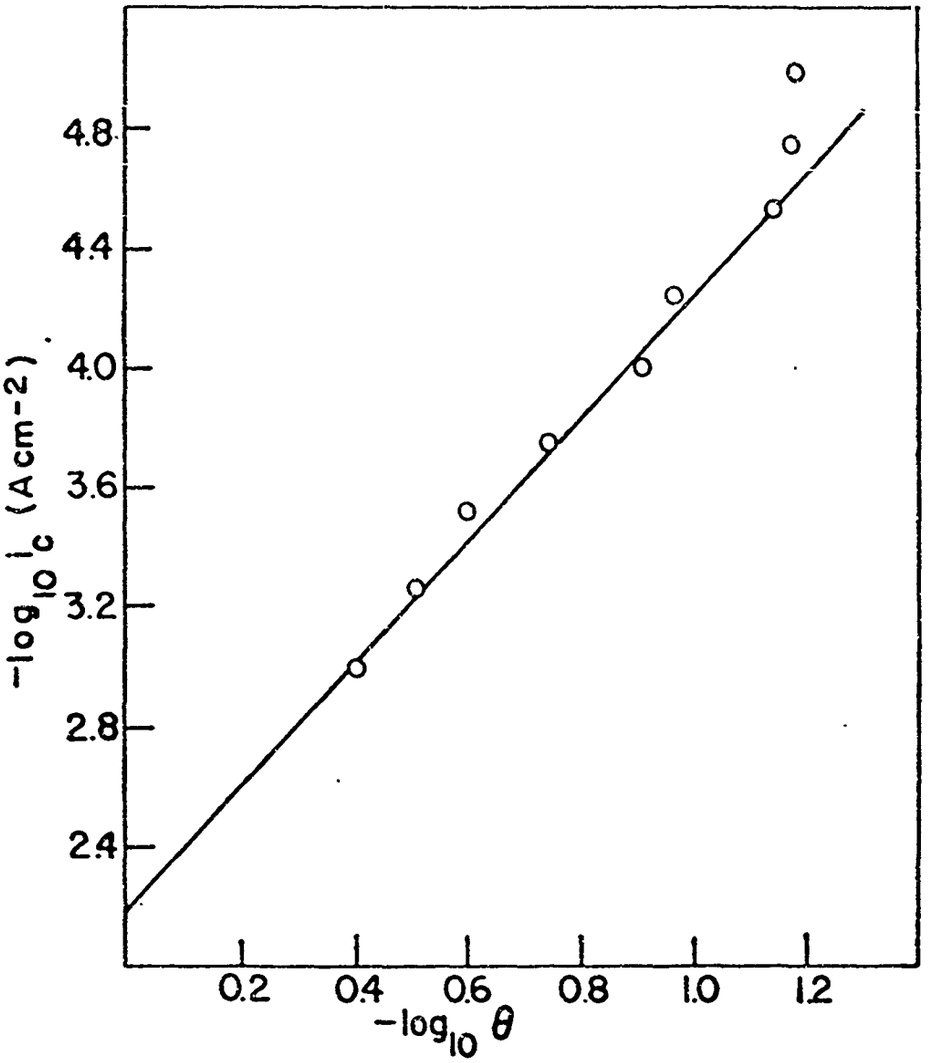
4.8
4.4
4.0
3.6
3.2
2.8
2.4
$-\log_{10} i_c$ (A cm^{-2})
0.2
0.4
0.6
0.8
1.0
1.2
$-\log_{10} \theta$

FIG. 19

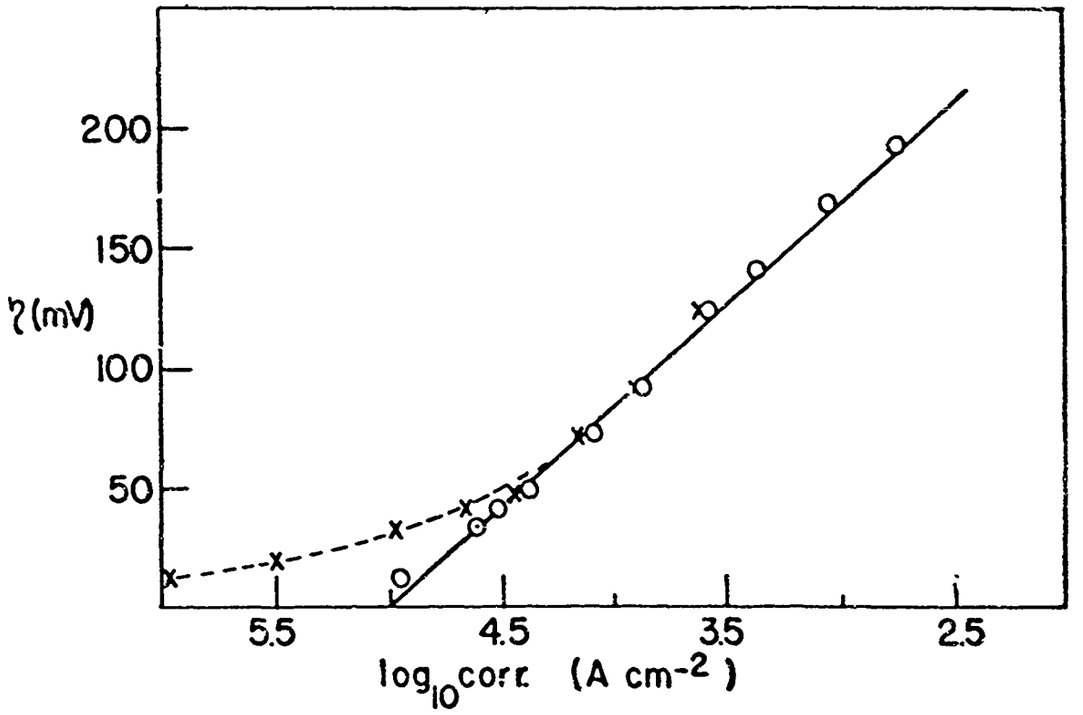
200
150
100
50
η (mV)
5.5
4.5
3.5
2.5
$\log_{10}$ corr. (A cm^{-2})

FIG. 20

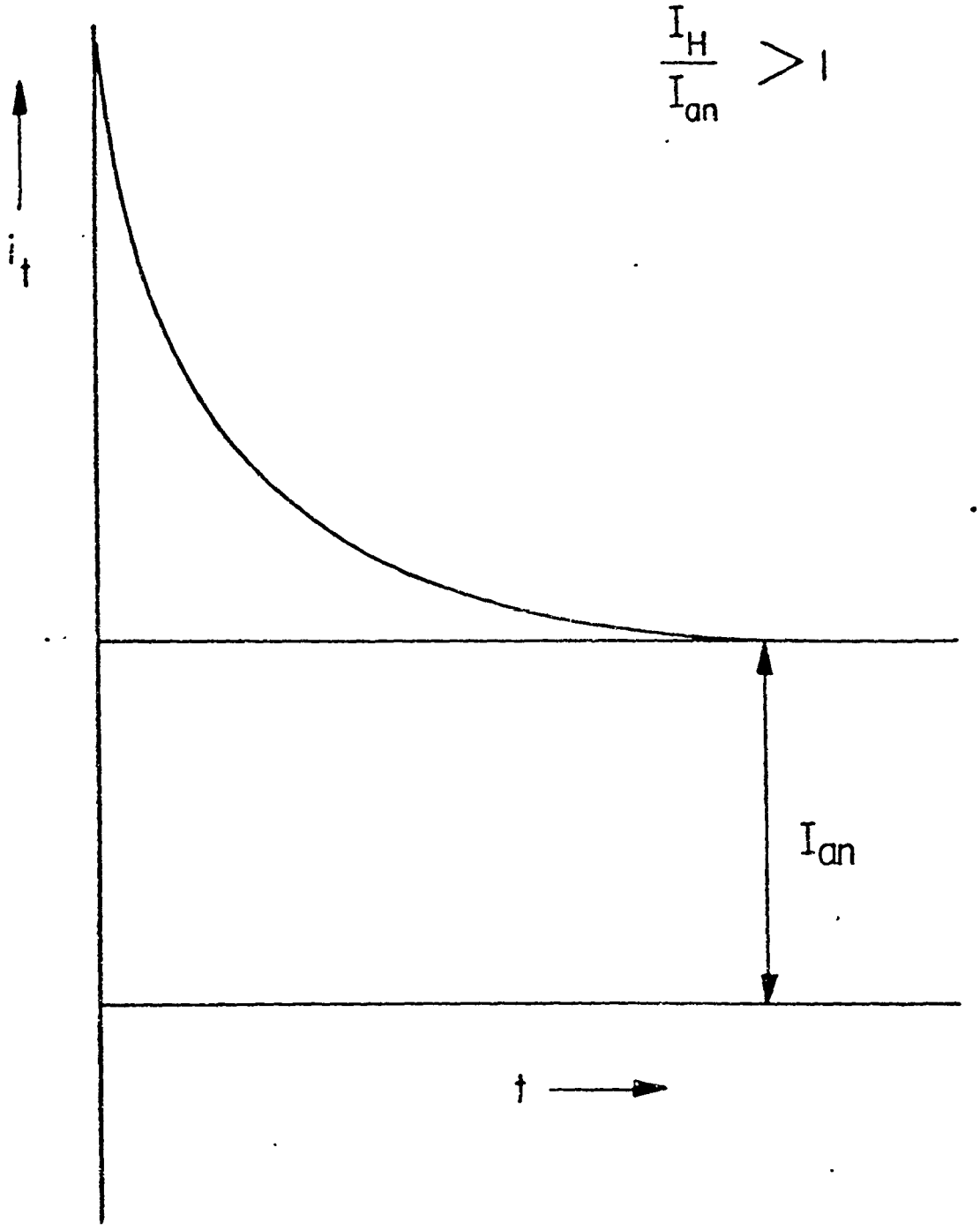

FIG. 21

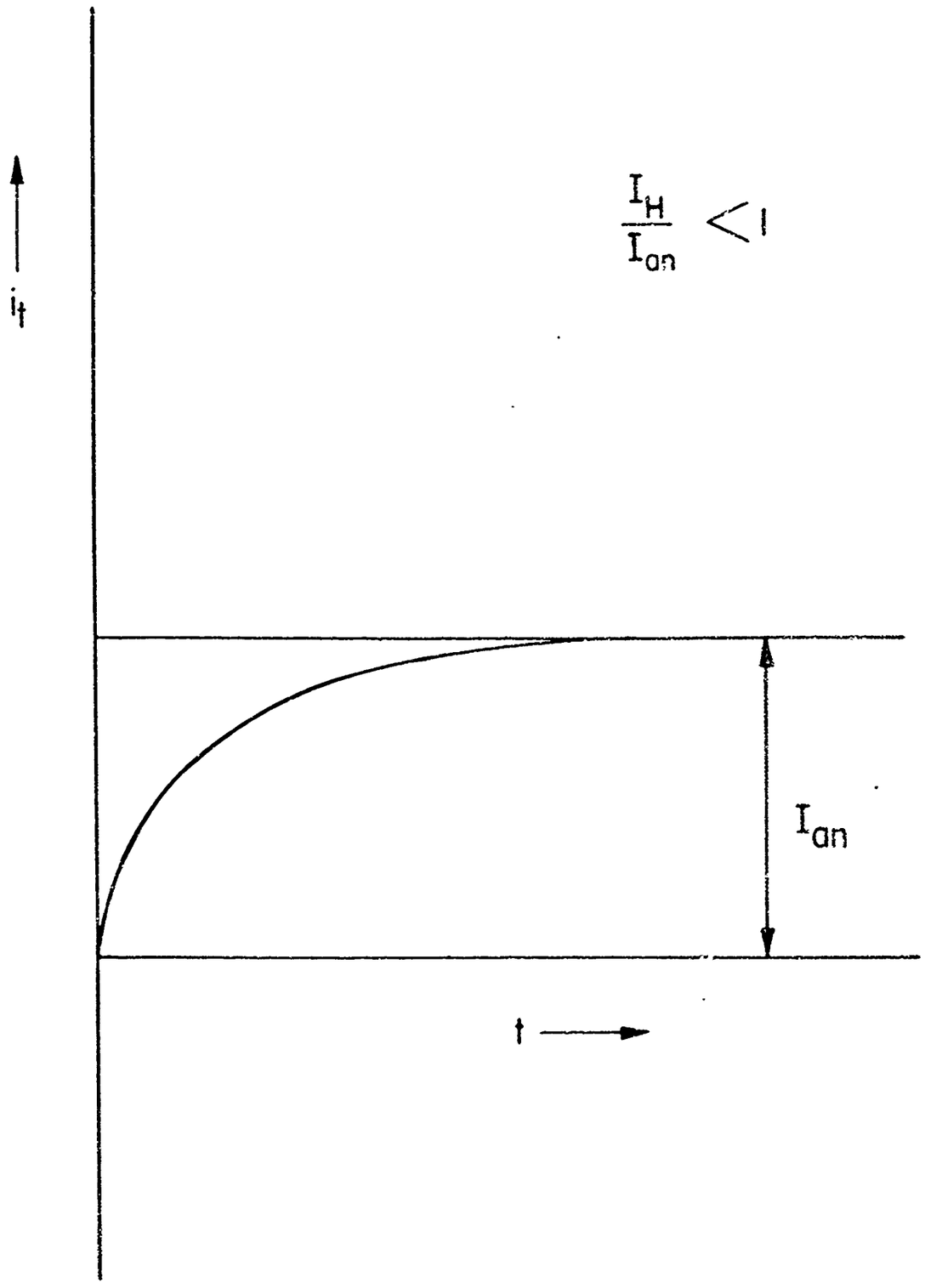

FIG.22

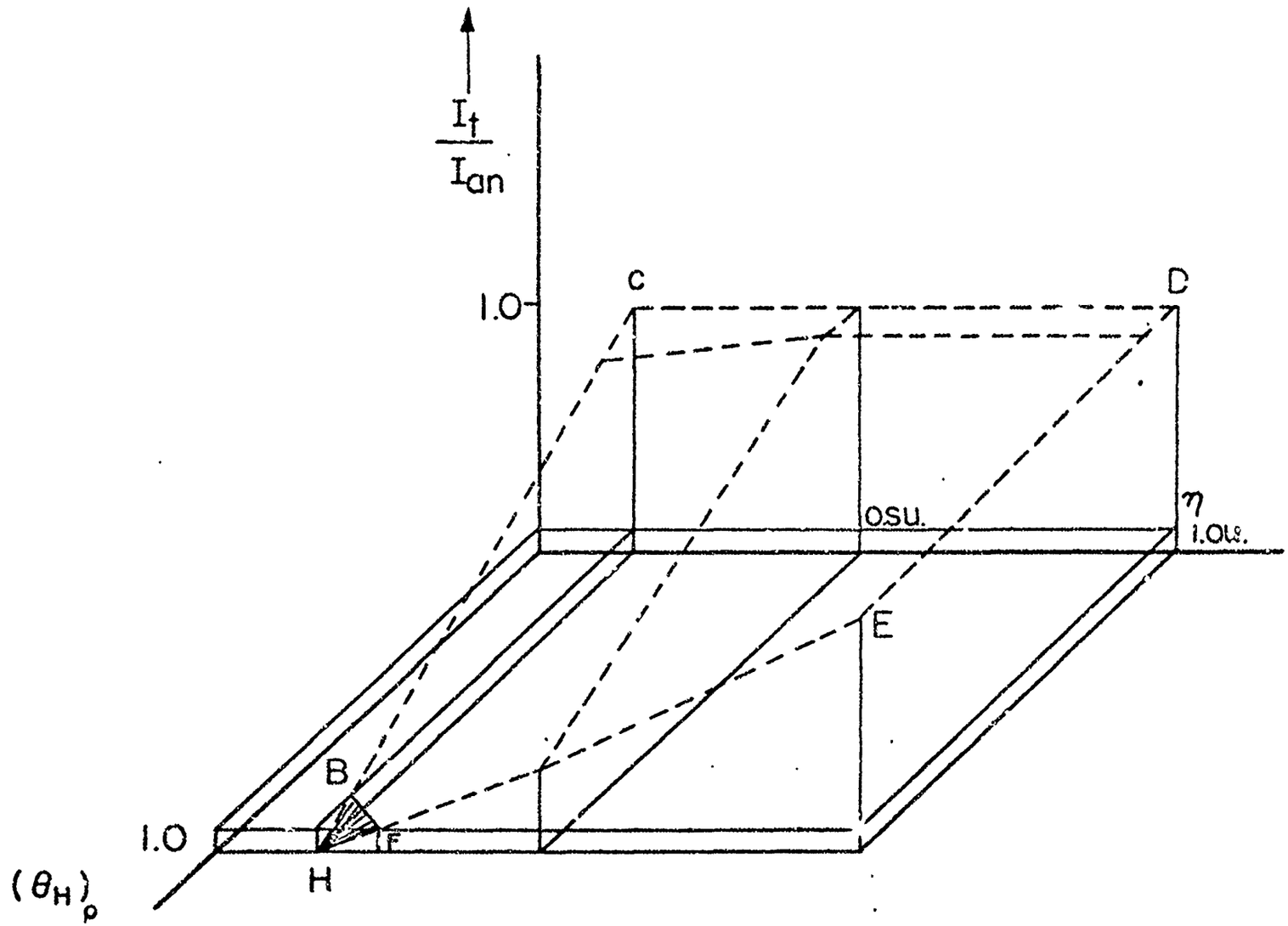

FIG.23

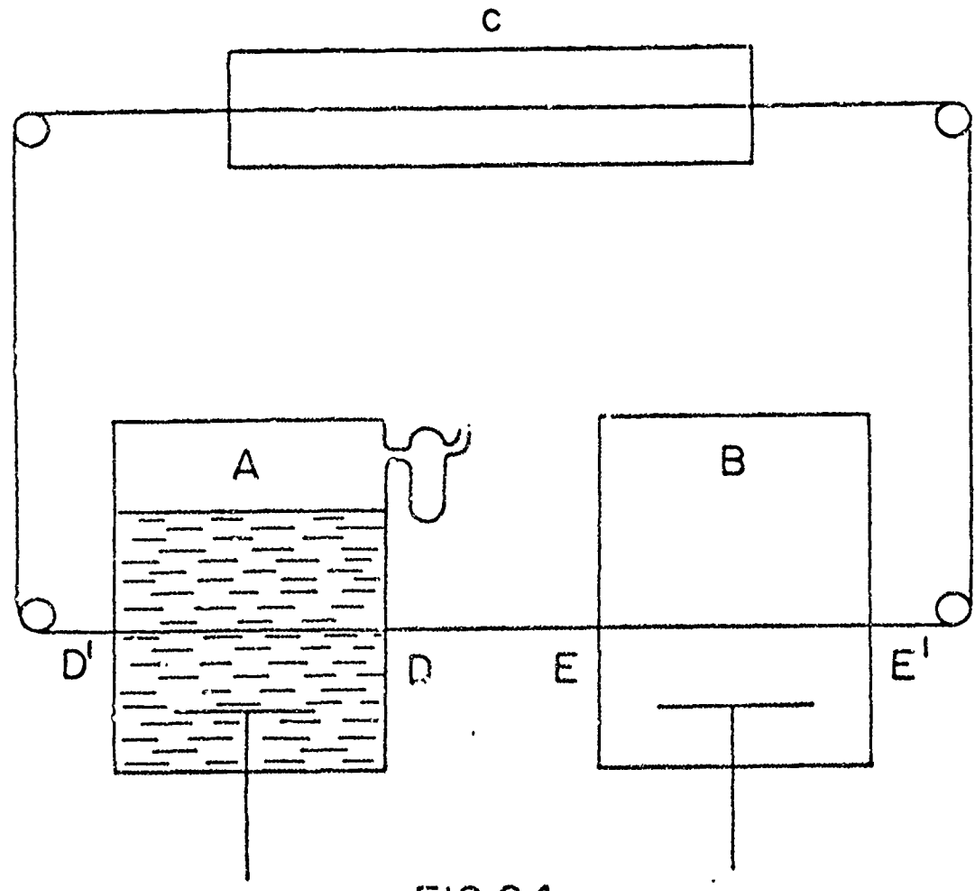

FIG. 24

FIG.25

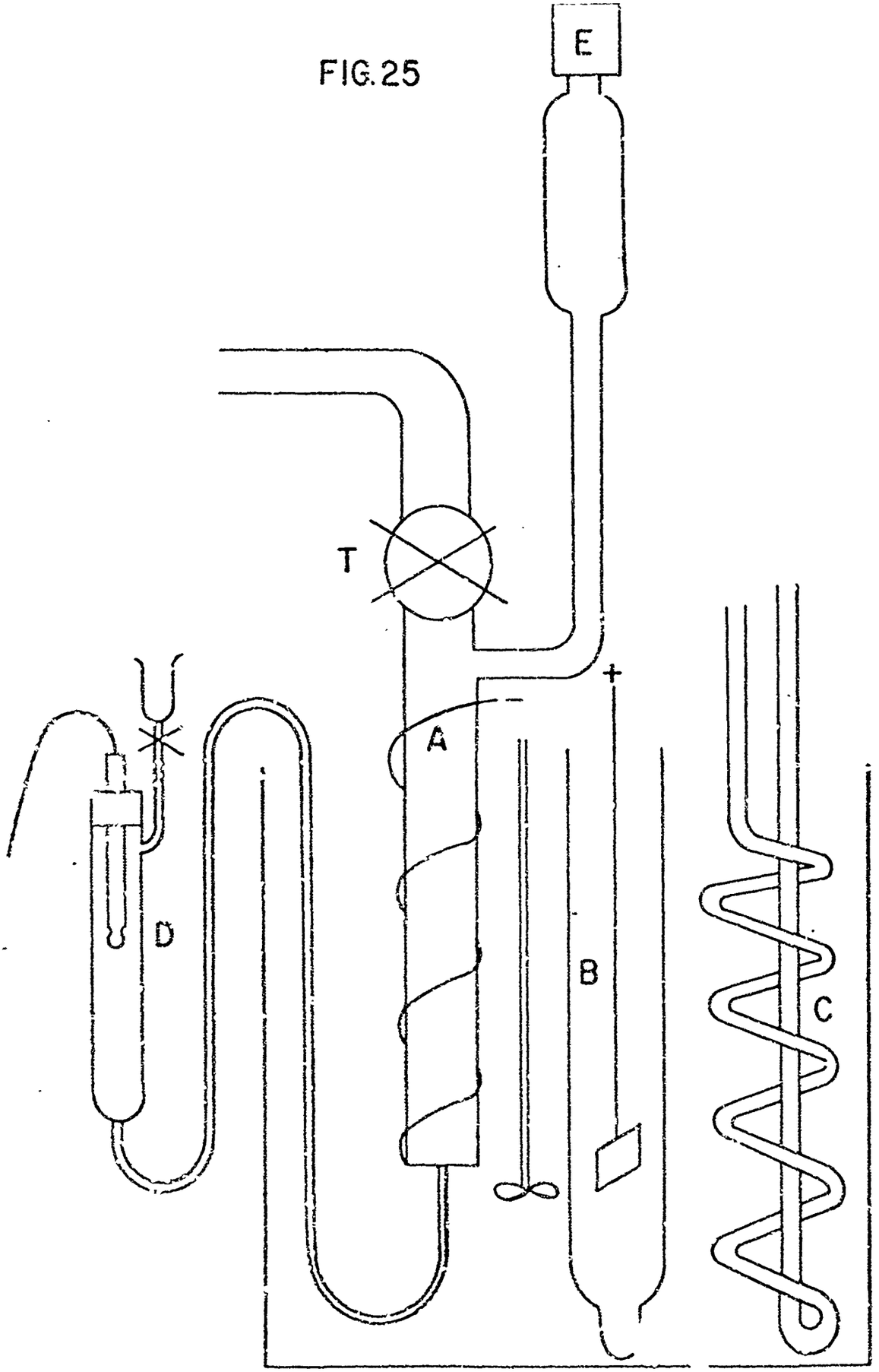

TIME (min)

FIG. 26

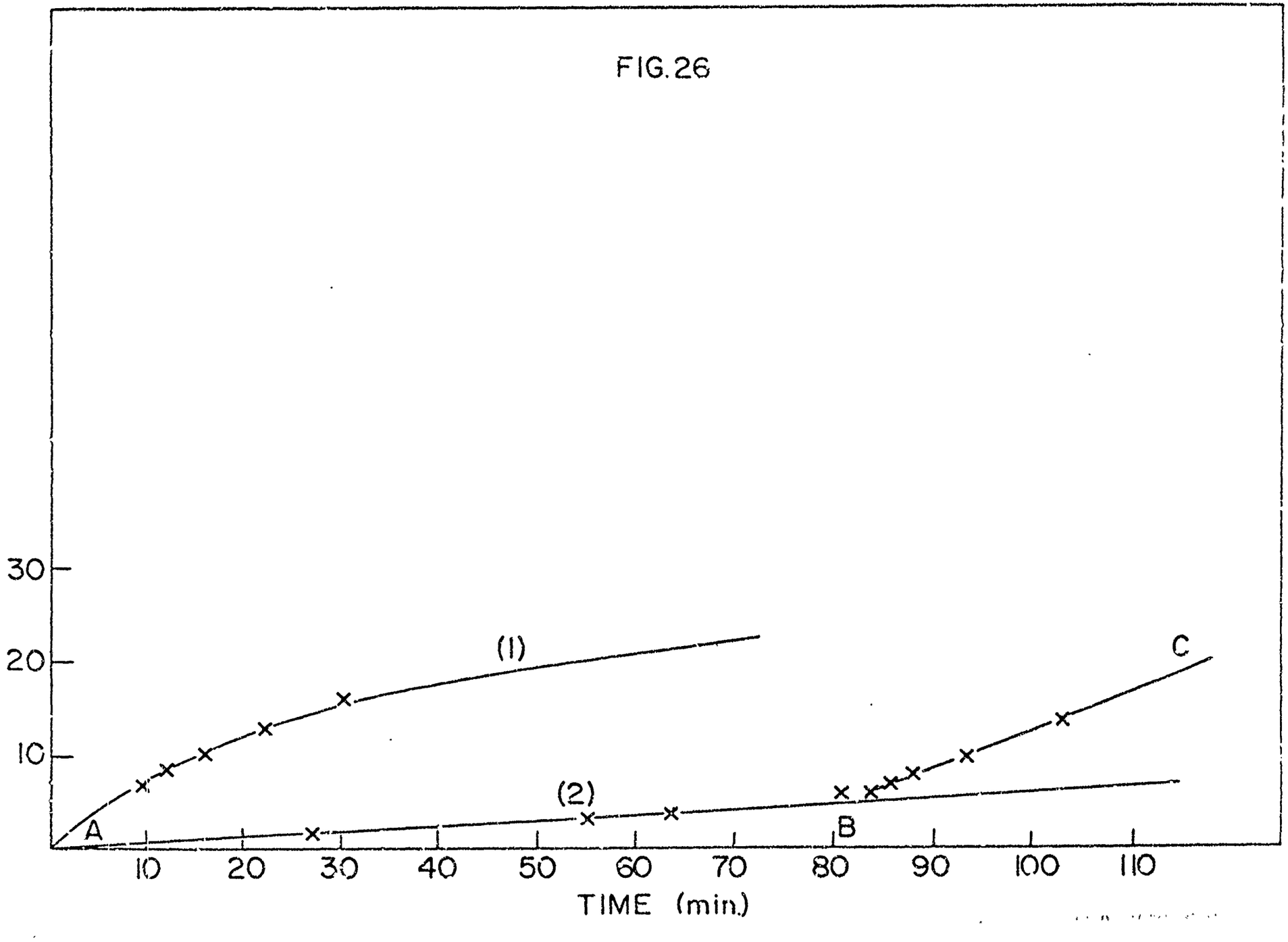

FIG. 27

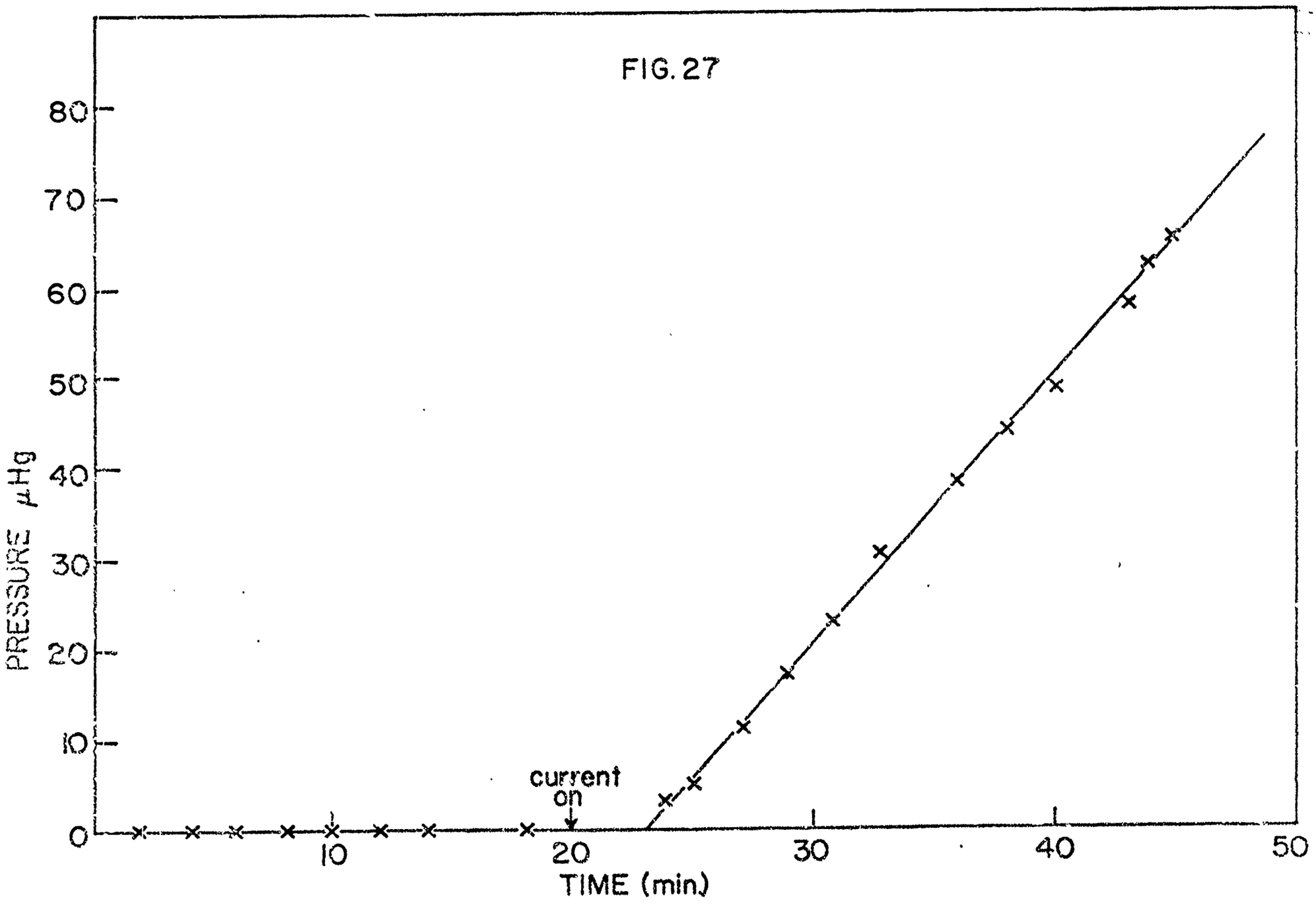
80
70
60
50
40
30
20
10
0
PRESSURE μHg
current on
10
20
30
40
50
TIME (min)

FIG. 28

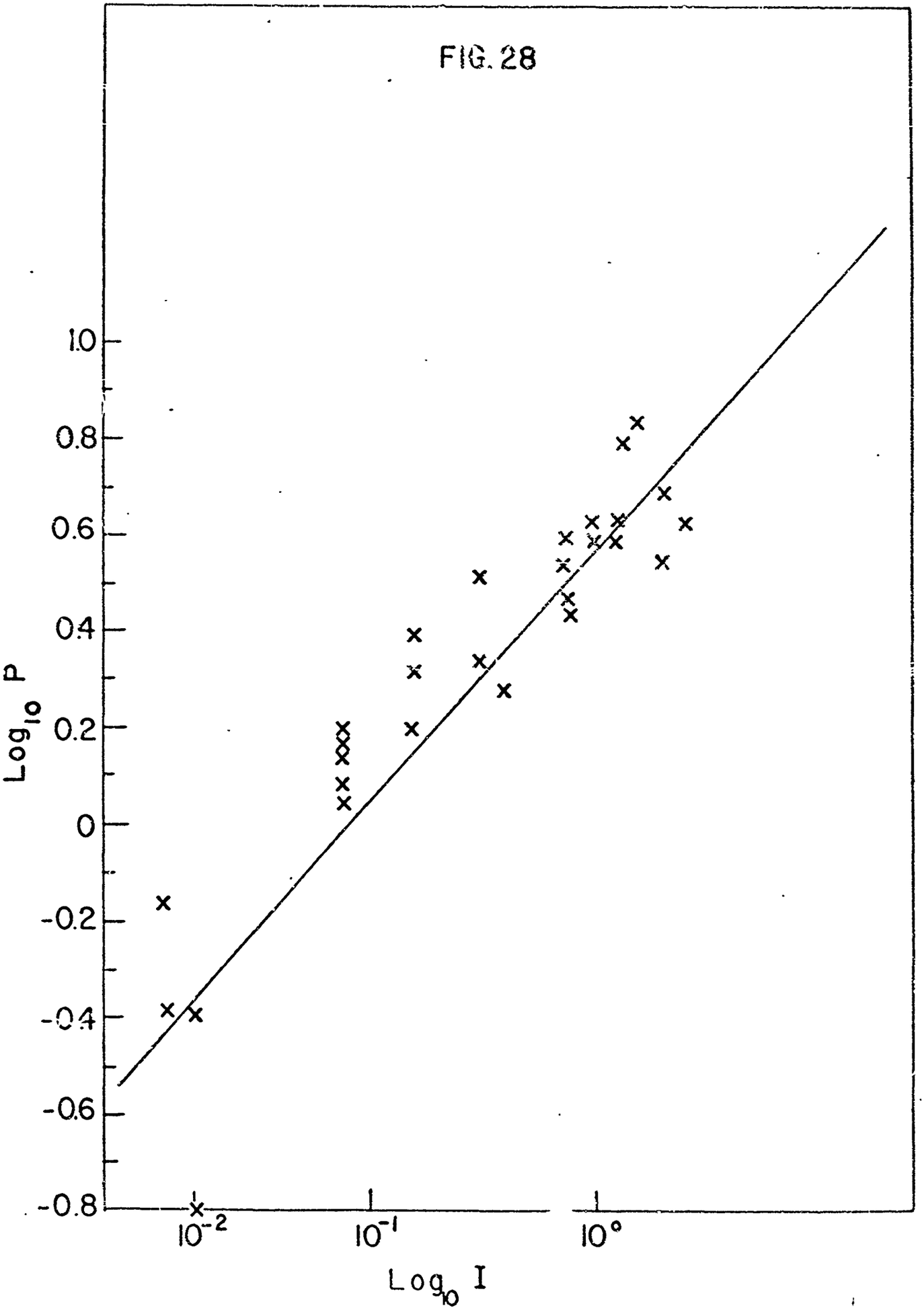

FIG. 29

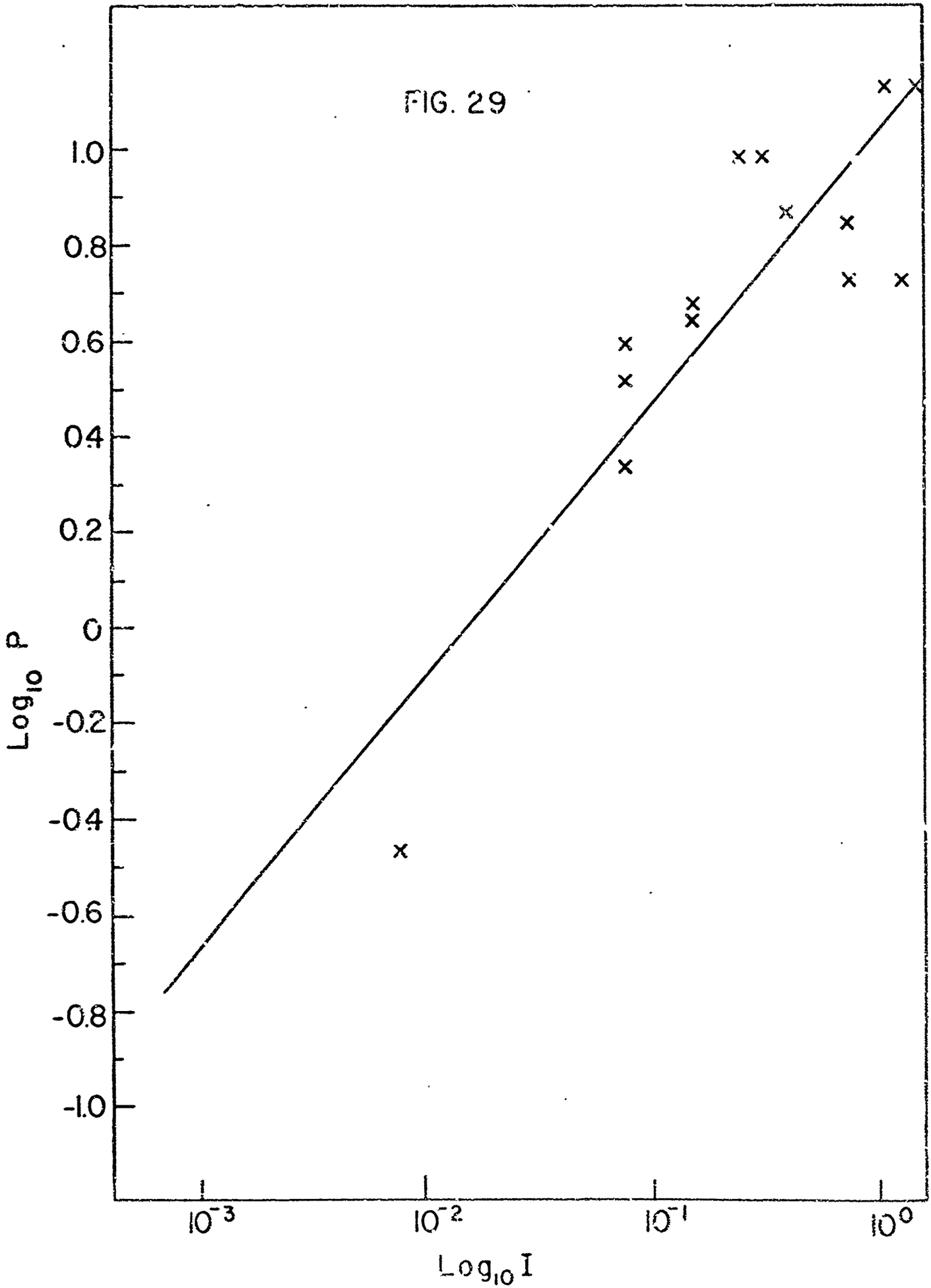

FIG. 30

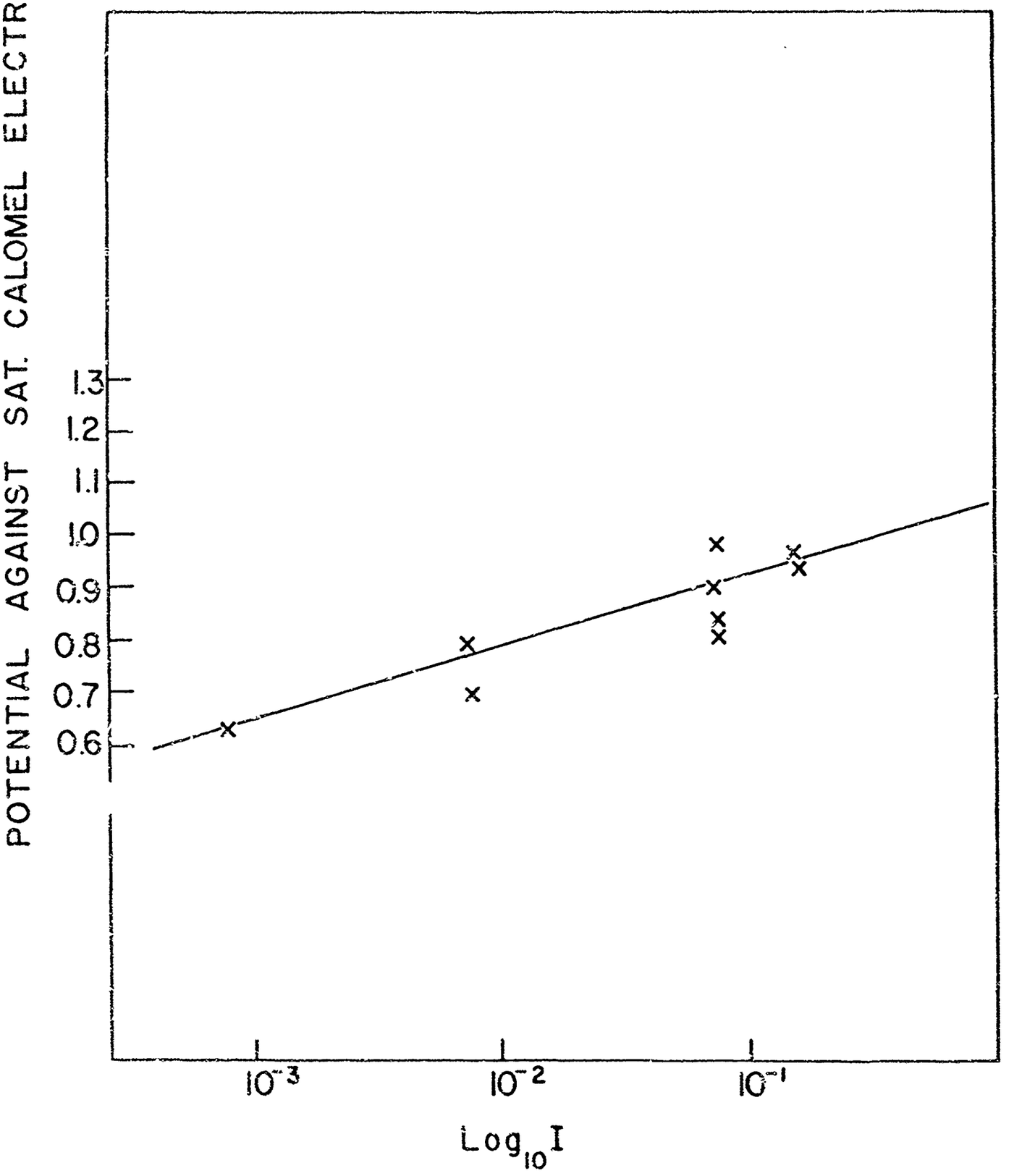
POTENTIAL AGAINST SAT. CALOMEL ELECTRODE
1.3
1.2
1.1
1.0
0.9
0.8
0.7
0.6
10^{-3}
10^{-2}
10^{-1}
$Log_{10} I$

TIME (hrs.)

FIG. 31

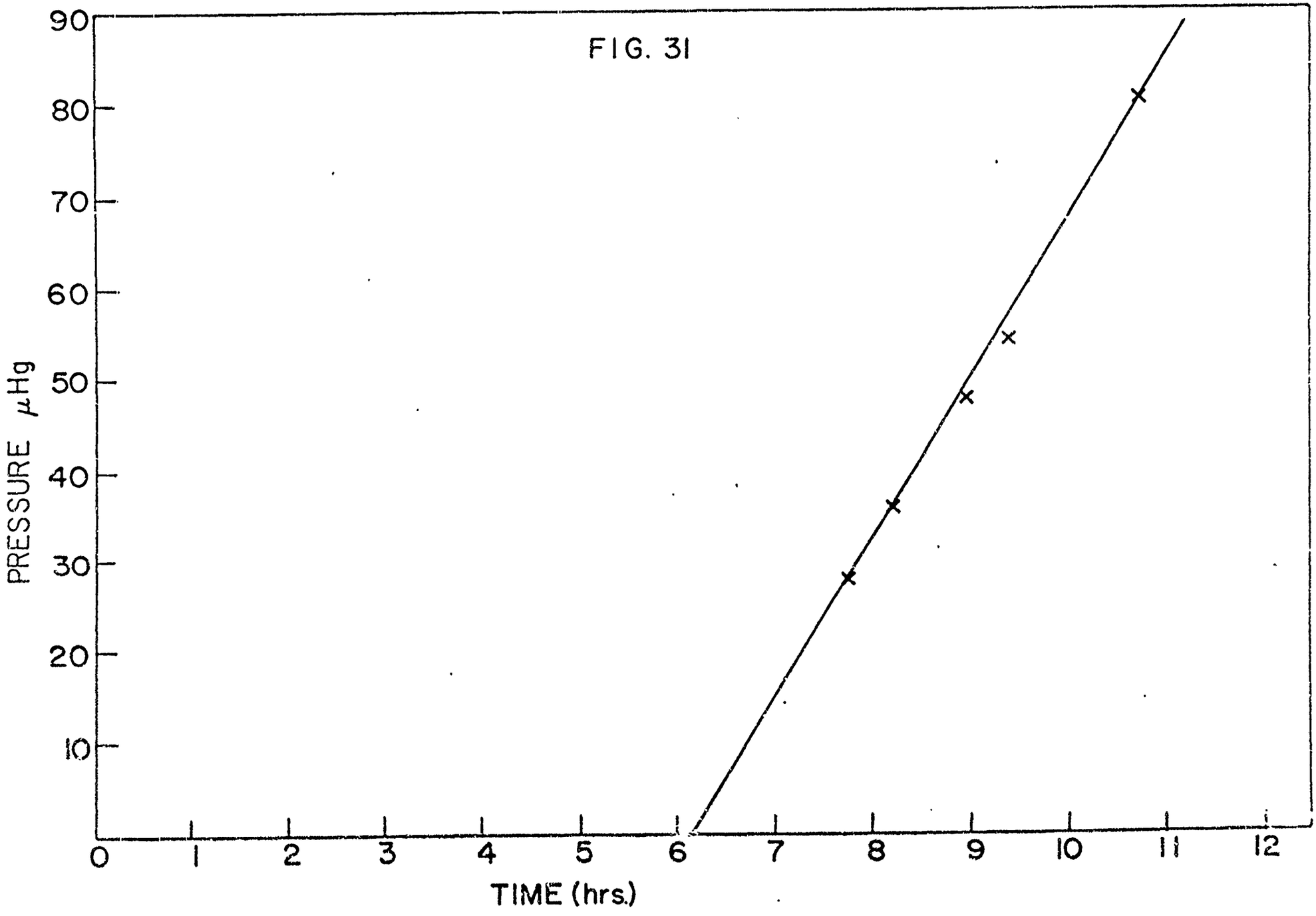

FIG. 32

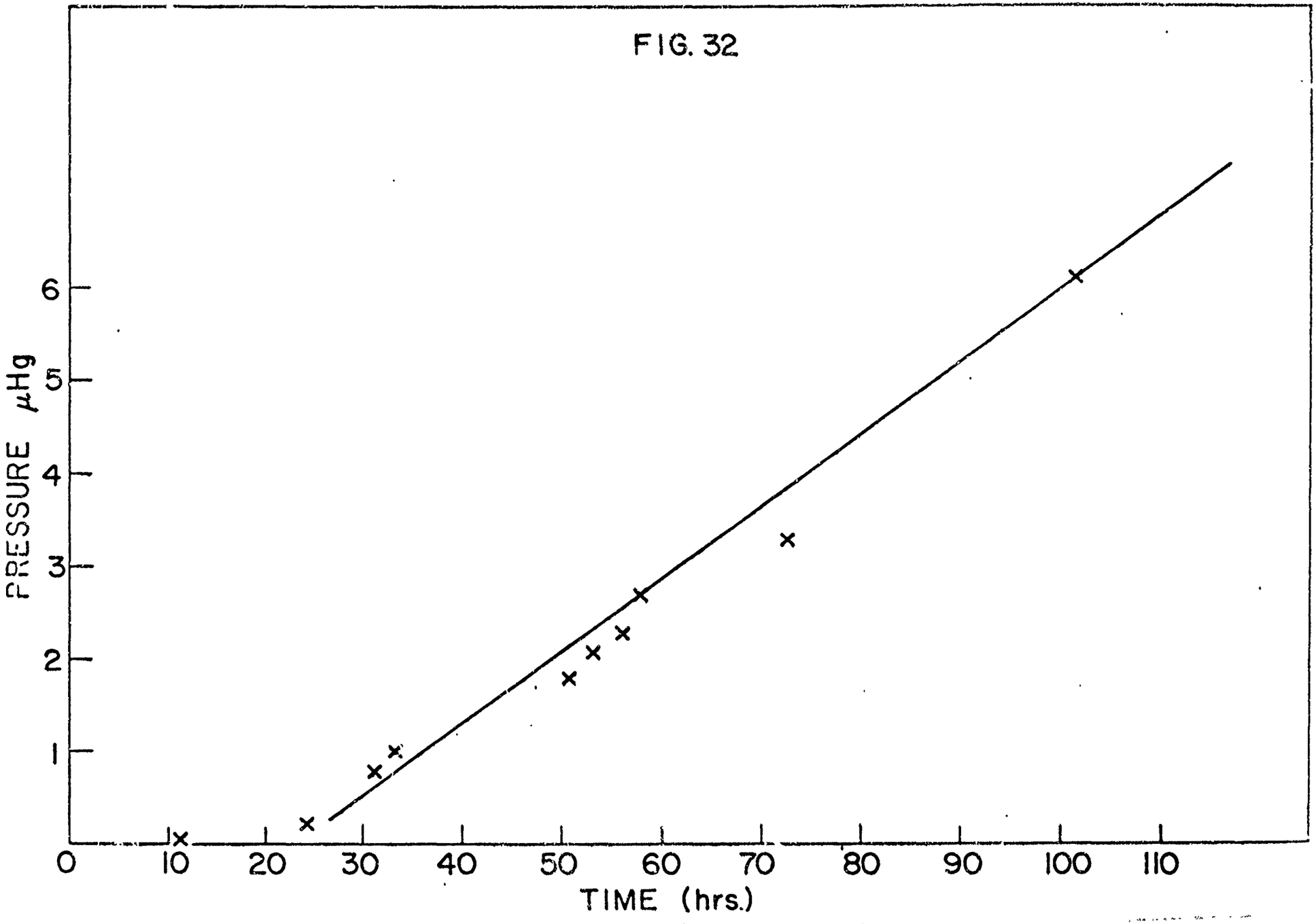

FIG. 33

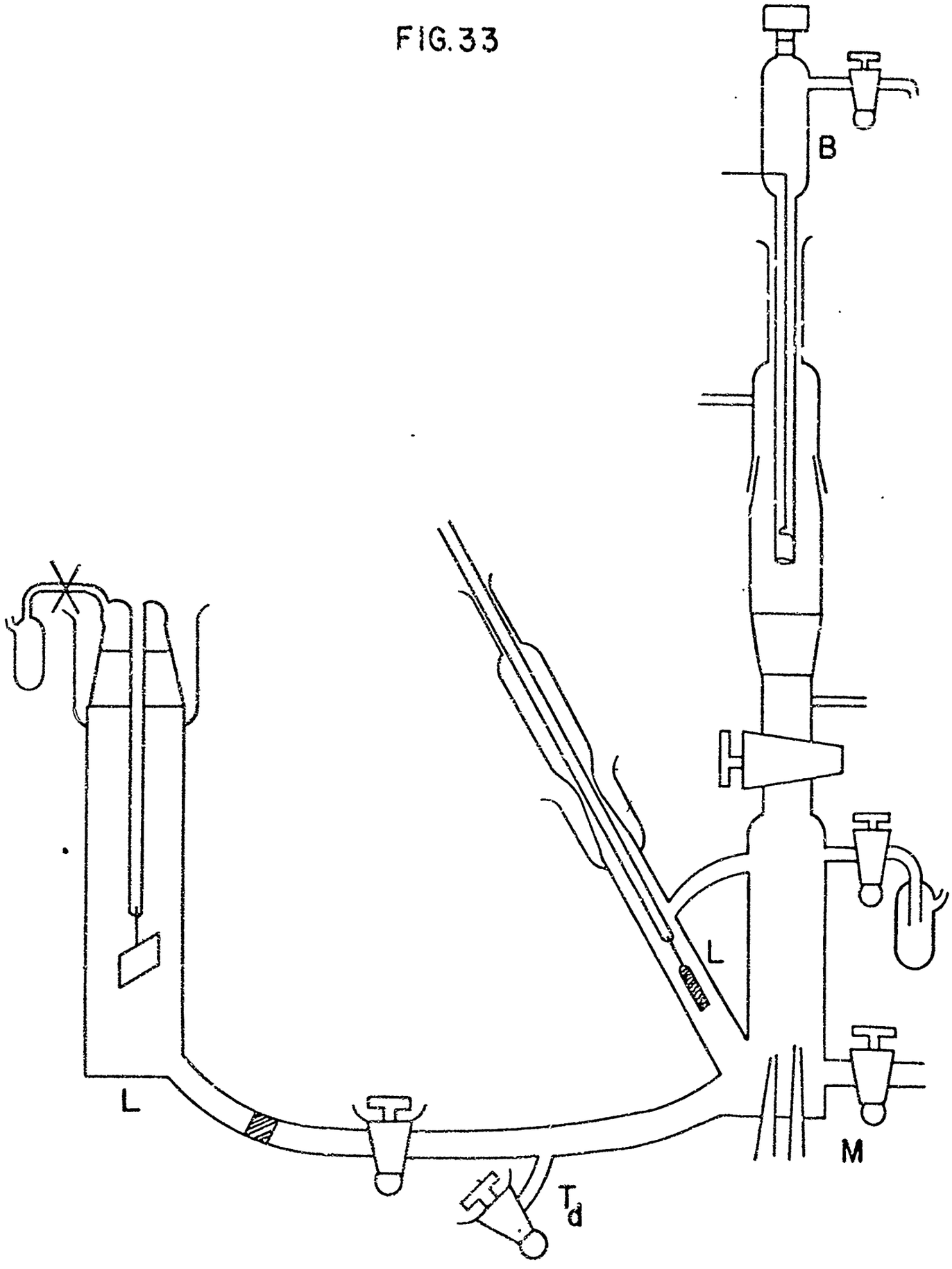

FIG. 34

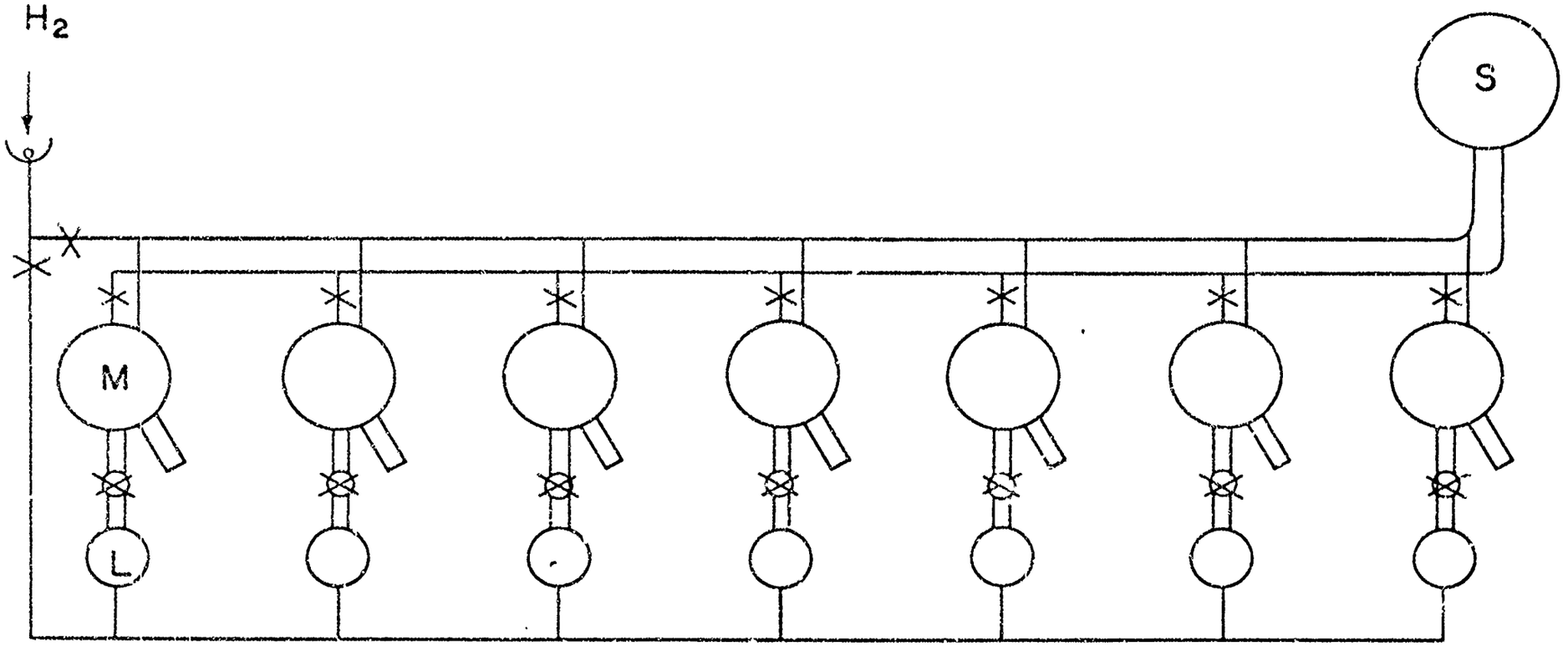

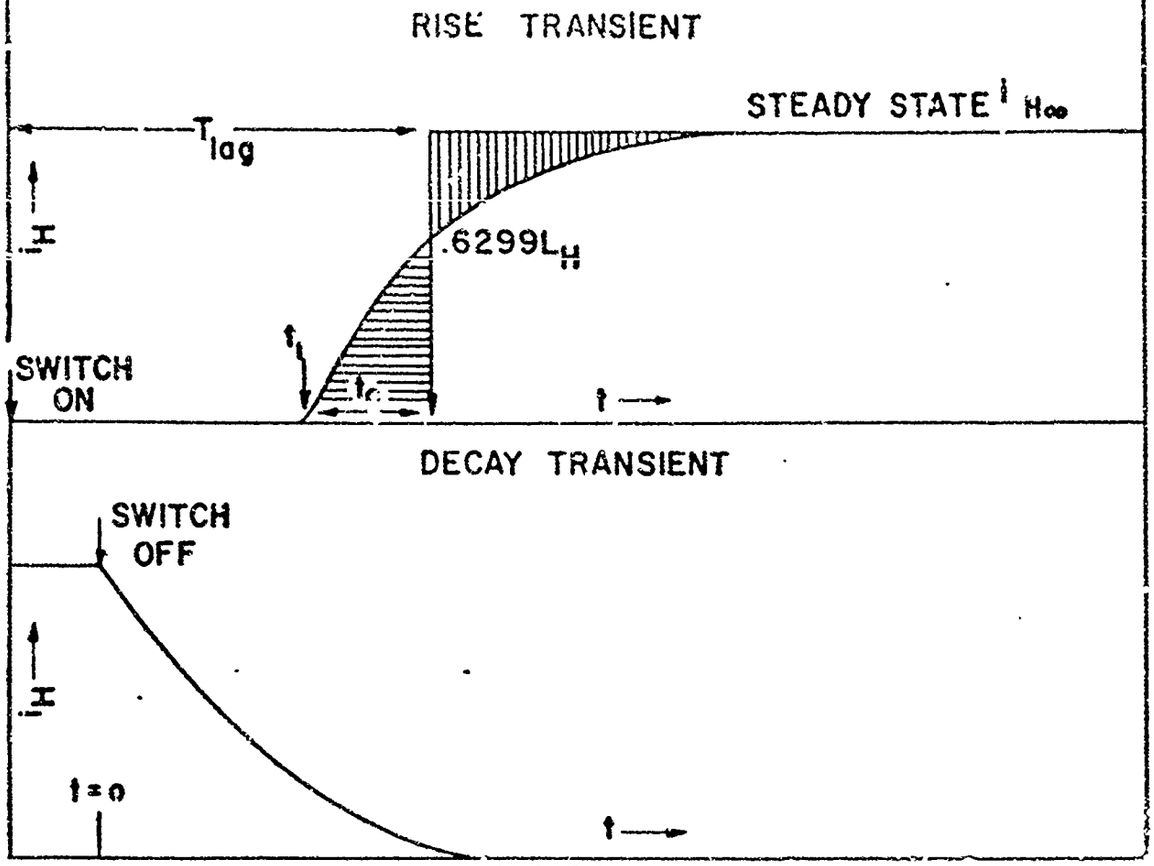
RISE TRANSIENT
STEADY STATE $i_{H\infty}$
T_{lag}
i_H
$.6299L_H$
SWITCH ON
t_1
t_c
t
DECAY TRANSIENT
SWITCH OFF
i_H
t=0
t

FIG. 36

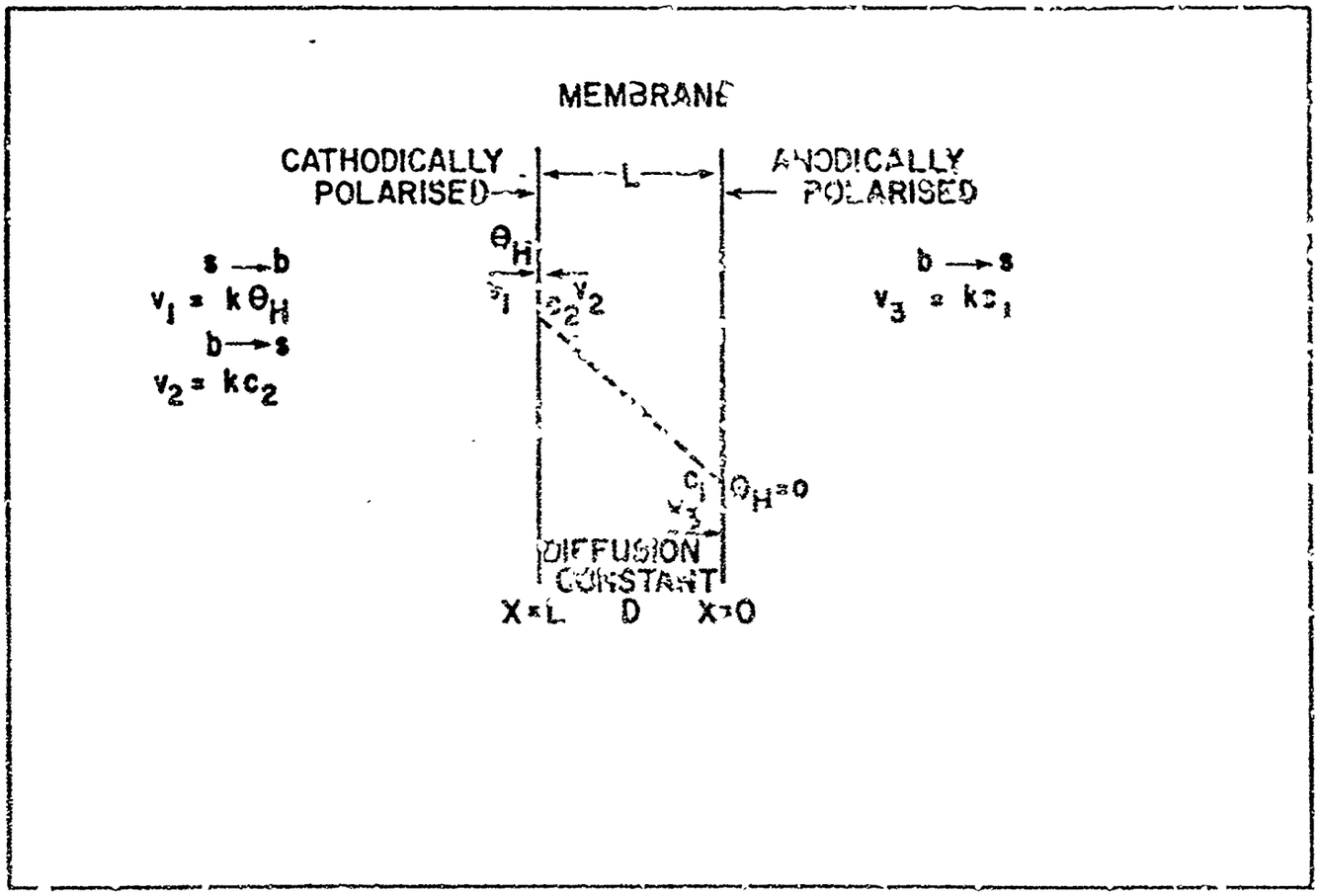
MEMBRANE
CATHODICALLY POLARISED
L
ANODICALLY POLARISED
θ_H
s → b
$v_1 = k\theta_H$
b → s
$v_2 = kc_2$
b → s
$v_3 = kc_1$
v_1
c_2
v_2
c_1
$\theta_H=0$
v_3
DIFFUSION CONSTANT
X=L
D
X=0

FIG. 35

FIG. 37

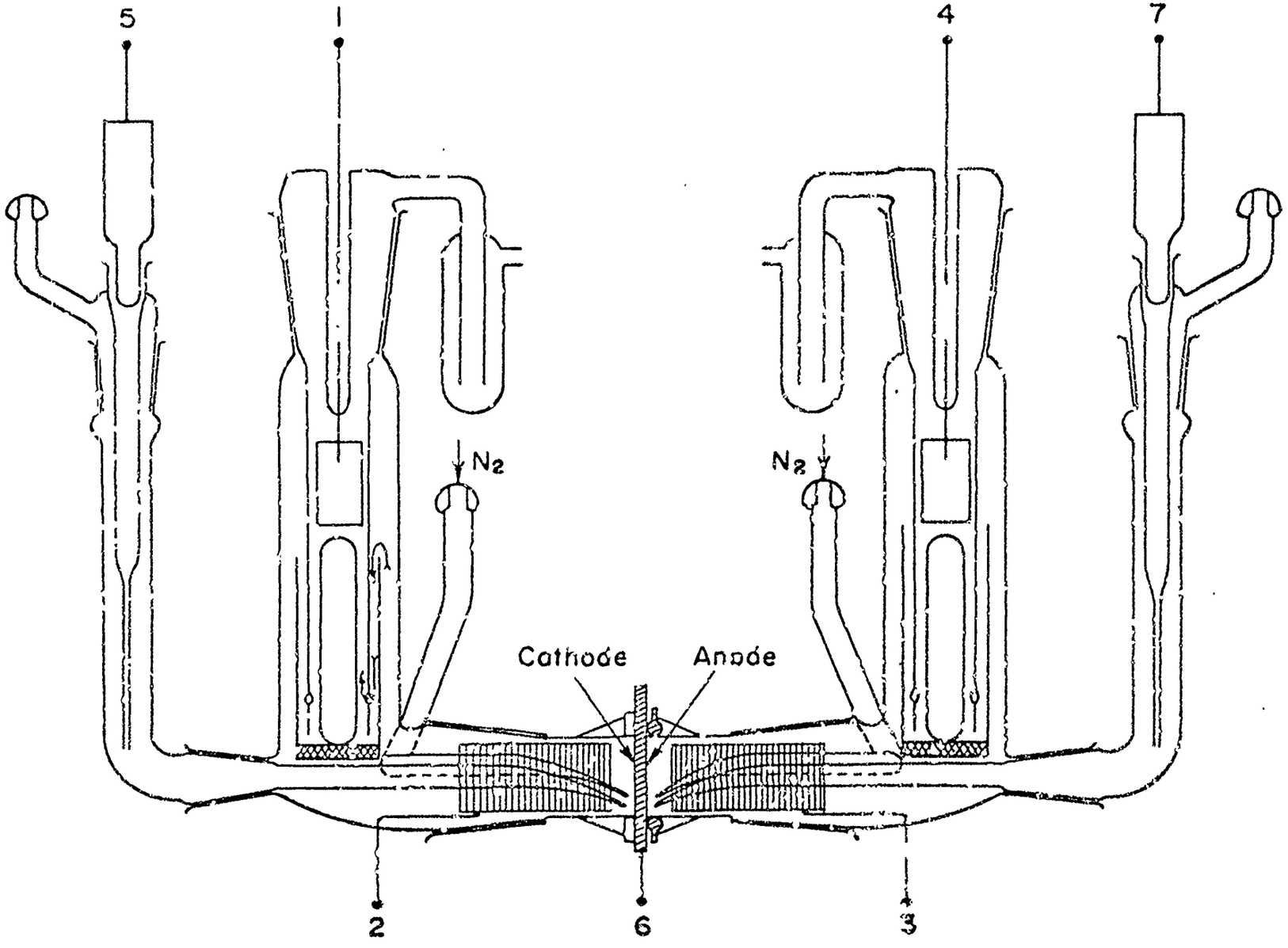

FIG. 38

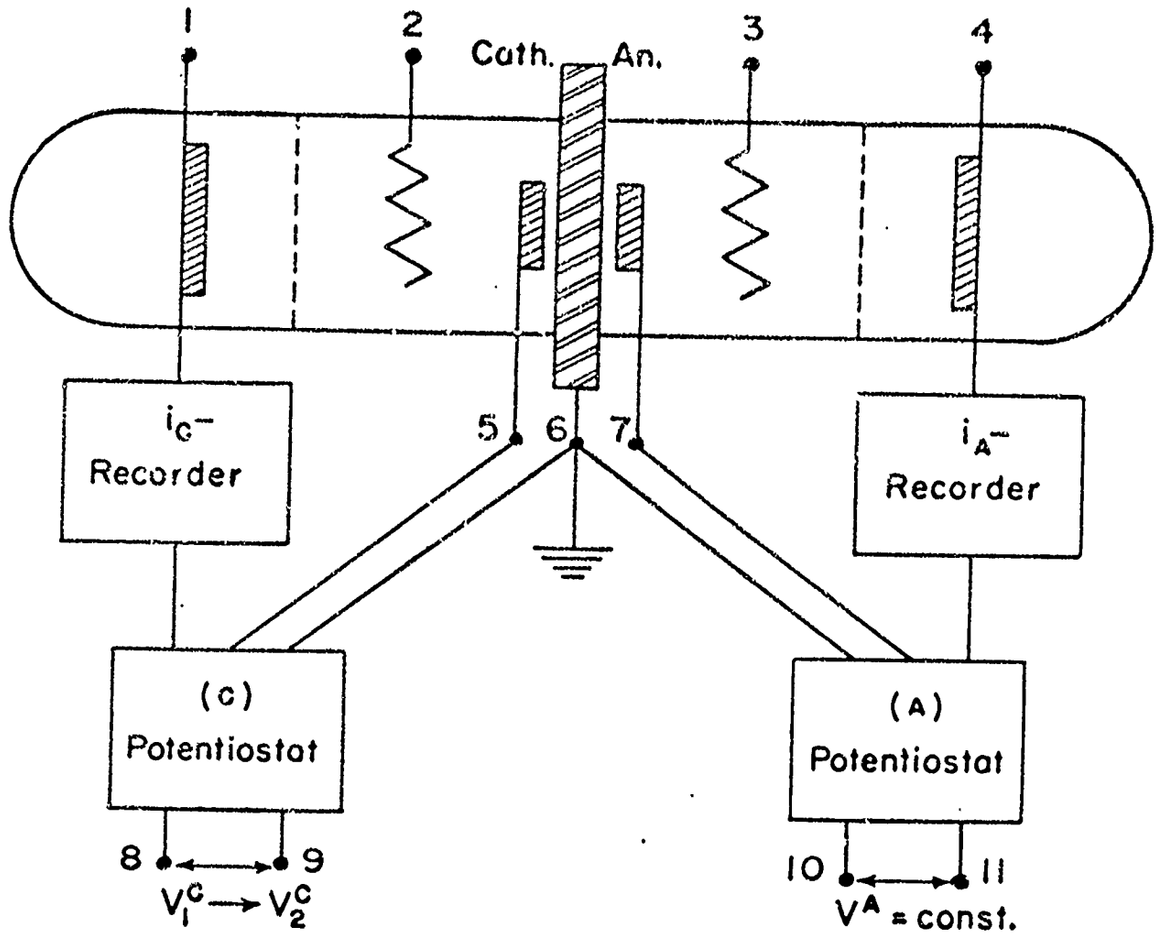
1
2
Cath.
An.
3
4
i_C – Recorder
5
6
7
i_A – Recorder
(C) Potentiostat
(A) Potentiostat
8
9
$V_1^C \rightarrow V_2^C$
10
11
V^A = const.

Log

FIG. 39

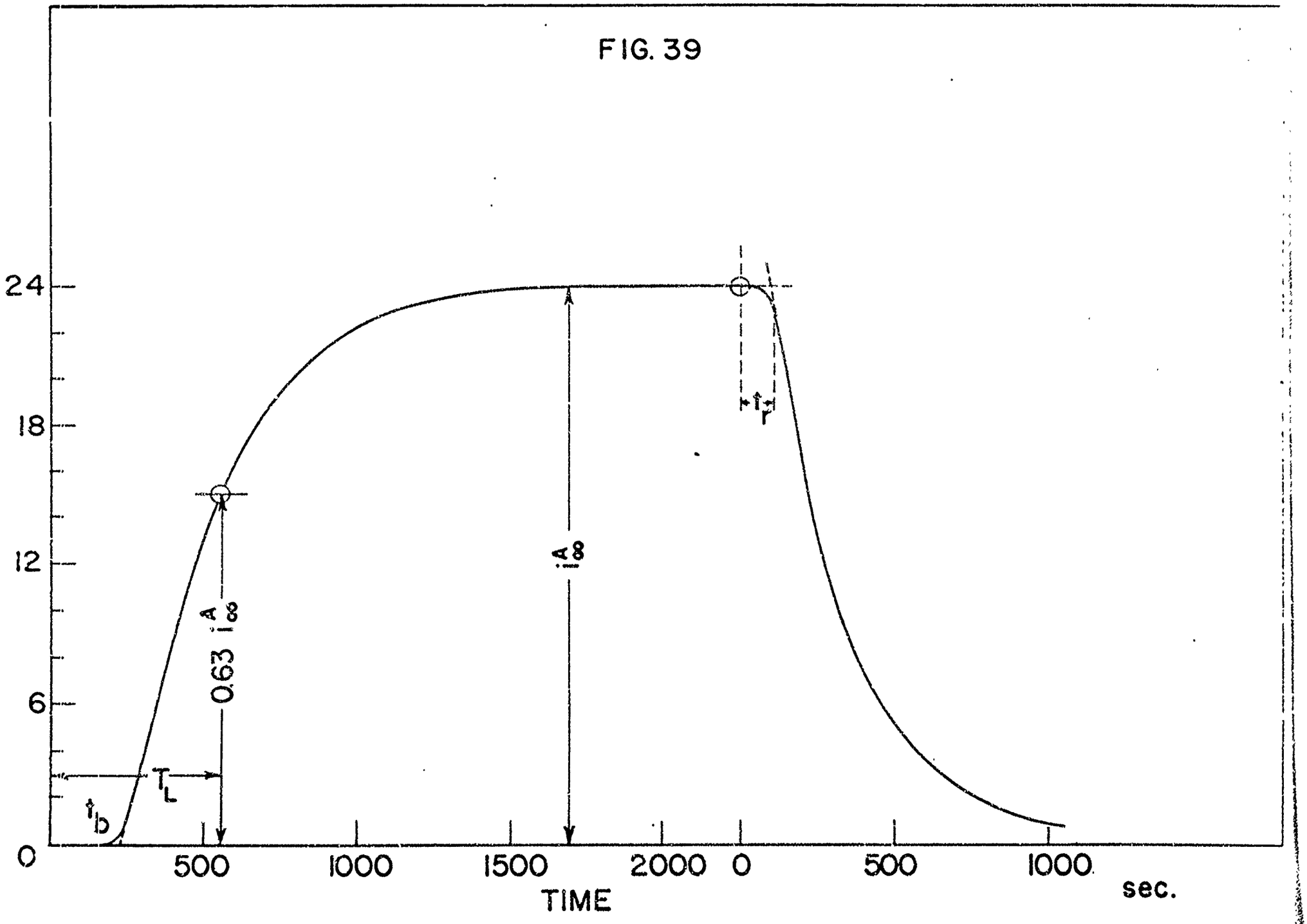
24
18
12
6
0
i_{∞}^{A}
0.63 i_{∞}^{A}
t_b
T_L
t_r
500
1000
1500
2000
0
500
1000
TIME
sec.

FIG. 40

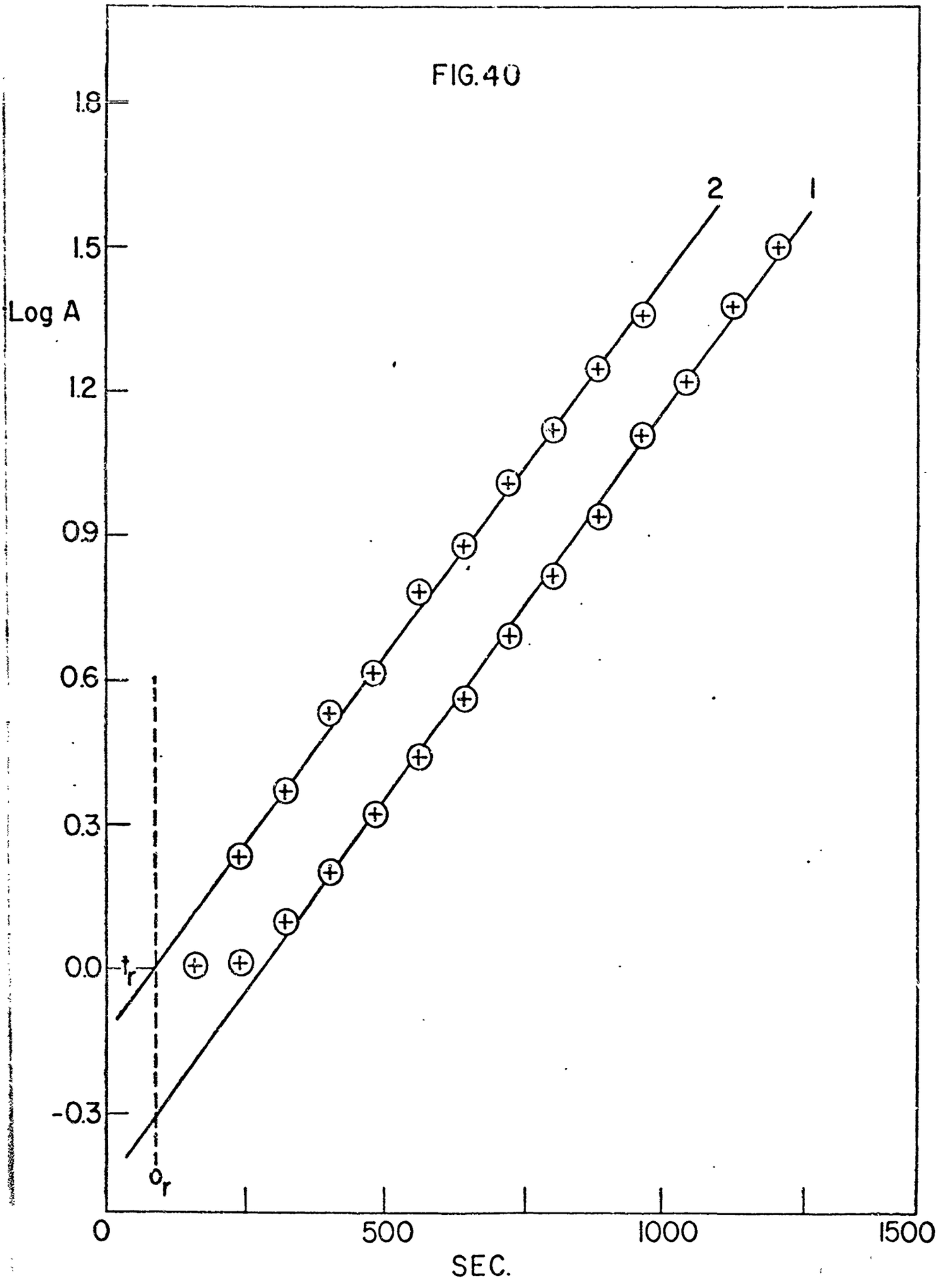

FIG. 41

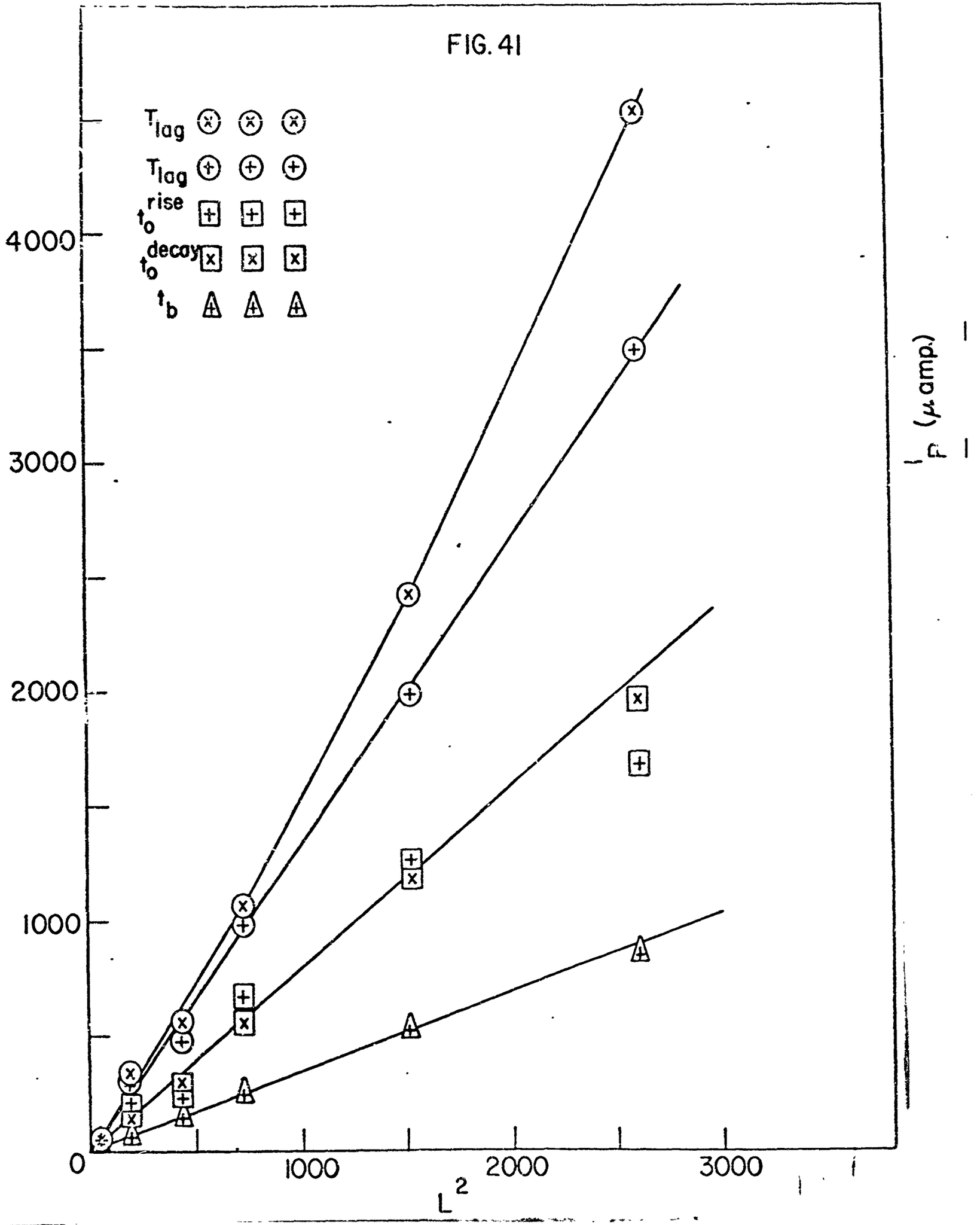
T_{lag}
T_{lag}
t_o^{rise}
t_o^{decay}
t_b
4000
3000
2000
1000
0
1000
2000
3000
L^2
I_R (μ amp.)

FIG. 42

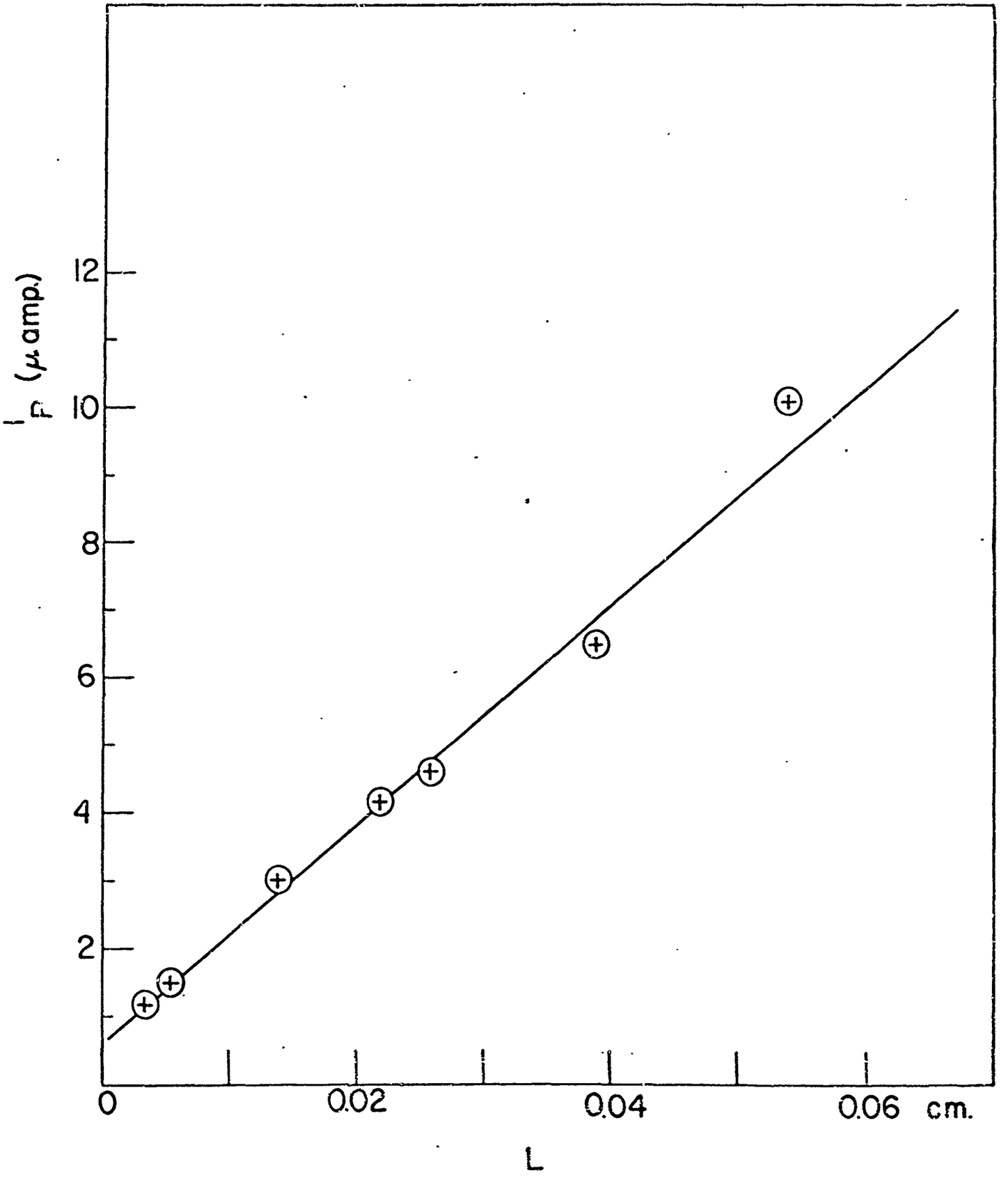

FIG. 43

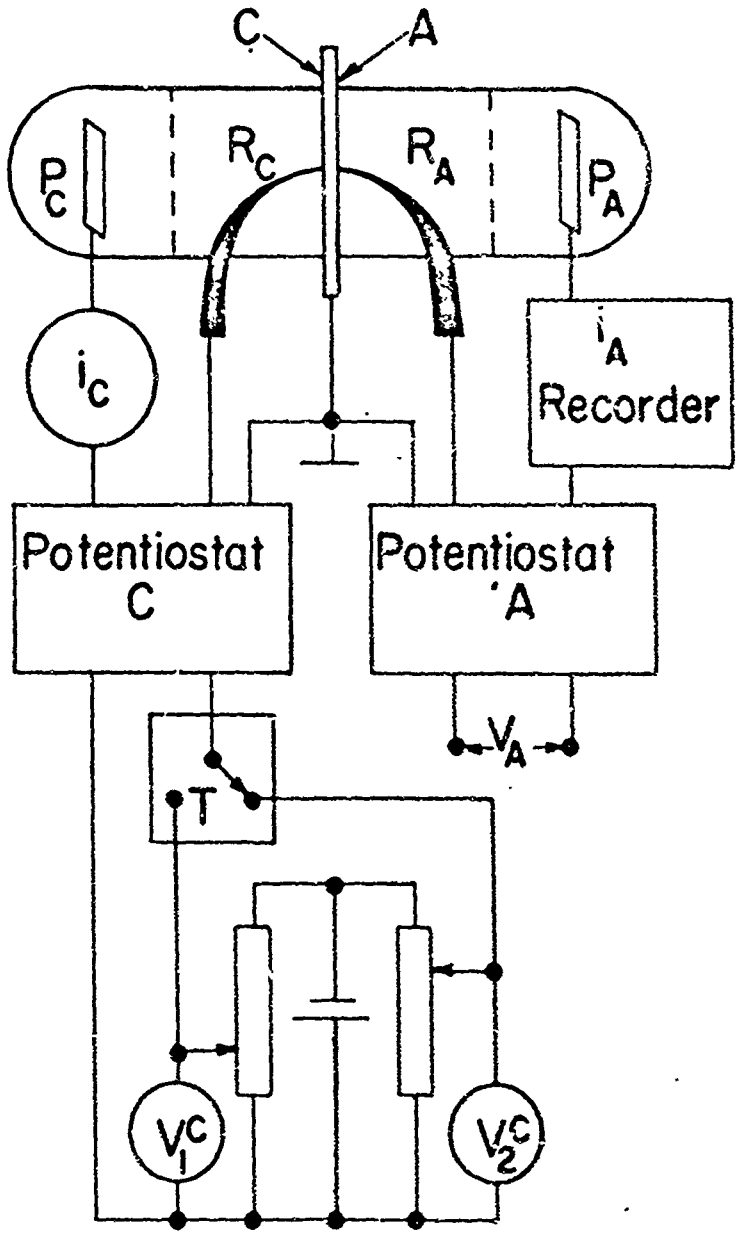
C
A
P_C
R_C
R_A
P_A
i_C
i_A
Recorder
Potentiostat C
Potentiostat A
V_A
T
V_1^C
V_2^C

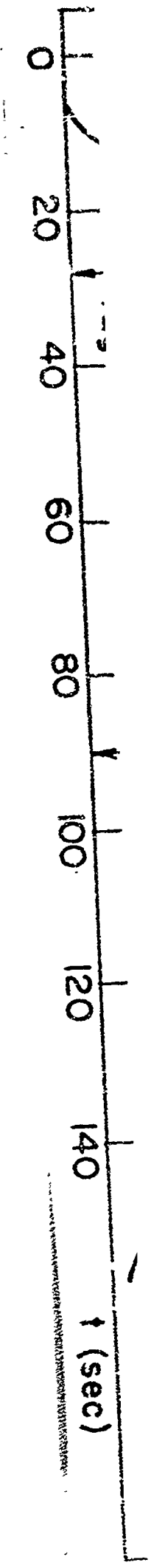
0
20
40
60
80
100
120
140
t (sec)

FIG.44

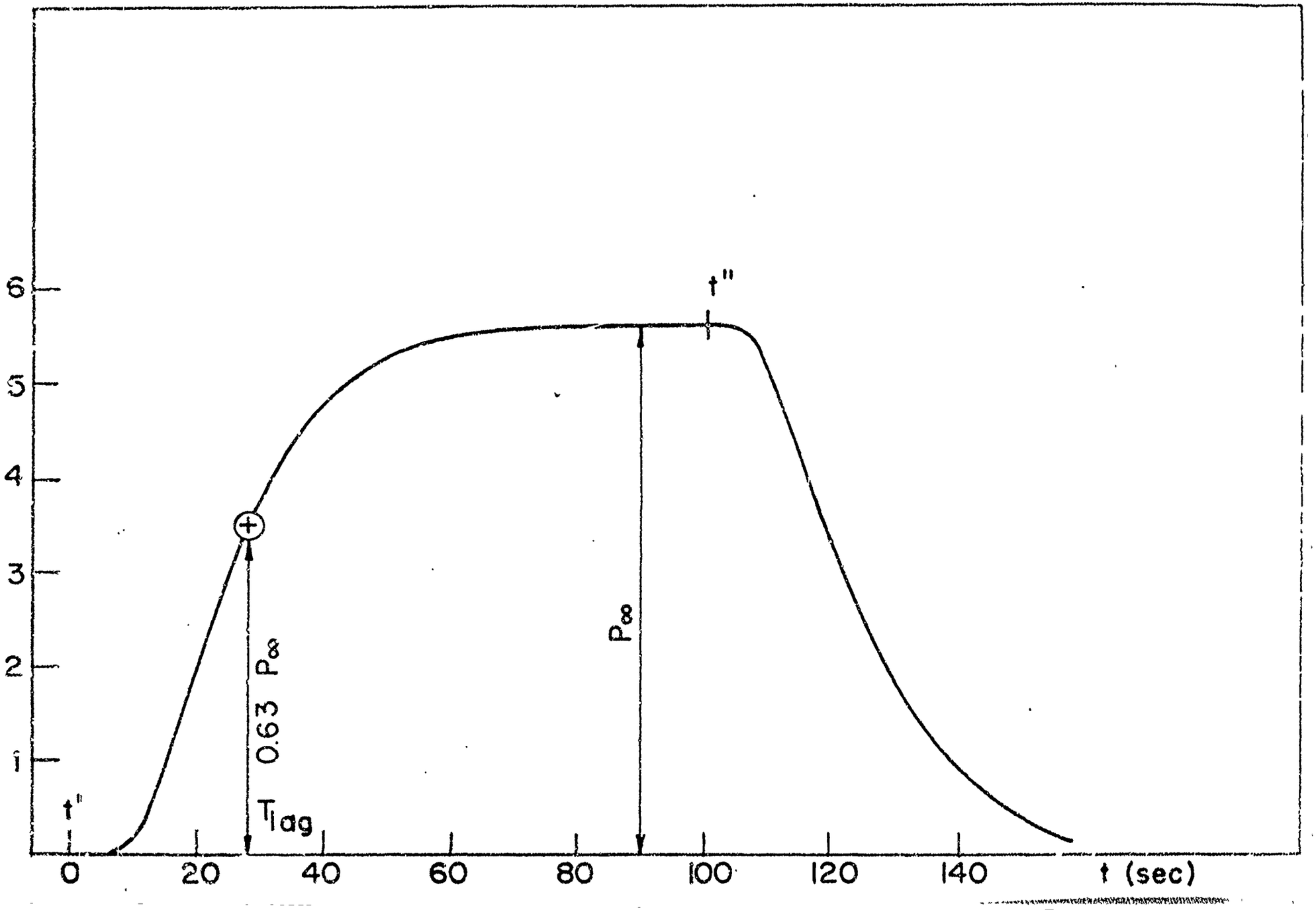

FIG.45

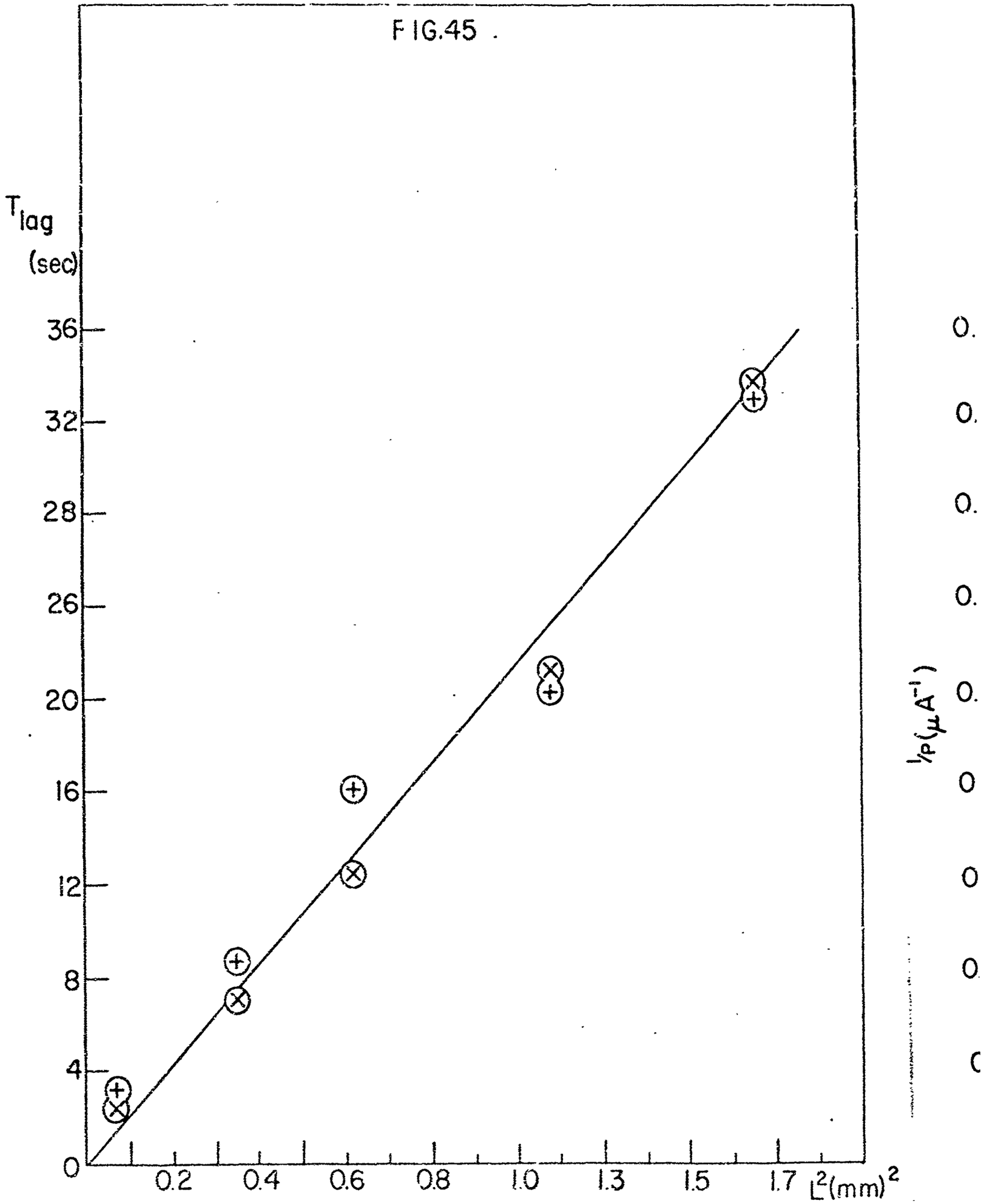
T_{lag} (sec)
36
32
28
26
20
16
12
8
4
0
0.2
0.4
0.6
0.8
1.0
1.3
1.5
1.7
$L^2(mm)^2$
$1/P(\mu A^{-1})$
0.
0.
0.
0.
0.
0
0
0
0

FIG. 46

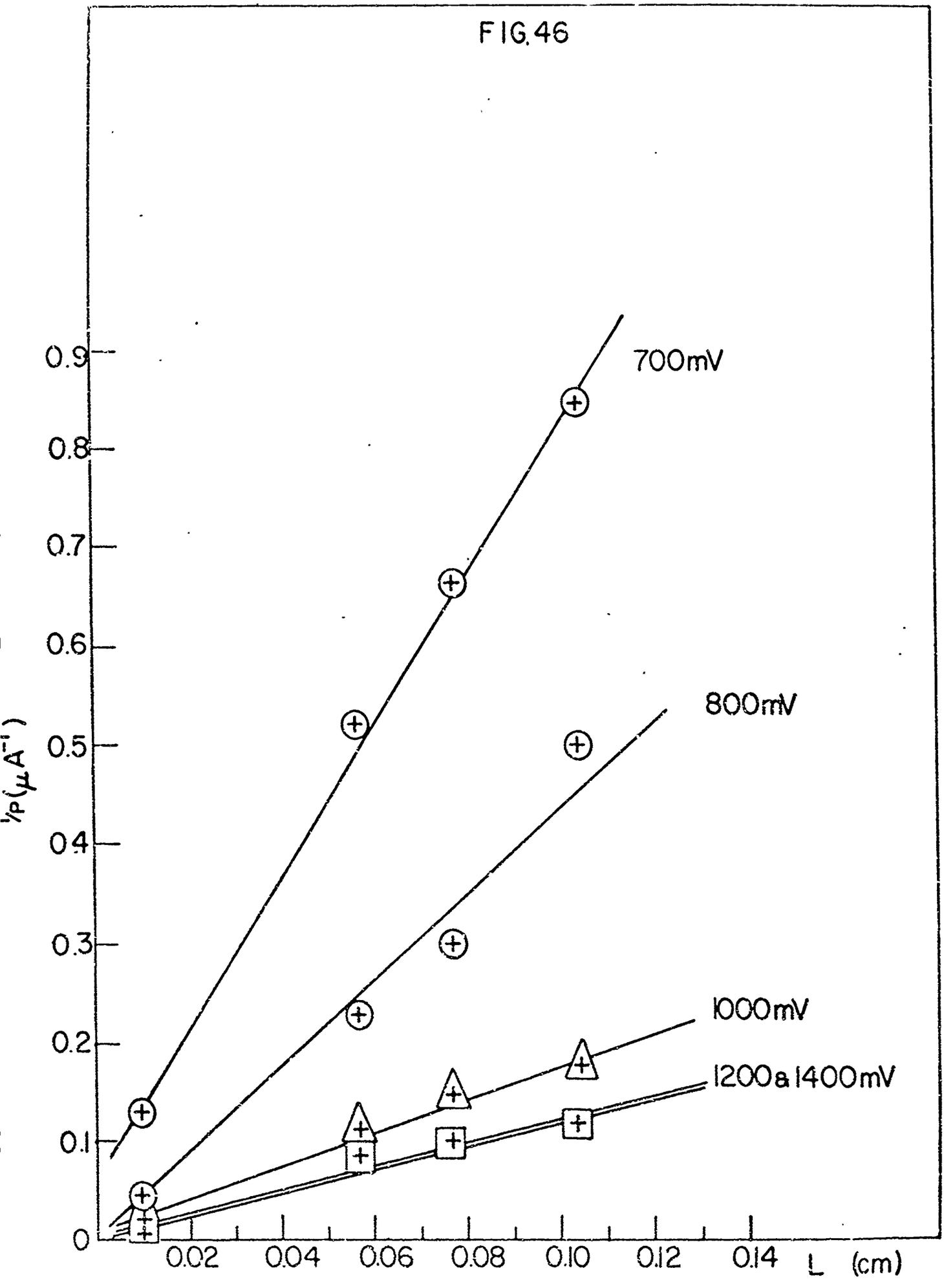
0.9
0.8
0.7
0.6
0.5
0.4
0.3
0.2
0.1
0
1/P (μA⁻¹)
700mV
800mV
1000mV
1200 a 1400mV
0.02
0.04
0.06
0.08
0.10
0.12
0.14
L (cm)

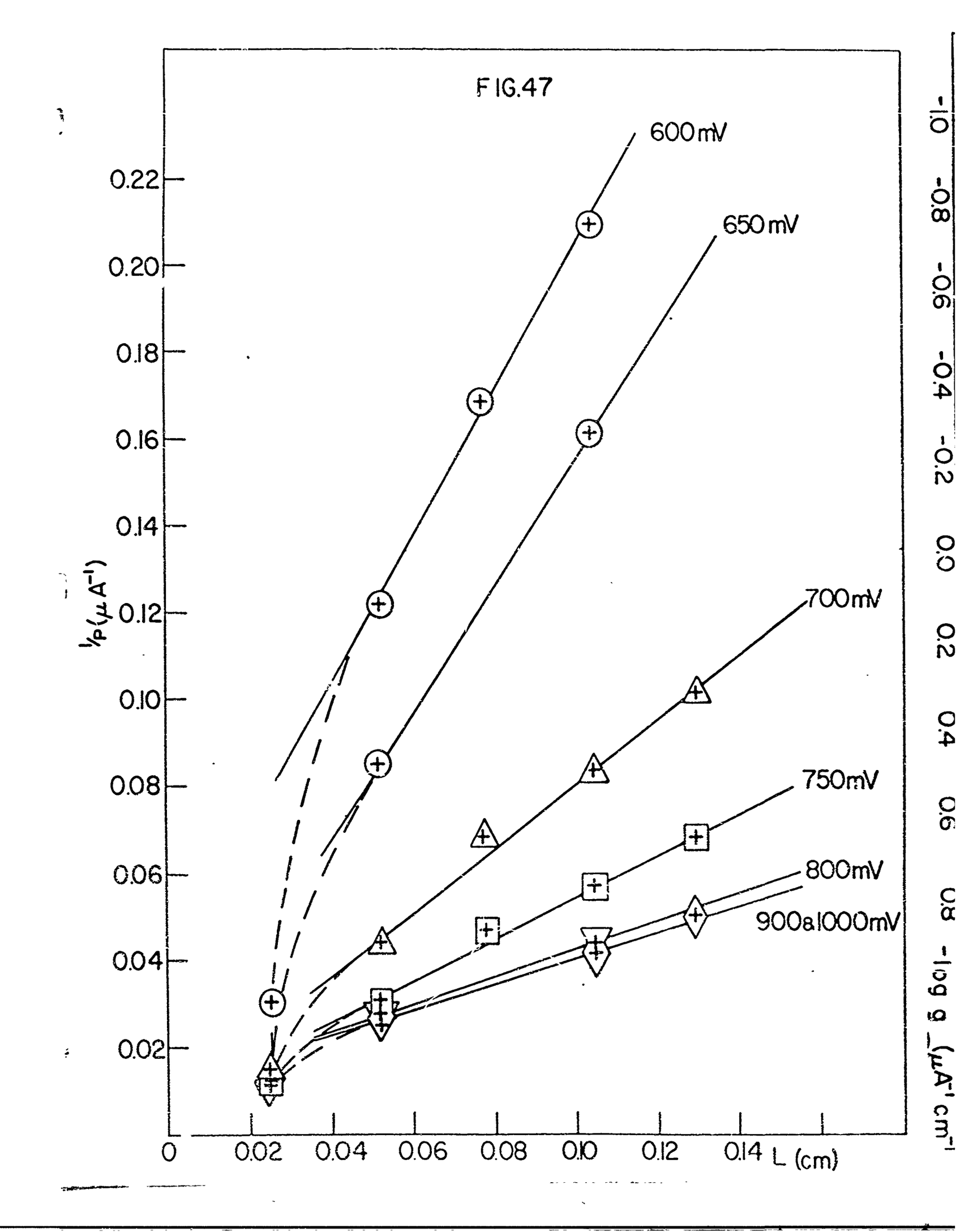
FIG.47
600mV
650mV
700mV
750mV
800mV
900&1000mV
0.22
0.20
0.18
0.16
0.14
0.12
0.10
0.08
0.06
0.04
0.02
$1/p\,(\mu A^{-1})$
0
0.02
0.04
0.06
0.08
0.10
0.12
0.14
L (cm)
-1.0
-0.8
-0.6
-0.4
-0.2
0.0
0.2
0.4
0.6
0.8
$-\log g\,(\mu A^{-1}\,cm^{-1})$

FIG.48

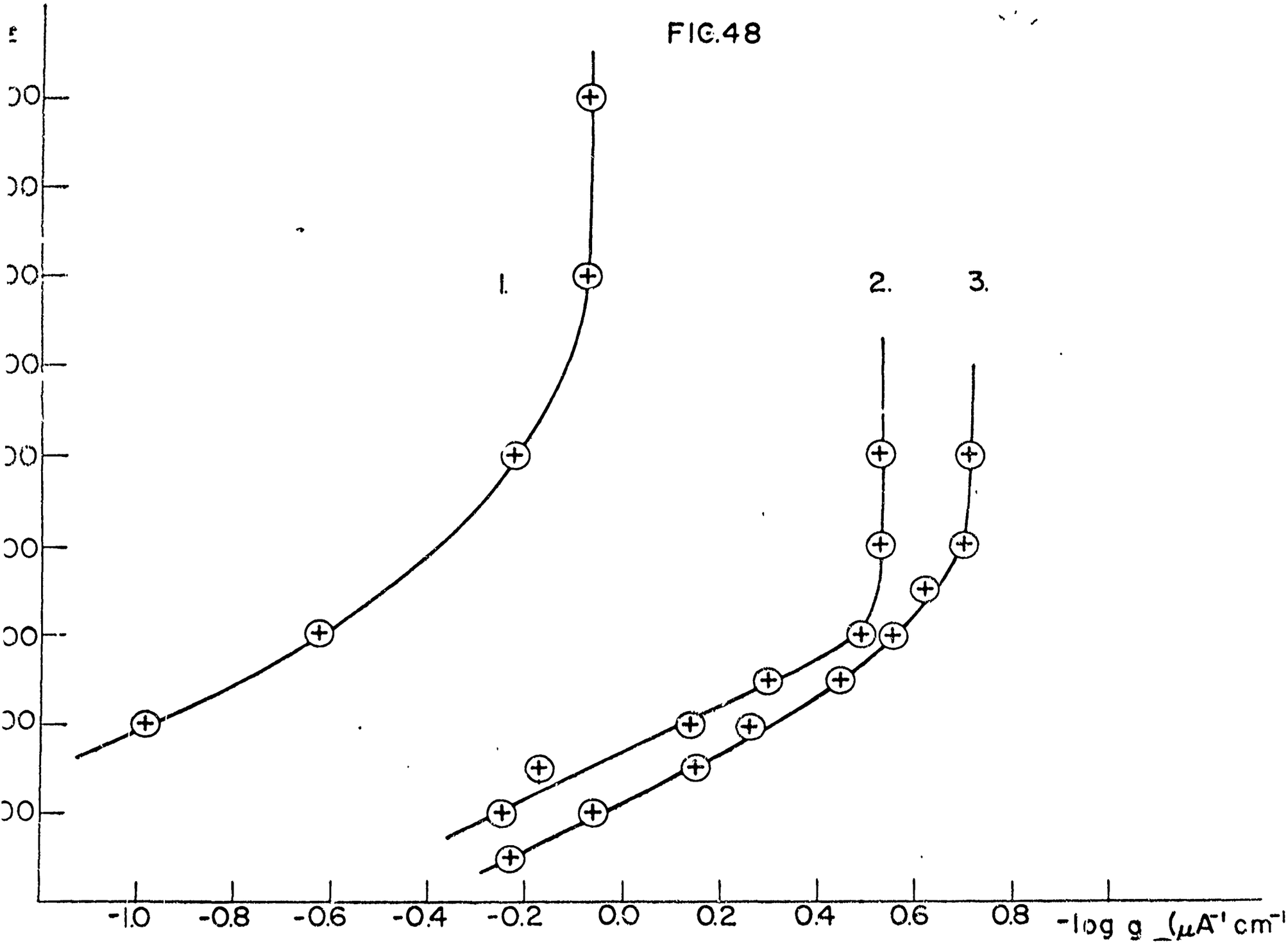

FIG.49

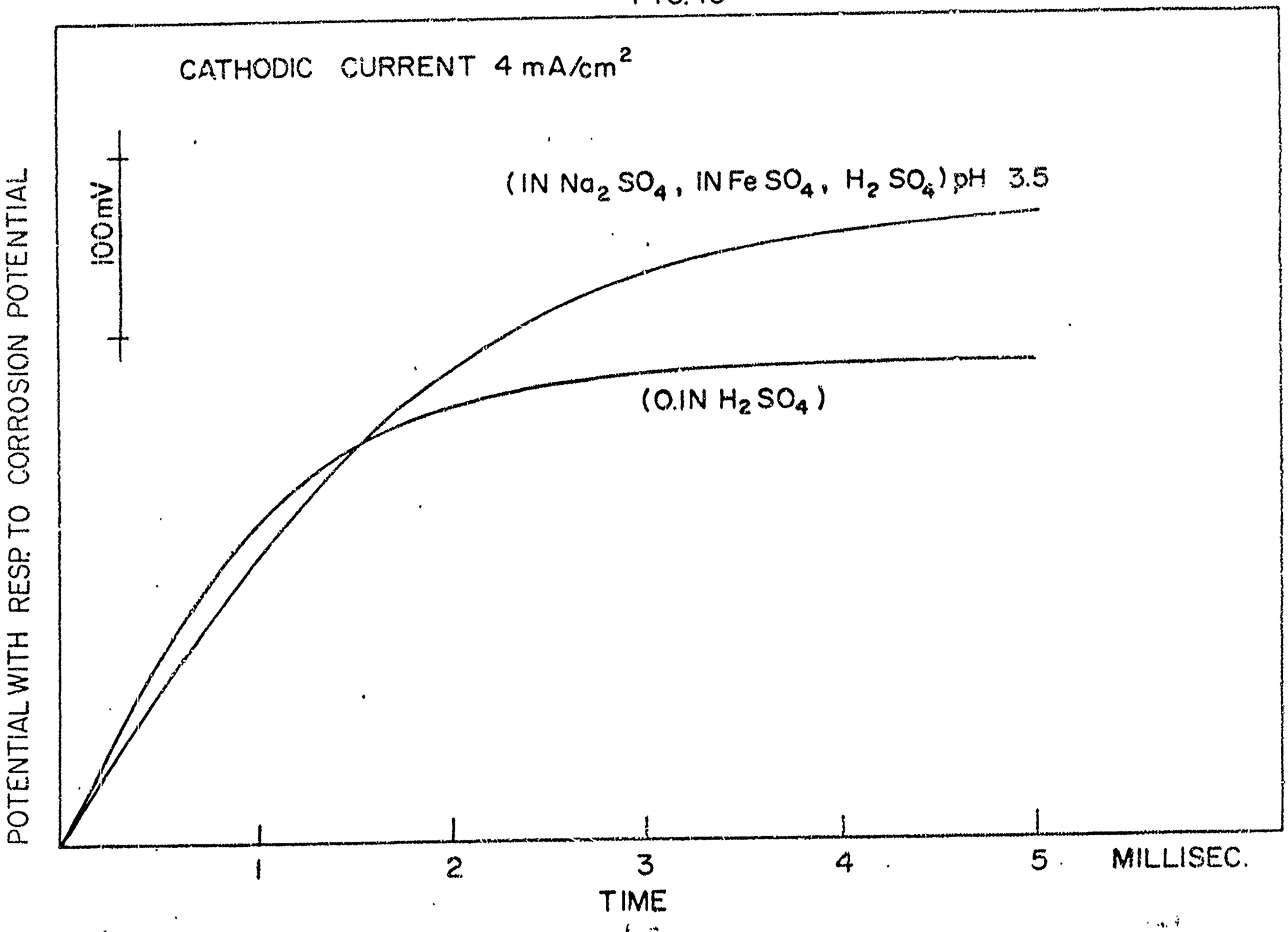
CATHODIC CURRENT 4 mA/cm²
100 mV
(1N Na₂SO₄, 1N FeSO₄, H₂SO₄) pH 3.5
(0.1N H₂SO₄)
POTENTIAL WITH RESP. TO CORROSION POTENTIAL
1
2
3
4
5
MILLISEC.
TIME

FIG.50

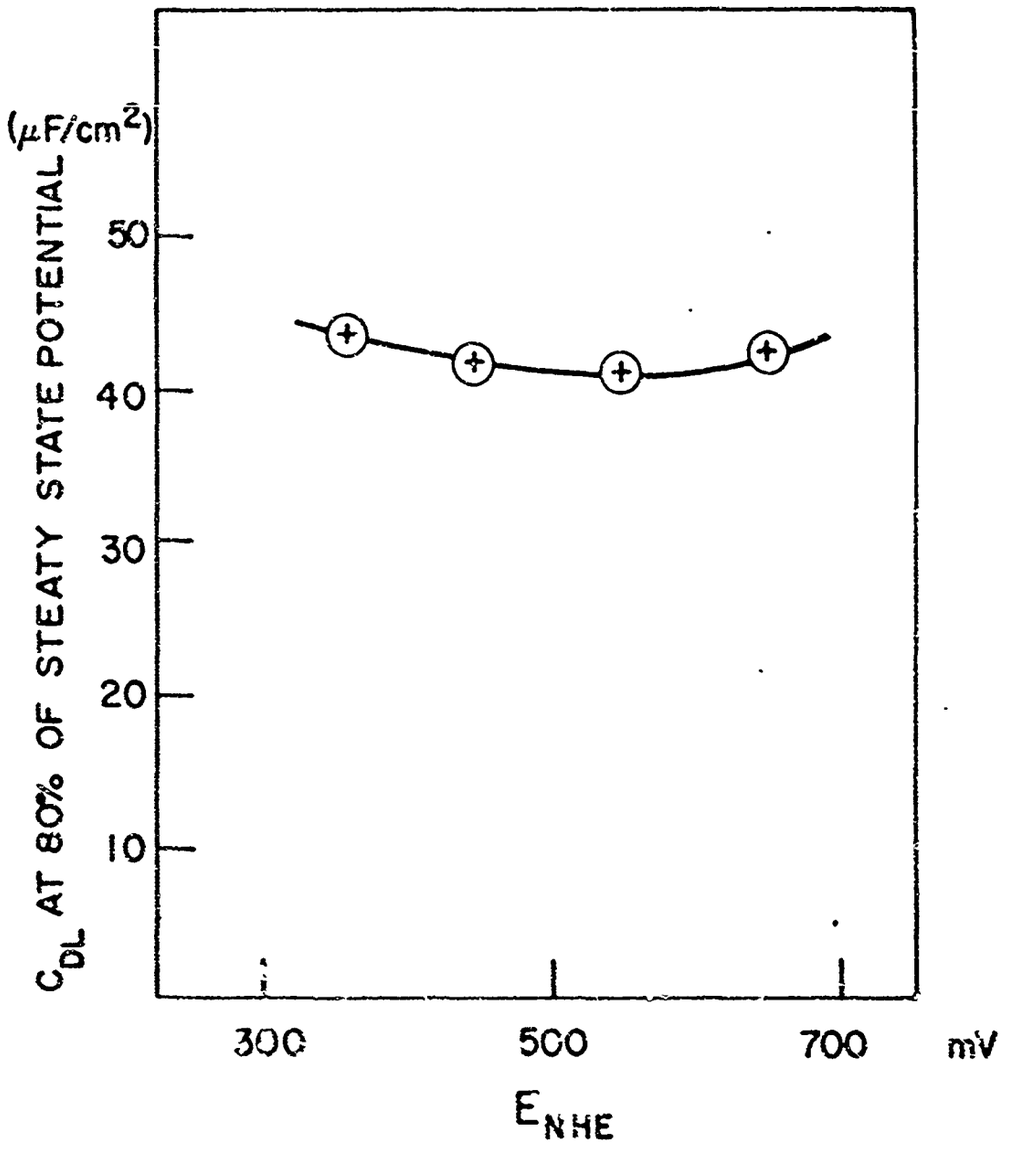
C_{DL} AT 80% OF STEATY STATE POTENTIAL
($\mu F/cm^2$)
50
40
30
20
10
300
500
700
mV
E_{NHE}